Spring 5-15-2019

A neural network for uncertainty anticipation and information seeking

Jensen Kael White
Washington University in St. Louis

WASHINGTON UNIVERSITY IN ST. LOUIS

Division of Biology and Biomedical Sciences
Neurosciences

Dissertation Examination Committee:
Ilya E. Monosov, Chair
Todd Braver
Suzanne N. Haber
Camillo Padoa-Schioppa
Lawrence Snyder

A Neural Network for Uncertainty Anticipation and Information Seeking

by
J. Kael White

A dissertation presented to
The Graduate School
of Washington University in
partial fulfillment of the
requirements for the degree
of Doctor of Philosophy

May 2019
St. Louis, Missouri

Table of Contents

List of Figures

Acknowledgements

The work that is presented in this dissertation would not have been possible without the tremendous assistance and guidance of my advisor, Dr. Ilya E. Monosov. I was incredibly lucky to have a mentor so dedicated to neuroscience and with such as passion for discovery. My work was knowledgeably guided by the comments and feedback from my thesis committee members, Dr. Camillo Padoa-Schioppa, Dr. Larry Snyder, Dr. Todd Braver, and Dr. Suzanne Haber, to whom I am incredibly grateful. I owe a special thank you to Dr. Ethan Bromberg-Martin, Dr. Sarah Heilbronner, and Dr. Suzanne Haber for their considerable contributions to our manuscript currently under review, from which the third chapter was adapted. Many thanks to Dr. Noah Ledbetter, Mr. Kaining Zhang, Ms. Julia Pai, Mr. Michael Traner, Dr. Ethan Bromberg-Martin, Dr. Ahmad Jezzini, Mr. Yang-Yang Feng, Ms. Jamie Moffa, and all members of the Monosov Lab past and present. You all provided insightful, engaging discussion and ensured that the lab was a stimulating place to spend (a lot of) time. Ms. Kim Kocher, whose superb animal care and lab management was only surpassed by her company and conversation, deserves a special thanks.

This work was supported by the Defense Advanced Research Projects (DARPA) Biological Technologies Office (BTO) ElectRx program under the auspices of Dr. Doug Weber through the CMO Grant/Contract No. HR0011-16-2-002, the National Institute of Mental Health under Award Number R01MH110594, and the McDonnel Center for Systems Neuroscience.

This work was expertly edited by the scientific editing network InPrint at Washington University in St. Louis.

With sincere respect and appreciation for laboratory animals across all scientific disciplines. Our species advances only through their sacrifice.

I am happy to give thanks to the many, many incredible people who I have had the opportunity to call friends while working at Washington University in St. Louis. Without you all, I surely would be neither where or who I am today. I also want to thank some of my oldest friends who, despite distance, have always been there for me.

I appreciate so much the love and support of my wonderful family. You have listened to my stories, my struggles, and even to me talk about my research. I love you all so much and truly cannot give enough thanks to have you in my life.

Finally, and most of all, I want to thank my amazing fiancée, Amanda Lee. You have been by my side through everything. Your companionship has made even the hardest days better; your intelligence and kindness always motivate me to be a better person. You are the love of my life, my partner in crime, and I cannot thank you enough for everything.

J. Kael White

Washington University in St. Louis

May 2019

Dedicated to my parents, Lin and Milo White.

Your compassion and perseverance never cease to inspire me.

You taught me to pursue not only what is true, but also what is right.

Abstract of the dissertation

A Neural Network for Uncertainty Anticipation and Information Seeking

by

J. Kael White

Doctor of Philosophy in Biology and Biomedical Sciences

Neurosciences

Washington University in St. Louis, 2019

Assistant Professor Ilya E. Monosov, Chair

In a world flooded with 'click bait', 'alternative facts', and 'fake news' one's ability to seek out, discern, and value information is of utmost importance. Although contemporary phenomena, these cultural ills take advantage of an evolutionarily-preserved drive for humans and nonhuman animals to monitor for and pursue opportunities to gain information. Indeed, in a natural environment where rewards are scarce and can be risky, animals often seek sensory cues as a source of information about future outcomes. Interestingly, humans and nonhuman animals will seek sensory information that provides advance information that predicts an outcome even when this information does not influence the event outcome or may even come at a cost to the eventual reward. This willingness to 'pay' for information, despite being unable to impact task outcome, indicates that the information itself has intrinsic value to subjects. But how and where in the brain are opportunities to learn new information about uncertain events signaled? How does the brain guide behavior towards pursuing this information? Elucidating these mechanisms would expand our understanding of how information seeking interacts with primary reward

seeking in naturalistic environments and could further inform theories of attention, learning, and economic decision-making.

Here, I demonstrate that connected regions of the anterior cingulate cortex (ACC), striatum, and pallidum contain neurons whose activity is selectively modulated by the presence and levels of outcome uncertainty. I describe the response of these neurons, many of which anticipate the resolution of uncertainty about an outcome— including when it is resolved through the animal seeking advance information. Finally, I demonstrate that the neural activity within areas of basal ganglia in this 'uncertainty circuit' causally contributes to information-seeking behaviors observed in nonhuman primates. This work demonstrates that connected regions of the brain previously associated with responses to primary rewards and motivation also contain a mechanism for anticipating uncertainty resolution and directing behaviors towards pursuing information that reduces uncertainty about upcoming events.

Chapter 1: Introduction to the dissertation

To begin this chapter, I provide an overview of information-seeking behaviors in human and nonhuman animals and how these behaviors might be useful in an uncertain world. Thereafter, I describe the role of the striatum in contributing to motivated and reward-related behaviors and as an integrator of cortical and midbrain signals. I then provide an overview of the organization of cortico-basal ganglia loops and the role of these networks in motivating animal behavior. Finally, I describe the connectivity and functions of connected areas of ACC and basal ganglia; I detail their roles signaling reward uncertainty and motivating reward-related behaviors and explain why this network is a good candidate for the signaling of upcoming uncertainty resolution and information availability. In sum, I will present an argument that these brain regions- already heavily implicated in motivating behavior towards primary reward- are ideal candidate regions for the investigation of the mechanisms by which the brain anticipates uncertainty resolution and drives behavior towards pursuing information about upcoming rewards.

1.1 Animals exist in an uncertain world and are motivated to reduce uncertainty through seeking information

We live in an uncertain world in which outcomes are variable, choices are risky, and the future is not often predicted with precision. Therefore, humans and other animals accurately estimating and reducing uncertainty can increase success in maximizing rewarding outcomes. Uncertainty can arise from a number of sources.[1] For example, someone could be uncertain about the past because of imperfections in memory, or uncertain about the current state of the world because of noisy or limited senses, such as imperfections in vision. This thesis will focus

primarily on outcome uncertainty, which arises when an animal is unsure about which events- or outcomes- will occur in the future. A common source of outcome uncertainty- and one which will be investigated extensively within this thesis- is that of economic risk, where the possible outcomes, timing, and probabilities of an outcome in a given situation are understood by the subject, but where the outcome itself remains unknown until the animal experiences the outcome event.[2,3]

For example, although one may understand the (dismally low) odds of winning in a lottery system such as the Powerball, the outcome of a ticket remains uncertain until when the numbers for the winner are drawn. Contrast this with an envelope that contains a dollar amount equal to the average yield of the lottery ticket (e.g.: $2.00). Where both objects share an expected value, the ticket has a degree of uncertainty (is risky) where the envelope has none (is safe). Humans and nonhuman animals often have strong preferences for choosing between certain and uncertain outcomes. For example, a gambling person might tend to choose the lottery ticket (risk seeking) while a more conservative person might tend to choose the envelope (risk averse).

How uncertainty guides behavior in humans and nonhuman animals is an interesting and ongoing topic of research in the fields of neuroscience, psychology, and economics. For example, uncertainty about an outcome can enhance learning[2–6], promote risk-seeking[3,7], and influence choice behavior[1,2,4,8] and emotional state.[1,9] Consistent with these observations of uncertainty's diverse influence on behavior, subsequent studies demonstrated that many brain regions are modulated by uncertainty. For example, human fMRI studies indicated that multiple regions of the brain, including the striatum[10,11] and many areas of the neocortex[12–14], are modulated by outcome uncertainty. Single-unit recordings indicated that the activity of individual neurons across the brain is modulated by reward uncertainty[15–22]. Although these

studies offer insight into how activity in different brain regions is modulated by uncertainty, the field has yet to determine the neural mechanisms by which the brain anticipates uncertain outcomes, values uncertain rewards, and drives behaviors towards reducing uncertainty about the future.

How is it that uncertainty about the future can be reduced? By obtaining information about an outcome in advance, animals can resolve uncertainty about an outcome prior to it occurring. Take, as an example, the risk-seeking gambler from above: imagine that she pulls the lever on a slot machine in which the symbols spin for 10 seconds before their identities are revealed and the outcome (i.e.: a win or a loss) occurs. In this scenario she would be in a state of uncertainty about the outcome until the symbols stop spinning and it occurs. Alternatively, imagine if the machine contained a button that, when pressed, would reveal the identity of the symbols immediately but the outcome would only occur 10 seconds after the lever was pulled. In this second situation uncertainty was resolved at an earlier timepoint through the delivery of advance information about the outcome. Importantly, the timing and the outcome of the gamble is constant across these scenarios; the only difference between them is that uncertainty was resolved in the latter at an earlier timepoint.

Pioneering behavioral experiments demonstrated that animals often prefer uncertain outcomes to be resolved at an early timepoint and will preferentially exhibit 'observing responses' which provide information about upcoming reinforcing outcomes.[23] This research has been replicated in subjects ranging from pigeons, to rats, to nonhuman primates[23–28] and suggests that animals across a wide range of species readily learn these observing behaviors. Indeed, in the field of economics, for example, similar preferences for this early information in human subjects were reported across a number of studies.[29–31] That is, when given the option to reveal

the outcome of an uncertain situation, humans will choose to do so at the earliest possible moment, even when this information cannot be used to impact the outcome or give the subject any advantage in the task. Interestingly, this desire is strong enough that both humans[31] and nonhuman primates[28] will exchange a portion of their upcoming reward in order to obtain this advance information about task outcome.

Despite the prevalence of these observing and information-seeking behaviors, the neural mechanisms that drive and maintain them remain unclear. One proposal is that these behaviors are supported by neural circuits that overlap with those that underlie conventional reward-seeking behaviors.[26] It is suggested that midbrain dopamine neurons, for example, are important for reward learning and motivated behavior.[32–36] The activity of many of these neurons transmits a reward prediction error (RPE).[35,37] An RPE is a signal of the difference between the expected value of an outcome and the delivered value of an outcome. RPE signals within the brain could contribute to computing the value of rewarding actions and reinforce actions that maximize primary rewards over a period of time.[32,33] Such a signal could contribute substantially to learning, memory, and motivated behaviors.[34] Although RPE-based reinforcement learning has the power to explain much of what motivates animals to pursue primary rewards[37–39], behaviors that show preference for this advance information would not be predicted by this model. Consider a secondary cue that gives information about a coin toss: a 50/50 chance of either a positive or negative outcome. Because the chances of this cue providing a positive RPE is the same as it providing a negative RPE, the secondary cue-seeking behavior would not be reinforced as the overall RPE would be neutral. Although multiple models have been proposed[27,40–42] to explain this gap in our understanding, the exact mechanisms that support these behaviors remain unclear.

A recent study[26] looking at midbrain dopamine neurons reported a similar response to advance information. Much like RPEs with primary rewards, 'information prediction errors' (IPEs) were higher when there was more information about outcome than expected and lower when there was less information about outcome than expected. Other information-related patterns of response are also observed in other motivational brain areas, including one of the major inputs to midbrain dopamine neurons, the lateral habenula[27] as well as areas of neocortex.[28] Taken together with the behavioral preferences for information seen in both human and nonhuman animals, these findings support the idea that the brain might use overlapping neural systems to motivate the pursuit of primary rewards and the pursuit of information about upcoming rewards.

Despite the importance of uncertainty resolution and information seeking to everyday life, the mechanisms that underlie these behaviors remains largely unknown. Where and how does the brain represent levels of uncertainty and availability of information? Further, which brain area or areas are capable of motivating animals to reduce uncertainty and seek information?

1.2 The striatum has a demonstrated role in reward-evaluation, reward-seeking, and other motivated behaviors

The striatum is the primary input structure of a set of subcortical structures known as the basal ganglia and has long been considered an integrator[43–47] of glutamatergic signals from cortex[48–50] and dopaminergic signals from the midbrain.[51–54] Of particular interest to this integration are medium spiny neurons (MSNs), which make up the vast majority of neurons found in the striatum and are a major target of midbrain dopamine neurons. The excitatory response of the MSNs to cortical input is modulated by dopamine as well as by the activity of largely inhibitory populations of local interneurons.[55–57] Within the striatum, synapses from

cortical inputs are preferentially contacted by projections from midbrain dopamine neurons relative to those that originate from thalamus.[55] These synaptic interactions are thought to underlie the roles of the striatum in supporting motivated, reward-related behaviors.

A large and growing body of literature has identified reward-related signals in the striatum and broadly implicates its role in motivational and reward-related behaviors. For example, early human PET experiments found increased levels of the neurotransmitter dopamine in subjects both with the stimulation of primary food reward[58] as well as rewarding epochs in a video game.[59] Later fMRI experiments verified that the striatum responds while subjects learned and anticipated rewarding outcomes[60–64] and that these responses could be influenced by varying the properties of these rewards, such as reward magnitude and timing.[62,65–67] Similarly, physiological recordings within the dorsal regions of this structure have demonstrated that activity in this region represents the anticipation[68,69] and delivery[70,71] of primary reward, action-dependent rewards[72–75], and that it contains signals capable of directing an animal's gaze towards rewarding outcomes.[76–79] In line with these findings, studies that manipulated striatal activity found that doing so changes reward-driven behaviors in a number of ways. Lesions and inactivations of the striatum yielded strong effects, including changes in reward-choice behaviors[80,81], and learning and habituation.[82–84] Injection of muscimol, a $GABA_A$ agonist into striatum resulted in decreases in reward-learning[85], choice[86], and feeding behaviors[80,81] and resulted in decreased performance in reward-related tasks, as well as slower response times to preferred rewards.[80,85] Additionally, pharmacologically manipulating activity in separate regions of striatum resulted in different effects during interactions with rewards.[87] In sum, these studies suggest that neuronal activity within the striatum is not only modulated by the presence and properties of reward, but that it also causally influences reward-driven action.

1.3 Cortico-basal ganglia networks contribute to and refine motivated behaviors

Projections from the frontal cortex to the striatum are organized and are thought to often follow stereotyped functional and topographical pathways.[45,50,88,89] An early anatomical study suggested[90] that these pathways compose closed "loops" from specific regions of cortex, to basal ganglia, to thalamus, and back to cortex. In this way, partially overlapping inputs from the cortex are integrated and refined along the progression of the circuit and "funneled" back into a single area of cortex. Activity across these circuits is segregated to specific areas with sensory, motor, or associative functions.[90] These neural circuits provide the framework for cortico-striatal interactions that could contribute widely to reward seeking and motivated behaviors.

Additionally, these closed loops explain observed similarities in function between anatomically-connected areas of cortex and striatum. For example, there are established projections[91–94] from motor, pre-motor, and somatosensory cortex to caudal dorsolateral striatum. Activity in this region of striatum contributes to sensorimotor behaviors, such as learned and innate sequential actions[95–99], motor learning and planning[72,100–104], and habit formation.[72,105–107] Similarly, projections from orbitofrontal and medial prefrontal cortex broadly innervate areas of rostromedial dorsal striatum as well as ventral striatum.[46,89,92,108] These areas of striatum contribute to goal-directed behaviors[109–111] and reward learning[112–115] and, further, dysregulation of these areas and their connections have been implicated in a number of mental illnesses.[116–121] Projections from additional areas of prefrontal cortex, such as the dorsolateral and medial prefrontal cortex- including areas of ACC- project broadly to rostrodorsal striatum.[48,122–124] This innervation could provide signals that influence more cognitive processes, such as working memory[125–130] and behavioral flexibility.[131–134] Taken together, the connections that compose the broad networks of cortico-striatal projections create a rough topographical organization between

cortex and the striatum that contributes broadly to a wide-ranging repertoire of motivated behaviors.

Although projections from cortex to striatum have often been considered parallel and segregated along this topographical map, there is growing evidence to suggest that the loops that they form are more overlapped than previously understood.[46,50,135,136] The processes by which information is exchanged across these circuits is believed to be at least partially dependent on cross-over connections that exist within and downstream of the basal ganglia.[136–139] These integrating nodes across cortico-basal ganglia loops that convey different properties of a situation could underlie evaluation of more complex object-outcome relationships than entirely segregated networks. In line with this concept, both associative and cognitive signals[63,101,107,109,114,140,141] have been reported broadly throughout areas of the striatum that were believed at one point to be largely dedicated to motor functions. Overall, it is currently understood that networks that encompass regions of cortex and basal ganglia contribute broadly to motivated behaviors, particularly to those which are directed at rewarding outcomes.

1.4 Signals related to uncertain rewards are present in anatomically-connected regions of cortex and basal ganglia that motivate behavior towards primary rewards

In order for the brain to promote information-seeking behaviors, neural mechanisms which monitor uncertainty should be tightly linked to those which underlie motivational processes. The striatum plays a key role in reward-seeking and motivational behaviors and as such might be an ideal candidate to fulfill this role. But where in the striatum might we expect to find uncertainty-related activity? Drawing inspiration from the cortico-basal ganglia loops discussed previously, it would likely be a region of striatum that share connections with areas of cortex and other areas of basal ganglia which have strong responses to uncertainty. In this way,

this region of striatum could process uncertainty signals from cortex and project them further into the basal ganglia to drive behavior.

Recently, single-unit recordings of neurons in ACC determined that largely separate populations of neurons respond to appetitive and aversive uncertain outcomes.[15] The mostly excitatory activity of different populations of these neurons signaled information about the uncertainty of juice rewards and air-puff punishments. These findings compliment the demonstrated role of ACC in the control of cognitive functions and motivated behaviors aimed at both optimizing rewards[142–146] and avoiding punishments.[147–149] Supporting this role are observations that the ACC contains individual neurons which respond to the presence of rewarding stimuli in ways which correspond to both the value of rewards[144–146,150] and the effort[151–153] required to obtain it. In line with these findings are hypotheses which suggest that ACC contributes to value-based decision-making behaviors.[143–145] A growing number of human imaging studies also reported higher-order signals related to learning and exploration, which are oftentimes related to the expectation of uncertain outcomes[4,9,154,155]

A recent study has identified a subset of neurons within VP that responded selectively to uncertainty. These cells showed a strong and consistent decrease in their firing before the delivery of uncertain rewards.[16] This study contributes to other proposals that areas of pallidum- particularly the ventral extent of the structure- are implicated in the mechanisms of reward and motivation. For example, self-stimulation studies reported that animals will repeatedly press a lever for pallidal stimulations[156–158] and that injection of bicuculline, a $GABA_A$ antagonist, resulted in increased food consumption.[159–161] Conversely, lesion studies found that damaging areas of ventral pallidum (VP) resulted in failures to eat and drink in rodents[162–164], indicating that the structure has a role in hedonic drive. Interestingly, one study of the ventral pallidum

found that lesioned animals not just reduce, but reverse, their pursuit of reward.[163] Clinical studies in humans with damaged pallidum found that a patient once addicted to alcohol and other drugs no longer experienced cravings and reported a depressive mood and a generally despondent demeanor[165]; similarly, a second patient with damage to an overlapping area reported the inability to feel strong emotions and a general lack of motivation following the lesion.[166]

But is there a striatal link between these cortical and basal ganglia uncertainty signals? Specific and overlapping areas of the dorsal striatum receive both glutamatergic projections from ACC and share mutual GABAergic connections with the ventral pallidum.[46,48,50] Interestingly, these areas of ACC and pallidum are also highly overlapped with those where uncertainty-responsive cells were reported.[15,16] Could it be that these regions of the dorsal striatum contain a mechanism for signaling levels of reward uncertainty? Further, might this interconnected network of brain structures, some of which have a demonstrated role in predicting uncertain outcomes and motivating behavior towards primary rewards, contribute to an animal's motivation to seek information about uncertain rewards?

1.5 Summary

For a brain area or areas to be implicated in motivating behaviors towards seeking information, they must not only monitor the environment for levels of uncertainty surrounding future events, but also anticipate when information that resolves this uncertainty is available. Further, it must be demonstrated that interrupting the activity of these areas causally reduces information-seeking behaviors. In the following chapters we will describe the experimental results of testing areas of ACC and basal ganglia for responses to outcome uncertainty and anticipation of information about upcoming outcomes. In Chapter 2 we report a selective and anticipatory response to uncertain reward delivery within the striatum, specifically regions of

caudate nucleus and putamen which border the internal capsule (icbDS). We interrogate this response further across various reward schedules and task conditions. We continue with Chapter 3 where we describe and compare the responses of anatomically-connected regions of ACC and basal ganglia (icbDS and VP) to reward uncertainty. We then test the response of each area when advance information about uncertain outcomes is available to determine if these areas are anticipating the delivery of uncertain outcomes, or if their response is to uncertainty resolution more broadly. Thereafter, we investigate looking behaviors which are associated with uncertainty and information-seeking and demonstrate that pharmacological manipulation of areas of this putative 'information-seeking' circuit results in decreased information-seeking biases. In sum, we identify a novel neural network which participates in signaling the resolution of reward uncertainty across multiple modalities and demonstrate that the activity of this network causally contributes to information-seeking behaviors in primates.

Chapter 2: Neurons in the primate dorsal striatum signal the uncertainty of object–reward associations

Adapted from:
J. Kael White & Ilya E. Monosov
Neurons in the primate dorsal striatum signal the uncertainty of object-reward associations.
Nature Communications, 2016. Article number: 12735 doi: 10.1038/ncomms1273

To learn, obtain reward and survive, humans and other animals must monitor, approach and act on objects that are associated with variable or unknown rewards. However, the neuronal mechanisms that mediate behaviors aimed at uncertain objects are poorly understood. Here we demonstrate that a set of neurons in internal-capsule bordering regions of the primate dorsal striatum, within the putamen and caudate nucleus, signal the uncertainty of object–reward associations. Their uncertainty responses depend on the presence of objects associated with reward uncertainty and evolve rapidly as monkeys learn novel object–reward associations. Therefore, beyond its established role in mediating actions aimed at known or certain rewards, the dorsal striatum also participates in behaviors aimed at reward-uncertain objects.

2.1 Introduction

To survive, humans and other animals must act on objects that have been previously associated with certain or reliable rewards.[107,167,168] However, learning, foraging and decision-making also require animals to monitor, approach and act on objects associated with variable or unknown rewards[4,18,155,169], even when the mean reward value of such uncertain objects is lower than that of other objects.[1,170,171] To date, the mechanisms that direct behavior towards uncertain objects are not well understood.

Expected (or certain) reward-driven behaviors are in part dependent on the caudate–putamen complex[73–75], also called the dorsal striatum (DS). In primates, the caudate nucleus in

particular has recently been shown to contain multiple mechanisms for directing gaze at objects associated with high reward values.[76–79] Here we asked if the primate DS also contains a mechanism to support behavior aimed at objects associated with outcome uncertainty.

Our experiments showed that a subset of neurons, mostly in the internal-capsule bordering regions of the DS (icbDS), was preferentially activated by visual objects associated with reward-uncertain outcomes. Furthermore, the icbDS reward-uncertainty responses greatly depended on the presence of visual objects associated with reward uncertainty because they were reduced when the object was removed before the uncertain outcome was delivered. These uncertainty responses occurred when subjects were presented with objects that were associated with uncertain either due to the subjects' lack of knowledge or due to known uncertainty (also called risk[3,172]) but carried no spatial or specific object information. Finally, during object–reward associative learning, icbDS neurons' uncertainty responses evolved rapidly as monkeys learned novel object–reward associations.

Our experiments suggest that uncertainty-sensitive neurons in the primate DS may play important roles in object-based behaviors under uncertainty.

2.2 Materials and methods

2.2.1 General procedures

Two adult male rhesus monkeys (*Macaca mulatta*) were used for the neurophysiology experiments in the DS (Monkeys B who is 6 years old; and Monkey W who is 5.25 years old). All procedures conformed to the Guide for the Care and Use of Laboratory Animals and were approved by the Washington University Institutional Animal Care and Use Committee. A plastic head holder and plastic recording chamber were fixed to the right side of the skull under general anesthesia and sterile surgical conditions. The chambers were tilted laterally by 35° and aimed at

the anterior portion of the striatum. After the monkeys recovered from surgery, they participated in the behavioral and neurophysiological experiments.

2.2.2 Data acquisition

While the monkeys participated in the behavioral procedures we recorded single neurons in the right DS. The recording sites were determined with 1 mm-spacing grid system and with the aid of magnetic resonance images (3 T) obtained along the direction of the recording chamber. This magnetic resonance imaging-based estimation of neuron recording locations was aided by custom-built software (PyElectrode). Single-unit recording was performed using glass-coated electrodes (Alpha Omega). The electrode was inserted into the brain through a stainless-steel guide tube and advanced by an oil-driven micromanipulator (MO-97A, Narishige). Signal acquisition (including amplification and filtering) was performed using Alpha Omega 44 kHz SNR system. Action potential waveforms were identified online by multiple time-amplitude windows with an additional template-matching algorithm (Alpha-Omega). Neuronal recording was restricted to single neurons that were isolated online. Neuronal and behavioral analyses were conducted offline in Matlab (Mathworks, Natick, MA).

Eye position was obtained with an infrared video camera (Eyelink, SR Research). Behavioral events and visual stimuli were controlled by Matlab (Mathworks, Natick, MA) with Psychophysics Toolbox extensions. Juice, used as reward, was delivered with a solenoid delivery reward system (CRIST Instruments). Juice-related anticipatory licking during the CS epoch was measured and quantified using previously described methods.[17]

2.2.3 Behavioral tasks

2.2.3.1 Reward-probability and reward-amount procedure (experiment 1)

The reward-probability and reward-amount behavioral procedure consisted of two blocks, a reward-probability block and a reward-amount block (Figure 2.1). In the reward-probability block, three visual fractal CSs were followed by a liquid reward (0.25 ml of juice) with 100, 50 and 0% chance, respectively. In the reward-amount block, three CSs were followed by a liquid reward of 0.25, 0.125 and 0 ml, respectively. Thus, the expected values of the three CSs matched between the probability and amount blocks. To control for neuronal object preference, we used two fractal sets (that is, for every CS there were two different fractals).

Each trial started with the presentation of a green trial-start cue at the center. The monkeys had to maintain fixation on the trial-start cue for 1 s; then the trial-start cue disappeared and one of the three CSs was presented pseudo randomly. After 2.5 s, the CS disappeared, and juice (if scheduled for that trial) was delivered. The monkeys were not required to fixate on the CSs. In each trial, the CS could appear in three locations: 10° to the left or to the right of the trial-start cue, or in the center. One block consisted of 18 trials with fixed proportions of trial types (each of the three CSs appears three times each block, 9/18 trials total).

In the remainder of the trials in each block (9/18), the monkeys chose amongst the task CSs. Each trial started with the presentation of a purple trial-start cue at the center, and the monkeys had to fixate it for 0.5 s. After the monkey fixated on the trial start cue for 0.5 s, a choice array was presented consisting of two fractals used in the Pavlovian procedure (shown in Figure 2.1A). The monkey had to continue to fixate until the trial start cue disappeared (0.5 s). Monkeys then made saccadic eye movements to their preferred reward-associated fractals and fixated them for 0.75 s to indicate their choices. Then, the unchosen stimulus disappeared, and the monkeys waited for 1 s to receive the scheduled outcome (associated with their chosen fractal).

The inter-trial intervals ranged from 3 to 6 s. Approximately one in five inter-trial intervals contained uncued events (chosen randomly). These could be either a juice reward alone (0.25 ml) or an ~70 dB 0.15 s auditory white noise burst paired with a brief change in screen color (same duration as the auditory stimulus).

Neuronal recordings did not begin until the monkeys chose the CSs associated with higher expected value over CSs associated with lower expected value >90% of the time. The monkeys' knowledge of the CSs was further confirmed when we measured the monkeys' licking behavior. The magnitude of licking was correlated to the reward value of the fractals in the reward-probability block ($P<0.001$; Spearman's rank correlation) and the reward-amount blocks ($P<0.001$; Spearman's rank correlation).

2.2.3.2 Five reward-probability and reward-amount procedure (experiment 2)

The reward-probability and reward-amount behavioral procedure consisted of two blocks, a reward-probability block and a reward-amount block. The trial structure was the same as in experiment 1. However, here the reward-probability block contained five objects associated with five probabilistic reward predictions (0, 25, 50, 75 and 100% of 0.25 ml of juice) and a reward-amount block that contained five objects associated with 100% reward predictions of varying reward amounts (0.25, 0.1875, 0.125, 0.065 and 0 ml).[17,18] One block consisted of 20 trials with fixed proportions of trial types (each of the five CSs appears four times each block).

2.2.3.3 Trace reward-probability procedure (experiment 3)

The temporal structure of this procedure was the same as in probability-amount procedure (experiment 1). The trace procedure contained four possible distinct CS fractals. The first two CSs were associated with 100% (CS 1) and 50% (CS 2) chance of 0.25 ml of juice. These CSs remained on the screen for 2.5 s and were followed by the scheduled reward outcome.

(same as in experiment 1). The other two CSs were also associated with 100% (CS 3) and 50% (CS 4) chance of 0.25 ml of juice but were only presented for 1 s. This was followed by a 1.5 s trace period, during which the screen did not contain any stimulus. The trace period was followed by the scheduled reward outcome. Therefore, in both trace and non-trace conditions, monkeys experienced two types of reward predictions (certain and uncertain) and experienced outcome delivery in 2.5 s after the initial CS presentation.

2.2.3.4 Object learning procedure (experiment 4)

Instead of using previously conditioned object fractals, monkeys were exposed to three novel CSs associated with 100, 50 and 0% chance of reward delivery. The task design and temporal structure of the trials were the same as in probability-amount procedure (experiment 1). However, the interleaved choice trials were choice trials amongst the three novel fractals.

2.2.3.5 Appetitive-aversive procedure

The procedure consisted of two alternating blocks: appetitive and aversive.[15] In the appetitive block, three visual fractal CSs were followed by a liquid reward (0.4 ml of juice) with 100%, 50% and 0% chance, respectively. In the aversive block, three visual fractal CSs were followed by an air puff with 100%, 50% and 0% chance, respectively. Airpuff (~35 psi) was delivered through a narrow tube placed 6–8 cm from the monkey's face. Temporal structure of the trials was the same as in other procedures, but here monkeys were not required to fixate the trial start cue. Each block consisted of 12 trials with fixed proportions of trial types (100%, four trials; 50%, four trials; 0%, four trials).

2.2.4 Data processing and statistics

Spike-density functions were generated by convolving spike times with a Gaussian filter (σ=50 ms). To display single neuron examples (Figs 1a, 3a, and 4a) spike-density functions were

generated by convolving spike times with a 100 ms Gaussian filter. A neuron was defined as uncertainty sensitive if its responses varied across the four possible reward predictions (100% 0.25, 50% 0.25, 100% 0.125 and 0 ml of juice) (Kruskal–Wallis test, $P<0.01$; analysis window: 100 ms after CS presentation until outcome) and if its response to the uncertain CS (50%) was significantly stronger or weaker than its responses to both 100 and 0% reward CSs (two-tailed rank-sum test; $P<0.01$). The same analysis window was used to study neuronal activity during the CS epoch in Figure 2.2C.

To normalize task-event-related responses, we subtracted baseline activity (the last 500 ms of the inter-trial interval) from the activity during the task-event-related measurement epoch. All statistical tests were two-tailed. For comparisons between two task conditions for each neuron, we used a rank-sum test, unless otherwise noted. For comparisons between two task conditions across the population average we used a paired signed-rank test, unless otherwise noted. Statistical threshold throughout this study is $P<0.01$ unless otherwise noted.

To assess the sensitivity of individual uncertainty-selective striatal neurons to task-related variables in Experiment 1 (Figure 2.2C), we obtained their response indices (difference between neuronal responses to two conditions divided by their sum). To assess CS spatial location sensitivity, we compared responses to the 50% CS when it was shown 10° to the right versus 10° to the left of center. To assess object-feature sensitivity, we compared responses to two distinct 50% CS fractal objects. Reward-value sensitivity was assessed by comparing neuronal responses to 100% 0.25 ml CS versus 0.125 ml CS. Reward-context sensitivity was assessed by comparing CS activity in certain reward trials (100% 0.25 and 0.125 ml CS trials) versus no reward trials. Uncertainty sensitivity was assessed by comparing responses to 50% reward CSs with 100% reward CSs. Reward prediction error sensitivity was assessed by comparing reward versus no-

reward responses after the 50% reward prediction (in the 250 ms window after the outcome). Neuronal responses during experiments 2–4 were measured in the last 500 ms before the trial outcome.

To calculate receiver-operating characteristic (ROC) that assessed neuronal discrimination of uncertainty, we compared spike-density functions of 100% reward CS trials and 50% reward CS trials. The analysis was structured so that receiver-operating characteristic area values >0.5 indicate that the activity in the 50% reward CS trials is greater than in the 100% reward CS trials values <0.5 indicate that the activity in the 100% reward CS trials is greater than in the 50% reward CS trials.

2.3 Results

2.3.1 DS neurons selectively signal reward uncertainty

To test if the primate DS contains neurons that are preferentially activated by visual objects associated with reward-uncertain outcomes, we recorded 141 single neurons from DS while two monkeys (B, n=103 neurons; W, n=38 neurons) participated in a behavioral procedure that was composed of two distinct blocks: a reward-probability block, in which three visual conditioned stimuli (CSs) predicted a 0.25 ml juice reward with 100, 50 and 0% chance; and a reward-amount block, in which three CSs predicted 0.25, 0.125 and 0 ml of juice (experiment 1, Figure 2.1A). For each block, we used two fractal sets that could appear in one of three spatial locations. Monkeys' knowledge of the task was tested with interleaved choice trials (Methods), and neuronal recordings did not begin until the monkeys chose the CSs associated with higher expected value over CSs associated with lower expected value >90% of the time (Figure 2.1B).

Uncertainty-sensitive neurons were defined as those that varied their responses across the task CSs (Kruskal–Wallis test; P<0.01) and displayed significantly stronger responses to the

50% CS than to both 100 and 0% reward CSs or weaker responses to 50% CS than to both 100 and 0% reward CSs (two-tailed rank-sum tests; $P<0.01$). We found that 45/141 neurons, mostly in the internal-capsule bordering regions of the striatum, were selectively activated by reward uncertainty ($n=19$ in monkey W; $n=26$ in monkey B). 0/141 neurons were selectively suppressed by uncertainty. An example uncertainty-sensitive (U+) neuron's CS responses are shown in Figure 2.1C. Its activity increased following the presentation of the CS that predicted 0.25 ml of juice reward with 50% chance until the uncertain outcome was delivered and the uncertainty was resolved. This example neuron did not strongly respond to other CS objects or task events.

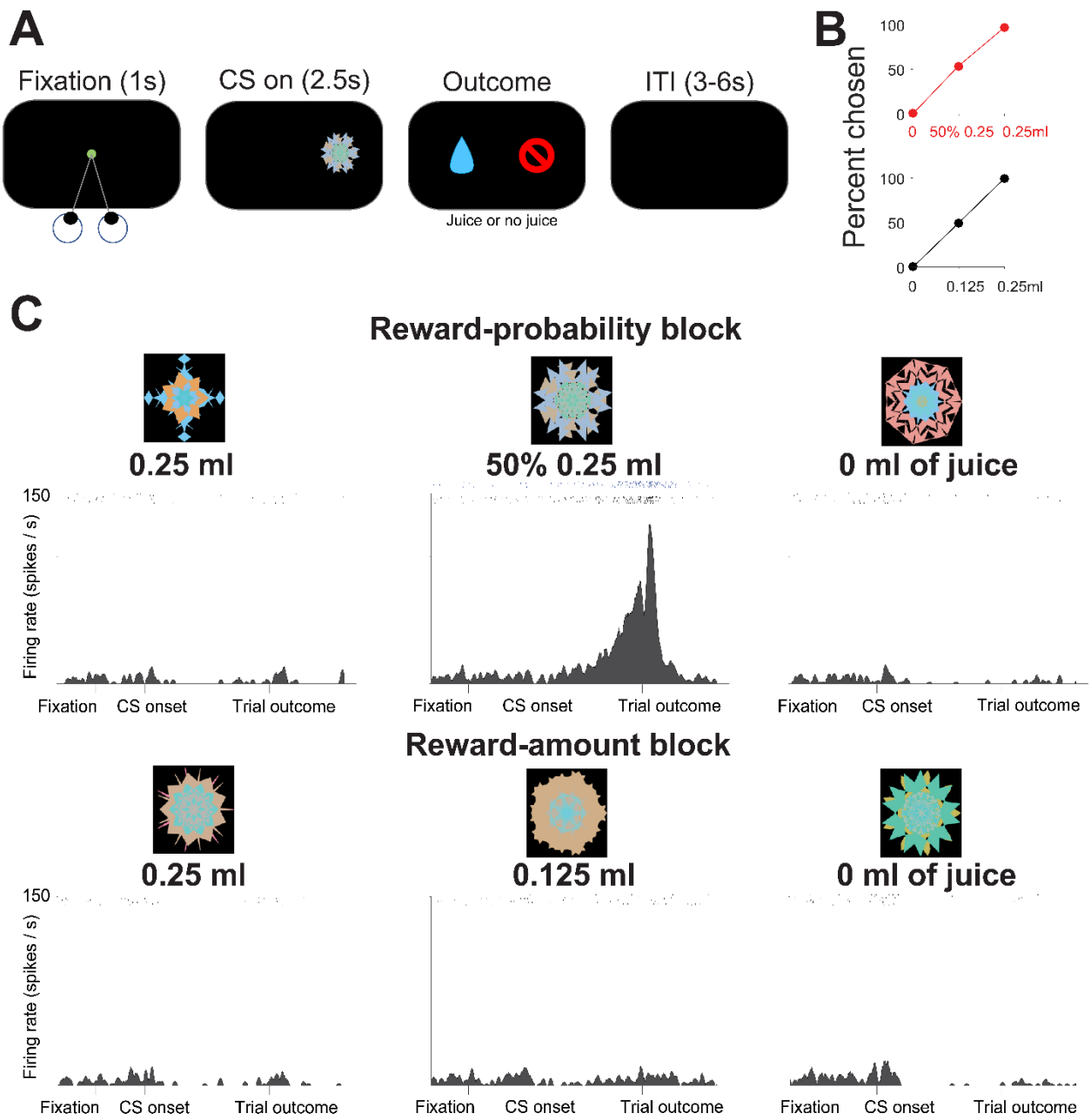

Figure 2.1: (**A**) Experimental procedure for experiment 1. (**B**) Monkeys' choice behavior in experiment 1**.** Choice percentage of a single reward-probability CS (x-axis) versus all the other reward probability CSs (red). Choice percentage of a single reward-amount CS (x-axis) versus all the other reward-amount CSs (black). Data compiled from 5602 trials. (**C**) Responses of a single uncertainty selective (U+) neuron in the internal capsule bordering region of the striatum to the presentation of six fractal objects (shown above rasters) associated with certain and uncertain predictions of juice reward. Dark blue raster plots indicate the activity in 50% CS trials in which reward was omitted.

All U+ neurons exhibited roughly similar responses (Figure 2.2A,B). On average, they were strongly activated by the presentation of the CS that predicted 0.25 ml of juice reward with 50% chance. This activation was most often a ramp-like increase in activity, which continued until the uncertain outcome was delivered and the uncertainty was resolved (Figure 2.2A).

Amongst single neurons, 44/45 U+ neurons responded more strongly to the CS object associated with 50% chance of 0.25 ml of juice than to the CS object associated with 0.125 ml of juice (Figure 2.2B) even though these CSs were associated with the same expected reward value.

Further neuron-by-neuron analyses revealed that amongst the task features of experiment 1, U+ neurons were consistently sensitive to reward uncertainty and to reward context (that is, difference between trials in which reward was possible versus trials in which rewards would not be delivered). This is shown in Figure 2.2C and in Supplementary Figure 2.2 for DS U+ neurons in caudate and putamen, separately. Most single U+ neurons did not encode information about expected values (defined as the difference between responses to objects associated with 0.25 and 0.125 ml of juice), spatial- and object-feature parameters (Figure 2.2C), or aversive outcomes (Supplementary Figure 2.3). However, 24/45 U+ neurons discriminated reward-associated CSs from CSs associated with no outcome delivery (Figure 2.2C, this reward-related enhancement can also be observed in the average activity in Figure 2.2A). Also, on average, U+ neurons responded to the delivery of expected/certain rewards with a weak but consistent phasic excitation (Figure 2.2A; $P<0.05$; sign-rank test). The observations in Figure 2.2 indicate that while U+ neurons were preferentially dedicated to signaling reward uncertainty, they were also sensitive to reward context (or expectation) and reward delivery.

While U+ neurons did not encode the locations of CS objects, thus far, it was unknown if they respond before or during saccades aimed at reward uncertain objects. To assess this further,

we studied the dynamics of U+ uncertainty selectivity during choice trials. We found that, on average, U+ uncertainty selectivity emerged after the monkeys fixated the object associated with reward uncertainty (Supplementary Figure 2.4). Therefore, U+ neurons did not trigger saccades aimed at reward-uncertain objects.

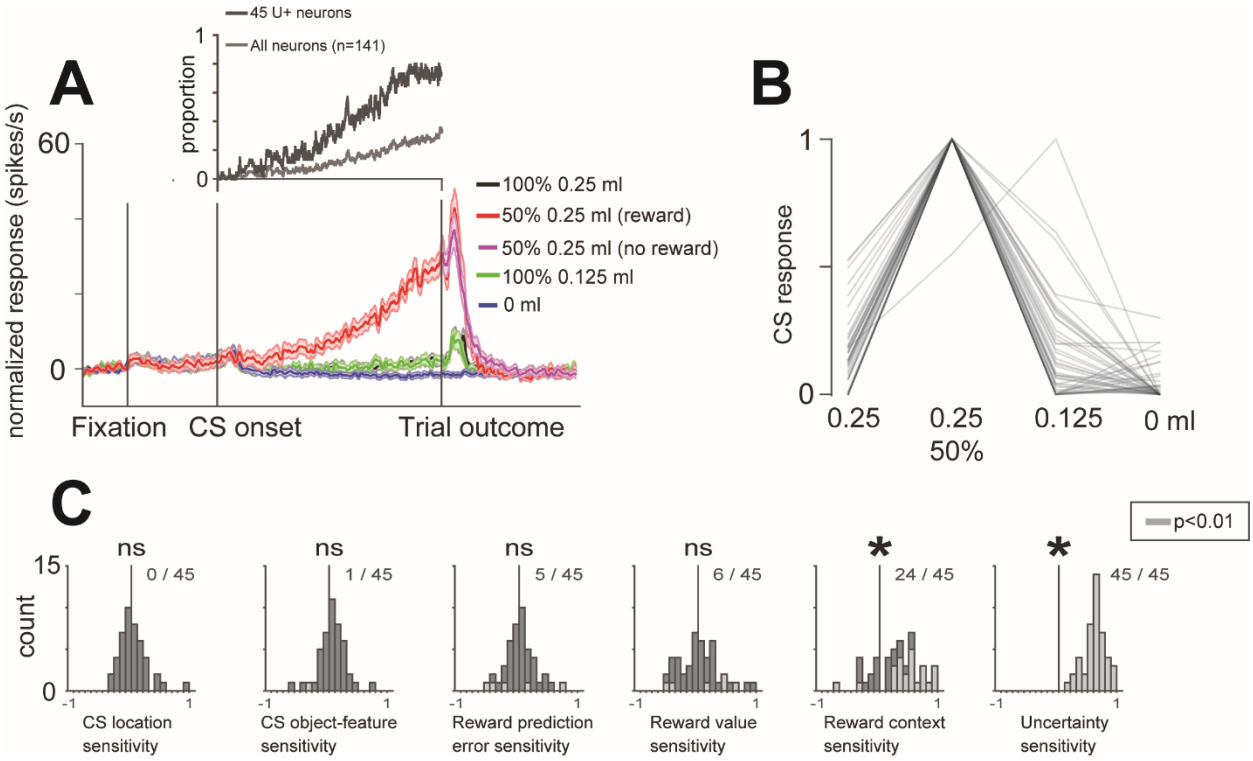

Figure 2.2: (**A**) Average responses of 45 U+ neurons to different reward predictions in the reward-probability and reward-amount procedure. Shaded region represents standard error. The inset shows proportion of neurons (of 45 U+ neurons and of all 141 striatal neurons) displaying uncertainty selectivity during the CS epoch in time. (**B**) CS responses of 45 U+ neurons for different reward predictions in the reward-probability and reward-amount procedure (normalized to the maximum CS response; from 0 to 1). In all, 44/45 neurons had the highest response for the 50% CS. (**C**) Sensitivity indices (Methods) for 45 striatal uncertainty-selective neurons for different behavioral/task variables. Asterisk above the histogram indicates significant deviation from 0 (P<0.01; sign-rank test). Significant individual neuron indices (P<0.01; Wilcoxon rank-sum test) are grey. The number of significant indices is indicated near the histogram.

Overall, the results of experiment 1 showed that the DS contains a subpopulation of neurons with striking sensitivity to objects associated with reward uncertainty. However, several important questions about these neurons remained unclear. First, are they sensitive to the level of uncertainty in a graded manner?[17,18] Second, do U+ neurons signal internal states related to the expectation of reward or are their uncertainty responses dependent on external cues or objects? Third, can U+ neurons support object learning under uncertainty? To answer these important questions, we selectively recorded from U+ neurons in the DS in experiments 2–4.

2.3.2 DS neurons are sensitive to the level of reward uncertainty

To test if U+ neurons were sensitive to the level of reward uncertainty, in experiment 2, we recorded 20 U+ neurons (14 in monkey B and 6 in monkey W) in a behavioral procedure in which monkeys experienced a reward-probability block that contained five objects associated with five probabilistic reward predictions (0, 25, 50, 75 and 100% of 0.25 ml of juice), and a reward-amount block that contained five objects associated with 100% reward predictions of varying reward amounts (0.25, 0.1875, 0.125, 0.065 and 0 ml of juice).[15,16] The expected values of the five CSs in the probability block matched the expected values of the five CSs in the amount block. Reward-uncertainty neurons in DS were identified during online screening as neurons that responded to any of the uncertain conditioned stimuli (25, 50 or 75% reward). The same preselection criteria were used in subsequent experiments in this study and in our previous reports.[17,18]

An example U+ neuron's responses to the 10 CS objects are shown in Figure 2.3A. It responded most strongly to the presentation of the 50% CS object, and less strongly to the presentation of the 25 and 75% CS objects. Moreover, it did not respond to the presentation of objects associated with certain reward predictions (0 and 100% reward CS objects and CS

objects in the reward-amount block). A similar result can be observed across the population of U+ neurons (Figure 2.3B,C). U+ neurons' average response was strongest for the presentation of the 50% CS object. Their responses were weaker for 25 and 75% reward-associated CS objects. On average, there was no significant difference between their responses to the 25% versus 75% CS objects, which have the same level of uncertainty but different expected values. Furthermore, as in experiment 1, during the reward-amount block, the neurons discriminated objects associated with rewards from objects associated with no reward (Figure 2.3C, black trace). In sum, experiment 2 showed that U+ neurons were sensitive to the levels of reward uncertainty.

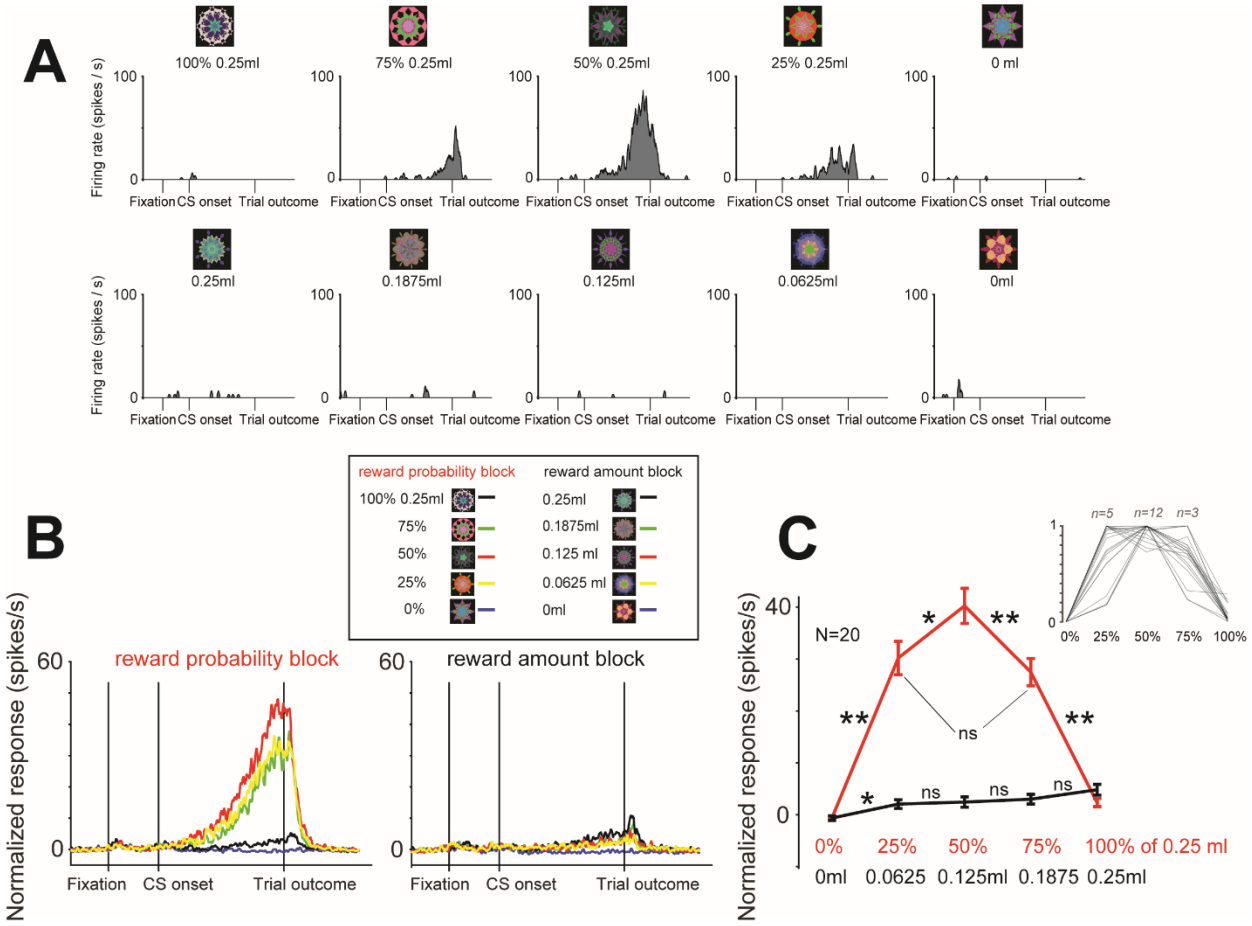

Figure 2.3: (**A**) Responses of a single uncertainty selective (U+) neuron to the presentation of 10 fractal objects associated with certain and uncertain predictions of juice reward. (**B**) Average responses of 20 U+ neurons in the reward-probability block (left) and reward amount block (right). (**C**) Average normalized responses of 20 U+ neurons for probability (red) and amount (black) CSs. Asterisks indicate differences between CSs (**P<0.01; *P<0.025; paired sign-rank test). The inset shows the single neuron's CS responses for different reward predictions in the reward-probability block (normalized to the maximum CS response; from 0 to 1). Numbers above the inset indicate the number of cells that exhibited the greatest response for 25, 50 or 75% CSs; 60% of the neurons exhibited greatest response for 50% reward CS.

2.3.3 U+ neurons are found most often in internal capsule-bordering regions of DS and are likely medium spiny neurons

The location of all recorded U+ neurons is shown in Figure 2.4A. U+ neurons were most often found within the anterior–dorsal putamen and caudate nucleus regions that bordered the internal capsule (Figure 2.4A, Supplementary Figures 2.1-2.2), prominently in the anterior putamen. In addition to reconstructing neuron location by recording sites and depths, we further verified their location using structural MRI. Following the successful recording of a U+ neuron, the electrode was temporarily fixed at the recording site and its tip's location in the target area was imaged (Figure 2.4B). We refer to this brain area as the icbDS. The low baseline discharge rate of U+ neurons (mostly <1 spikes per s; Figure 2.4C) suggests that they are medium spiny neurons[70,74,77,173,174]—the chief output neurons of the striatum.

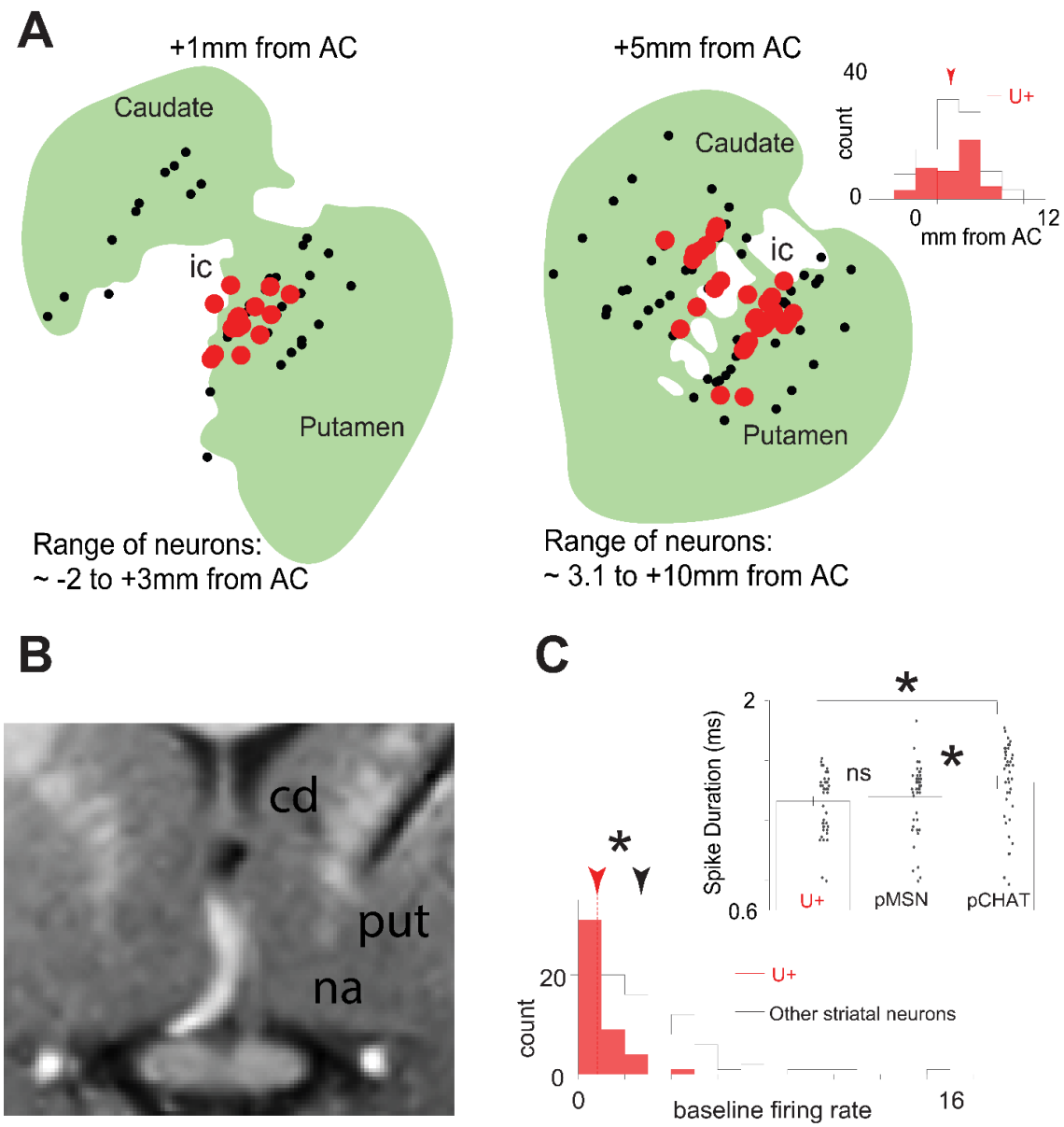

Figure 2.4: (**A**) Estimated locations of 45 U+ neurons (red dots) in the internal capsule bordering striatum shown on two coronal slices. Ranges of the neurons on each slice and the distance of each slice from the center of the anterior commissure (AC) are indicated. Black dots indicate other recorded neurons. Insert is the histogram of recording locations along the anterior-posterior axis. (**B**) A coronal T1 magnetic resonance (MR) image taken with a tungsten electrode at the location of an identified U+ neuron. (**C**) Histogram of baseline firing rates of recorded neurons. Inset shows spike duration (trough-to-trough) for all U+ neurons (left), non-uncertainty-selective putative medium spiny neurons (neurons with a baseline firing rate of < 3 spikes/second), and non-uncertainty-selective putative cholinergic interneurons (CHAT) neurons (neurons with a baseline firing rate >= 3 spikes/second). Error bars indicate standard errors. Single neuron data points are shown as scatters. Asterisks indicate significant differences (Wilcoxian rank sum test; $p < 0.05$).

2.3.4 icbDS uncertainty responses are object-dependent

The results of experiments 1 and 2 are consistent with two possible scenarios. First, U+ responses may signal internal states related to reward expectation, particularly with the expectation of uncertain rewards. A second scenario is that U+ responses may signal the uncertainty of the object–reward associations, rather than the internal state associated with reward uncertainty. To distinguish between these alternatives, monkeys were presented with four CSs (experiment 3). Two distinct CSs were associated with 100 and 50% chances of reward and were kept on the experimental presentation screen for 2.5 s, until the time of the trial outcome (same trial structure as in Figure 2.1A). Two other CSs were also associated with 100 and 50% chances of reward and were present on the screen for 1 s and outcomes were delivered in 1.5 s after the removal of the CSs (the 1.5 s period during which the CS is not present is referred to as a trace period). Therefore, for all CSs, reward was delivered 2.5 s after CS onset. Monkey performance indicated that they understood the procedure and were similarly motivated by trace and no-trace 50% reward predictions (Supplementary Figure 2.5).

We identified U+ neurons in icbDS and recorded their activity in this paradigm (n=32 neurons; 11 in monkey W and 21 in monkey B). An example U+ neuron is shown in Figure 2.5A. This neuron robustly discriminated 50% reward-associated CS object (uncertain condition) from the 100% reward-associated CS object (P<0.01; rank-sum test). Surprisingly, the removal of the uncertain CS (trace condition) before the outcome was delivered completely abolished its uncertainty selectivity (Figure 2.5A, green and blue traces). Similar results were found for most of the U+ neurons (Figure 2.5B). The discriminability of striatal uncertainty signals was greatly diminished when the uncertain object was not present at the time of the outcome (Figure 2.5C). Many U+ neurons' uncertainty signals were completely abolished (Figure 2.5B,C). These results

indicate that U+ neurons' reward-uncertainty responses are related to the presence of the uncertain object.

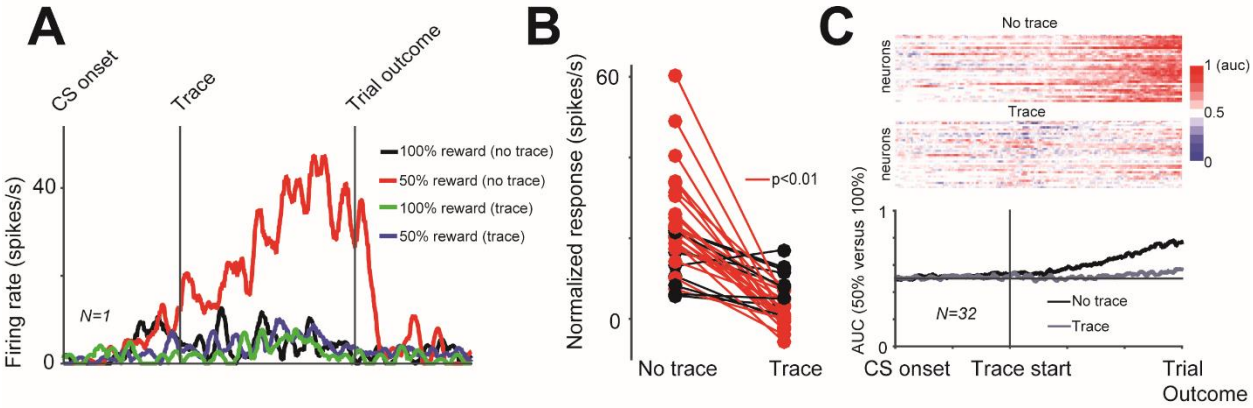

Figure 2.5: (**A**) Responses of a single U+ neuron to 100 and 50% reward predictions without a trace period (CS objects remained until the outcome) (black and red), and with a trace period (CS objects disappeared after 1 s) (green and blue). (**B**) In all, 22/32 neurons displayed significant differences in reward-uncertainty responses across the no-trace and trace conditions (red; rank-sum test; $P<0.01$; 26/32 were significant with a 0.05 threshold). All significant changes were reductions of uncertainty responses. Normalization was performed by subtracting 100% CS responses from 50% CS responses (for trace and no-trace conditions, separately). (**C**) Single neuron (insets above) and population reward-uncertainty discriminability was greatly diminished in the trace condition. AUC, area under receiver-operating characteristic curve.

In the basal forebrain (particularly in its medial regions), some neurons also signal reward uncertainty with ramp-like responses[17], however, additional experiments revealed that their uncertainty-selective signals persist during the same trace-conditioning procedure used to study U+ neurons (Supplementary Figure 2.5). Consistent with this observation, other reward-related signals are preserved during trace conditioning in brain regions that are interconnected with the basal forebrain, such as in the dorsal raphe[175] and in the amygdala.[176] These observations suggest that basal forebrain and related limbic structures signal values and uncertainty of internal states (perhaps somewhat independently of the external environment), whereas the U+ neurons in the basal ganglia signals are related to the presence of cues associated with reward uncertainty.

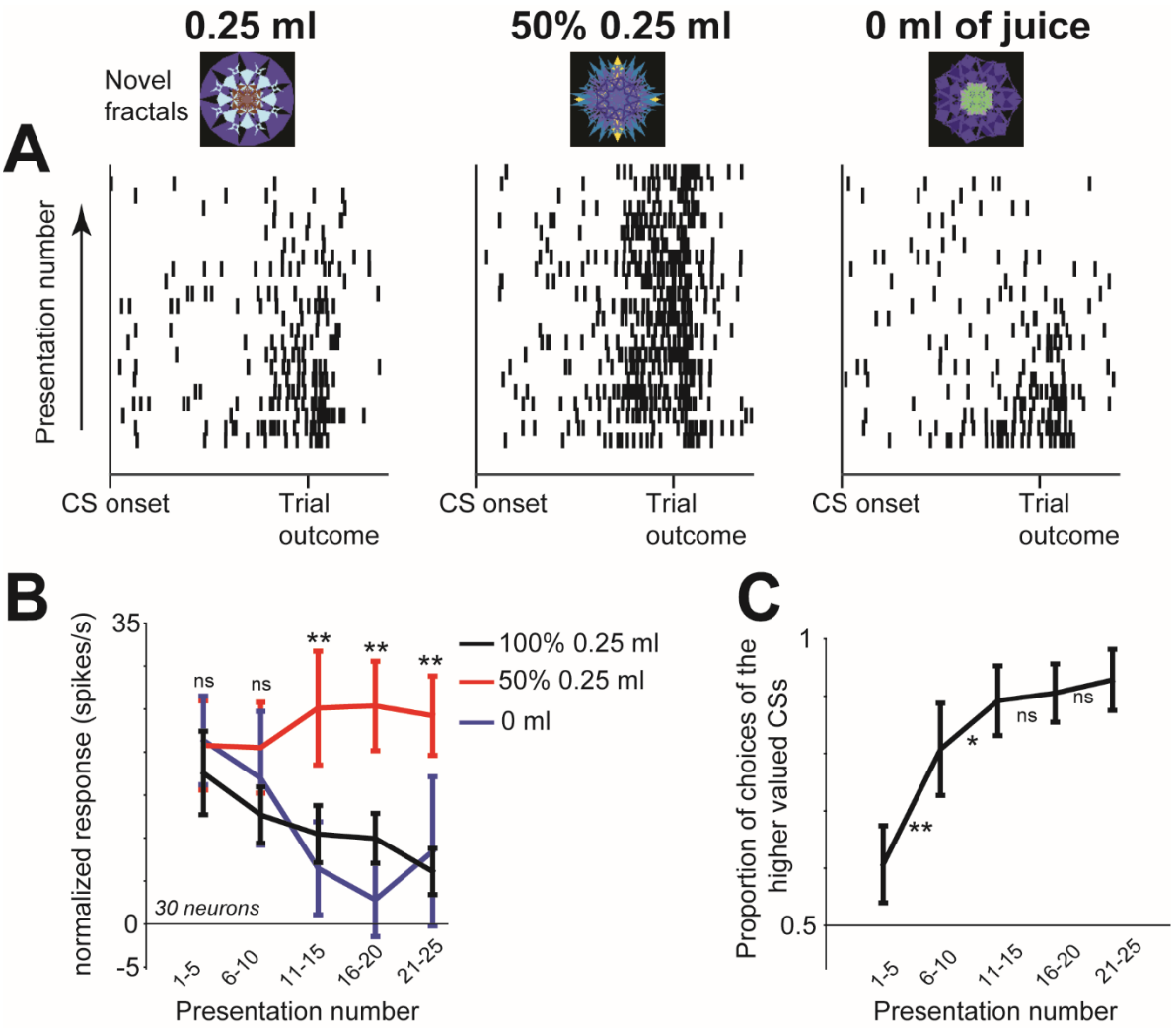

Figure 2.6: (**A**) Single neuron's responses (shown as single trial rasters) to the presentation of three novel objects shown in the order of the monkey's experience (bottom to top). (**B**) Binned neuronal population response across learning (30 learning sessions, 30 neurons) shown separately for 100, 50 and 0% reward-associated novel objects. Asterisks indicate significant variance across the three conditions (P<0.01; Kruskal–Wallis test). Neuronal responses are shown separately for Pavlovian and choice trials in Supplementary Figure 2.6. (**C**) Monkeys' choices during learning. Proportion of choices of the higher-valued fractal CS objects during randomly interleaved choice trials (binned like neuronal activity in **B**). **P<0.01, *P<0.05 (sign-rank test assessing difference between bins).

2.3.5 icbDS uncertainty responses are rapidly shaped by learning

The previous data prompted us to assess how U+ neuronal responses are shaped by the learning of novel object–reward associations (experiment 4). Thus far, we had tested the responses of U+ neurons to reward uncertainty arising from knowledge about reward variability associated with 50% reward CSs (also called known-uncertainty or risk). However, if uncertain object–reward signals in the DS contribute to object learning, then U+ neurons should also signal uncertainty that is due to a lack of previous object–outcome associations (also called ambiguity)- an uncertainty that can be identified and resolved by learning. To test this, we recorded the activity of identified U+ neurons in a Pavlovian procedure in which three novel fractals were used as CSs associated with 100, 50 and 0% reward probabilities (n=30 neurons; 11 in monkey W and 19 in monkey B). One example U+ neuron is shown in Figure 2.6A. At the start of learning, this neuron showed a strong increase in response to all the novel CSs. As the CSs were repeatedly experienced, the neuronal activity started to decrease for certain CSs (0 and 100%) and remained roughly the same for the reward-uncertain CS (50% reward prediction). The population of 30 U+ neurons shows a similar pattern (Figure 2.6B and Supplementary Figure 2.6). The neuronal responses to certain object–reward associations decreased as the monkeys learned (Figure 2.6C). These results demonstrated that U+ neurons signal object–reward uncertainty of unknown or novel objects and that the DS uncertainty responses can be rapidly shaped by learning, even within a single experimental session.

2.4 Discussion

In the caudate–putamen complex we found a population of neurons that signal uncertainty of object–reward associations. These U+ neurons were often found in the icbDS.

Their uncertainty-selective responses depended on the presence of objects associated with reward uncertainty and evolved rapidly as monkeys learned novel object–reward associations. Which brain regions supply reward uncertainty signals to U+ neurons? Their average location in the striatum may provide a clue. U+ neurons were most often found within the anterior putamen and caudate regions that bordered the internal capsule, prominently in the anterior putamen. icbDS receives inhibitory inputs from the ventral pallidum[177], where some neurons are inhibited by reward uncertainty (Supplementary Figure 2.7).[16] Given the uncertainty-excitatory responses of many icbDS neurons (Figure 2.2), we hypothesize that the inhibition of pallidal neurons by uncertainty may open a gate, so that U+ neurons can selectively respond to cortical inputs carrying sensory information about objects[90,108] and about their reward value or uncertainty.[20] Although precisely which cortical regions send uncertainty and other signals to U+ neurons remains to be assessed, recent work has demonstrated the presence of reward-uncertainty responsive cells within regions of anterior cingulate cortex (ACC).[15] Notably, areas of DS that overlap with where we report these U+ neurons receive excitatory inputs from this region of ACC.[48,49,50(p)] The differences in response to uncertainty of ACC and icbDS, however, have yet to be assessed.

The task responses of striatal U+ neurons differentiated them from reward uncertainty-selective neurons in the anterodorsal septum and the medial basal forebrain. For example, during object learning, anterodorsal septal uncertainty-selective neurons responded preferentially to knowledge-based uncertainty (often called risk), after monkeys learned the uncertain stimulus–response association.[18] In contrast, during a similar object-learning task, U+ neurons responded strongly to novel stimuli, whose conditioned stimulus–unconditioned stimulus relationship was not yet learned (Figure 2.6). Unlike U+ neurons, medial basal forebrain reward uncertainty-

sensitive neurons slowly learned to discriminate between certain and uncertain reward-predicting objects.[17] This slow learning was not correlated with the fast time course of the monkeys' object–reward associative learning. [17] These data are consistent with the observation that there are no known connections from the medial basal forebrain or septum to the striatum and suggest that U+ neurons belong to a mostly distinct system for signaling uncertainty of objects that may be particularly well suited to contribute to object learning.

It is noteworthy that U+ neurons did not encode all types of uncertainty, or only uncertainty.[3,18] First, they did not respond to uncertainty about punishments. Second, on average, they discriminated reward-associated CSs from reward-unassociated CSs (Figure 2.2A,C). In fact, similar reward-related tonic activity shifts were observed in other neurons that encode reward uncertainty.[15,16] It remains to be tested whether they are due to context value (or relevance), or if they are due to uncertainty that could exist even during the expectation of 'certain' rewards (for example, due to errors in the estimation of reward timing). Third, U+ neurons' uncertainty responses were abolished by the removal of the CS before the trial outcome (during trace conditioning). This suggests that striatal U+ neurons' responses depended on the presence of the uncertain CS object. This finding further differentiated striatal U+ neurons from uncertainty-enhanced neurons in the medial basal forebrain whose uncertainty selectivity persisted when the CS object was removed before the trial outcome (Supplementary Figure 2.5).

Our study in monkeys and a previous human brain-imaging study[10] suggest that icbDS is a prominent node for processing information about reward uncertainty. However, it is possible that there are other striatal mechanisms for signaling uncertainty, and/or for integrating uncertainty with stimulus-feature information, movement kinematics and values.[178,179] Indeed, different areas of the primate striatum learn and signal values in distinct manners[73,76,78,79,106,178–

[181] to support their different roles in action, decision-making, and learning and memory.[48,49,73,76,77,79,90,106,178,179,182] How uncertainty guides computations across different striatal subregions must therefore be an important direction of future studies. Objects in the environment are important because they signal rewards or dangers, or because they represent an opportunity to learn and change one's state. In this study, we showed that the basal ganglia signals reward uncertainty of object–reward associations—a critical variable for monitoring and learning from objects. These results demonstrate a novel role for internal-capsule bordering putamen and caudate in controlling behaviors in uncertain contexts.

2.5 Supplementary material

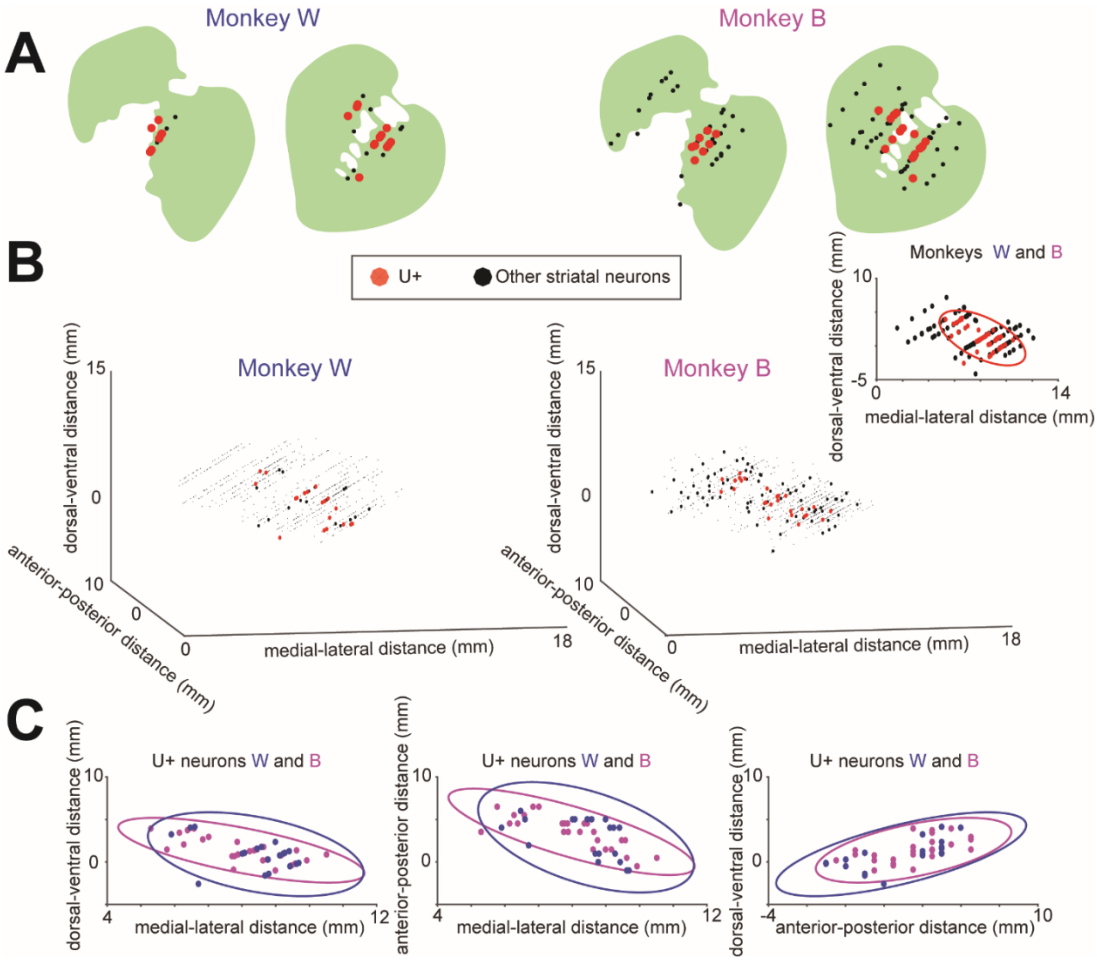

Supplementary Figure 2.1: Supplementary information about the location of U+ neurons (**A**) Estimated locations of U+ neurons (red dots) in the internal capsule bordering striatum shown on two coronal slices for each monkey. Formatting, anterior-posterior ranges of the neurons on each slice, and the distance of each slice from the center of the anterior commissure (AC) are as in Figure 2.4. (**B**) Three dimensional scatters of neuronal locations relative to the center-top of the AC. Red dots – U+, Black dots – other recorded striatal neurons, small black dots – neurons that were encountered (but not recorded) during experiments to map the extent of the caudate and putamen and to verify locations of the internal capsule and AC. Inset – locations of recorded neurons from two monkeys shown in two planes (medial-lateral versus dorsal-ventral) relative to the center-top of the AC. 95% confidence ellipse (red) around the U+ neurons includes 44 U+ neurons and 65 other recorded striatal neurons; 13 of those 65 neurons displayed significant correlations with the expected reward values of the CSs (correlations were assessed as relationship between the size of expected rewards in the reward amount block and neuronal activity during the CS epoch; Spearman's rank correlations; $p<0.05$; tested using a permutation test; 10,000 shuffles). (**C**) U+ neurons shown for two monkeys separately (magenta and blue) relative to the center-top of the AC. Each plot compares two different anatomical planes. 95% confidence ellipses of the two monkeys in all planes were highly overlapped.

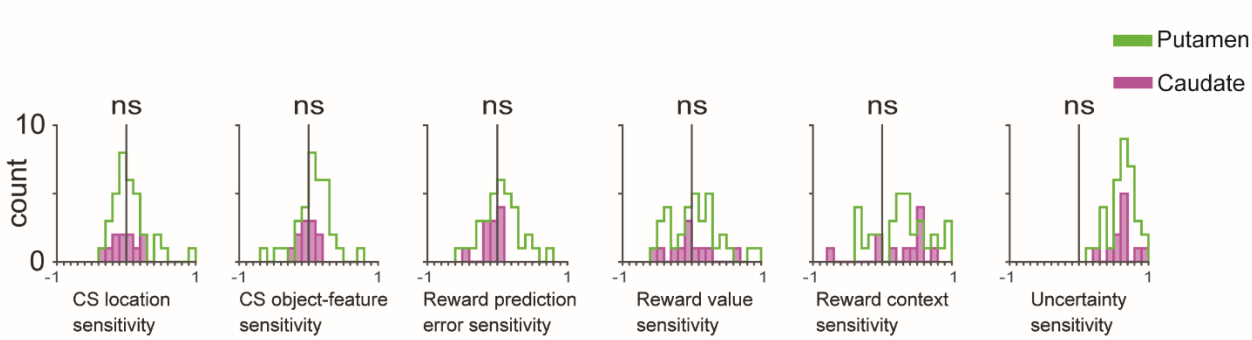

Supplementary Figure 2.2: Sensitivity indices comparing U+ neurons in the putamen versus caudate nucleus. Sensitivity indices (same as in Figure 2.2) are shown separately for putamen and caudate U+ neurons. There were no significant differences between neuronal task-responses amongst populations of putamen and caudate U+ neurons (ns; Wilcoxon rank sum test).

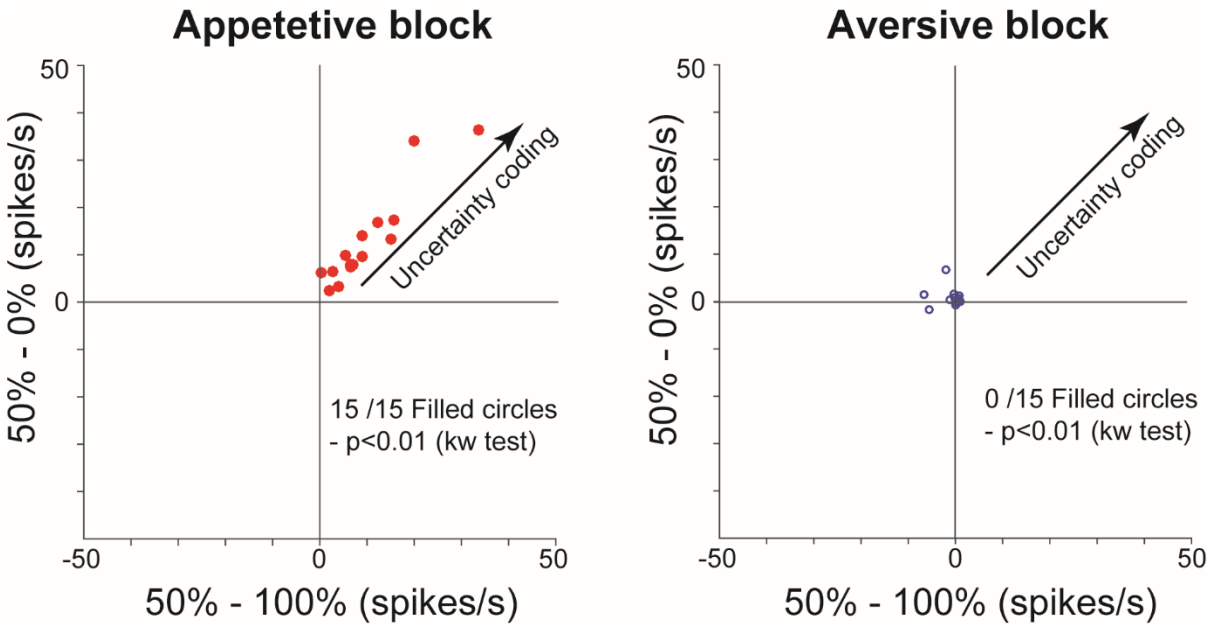

Supplementary Figure 2.3: U+ neurons' responses in the Appetitive-Aversive procedure. For each neuron (indicated by a circle; n=15; Monkey B), we plotted the differences in response magnitude between 50% reward CS and 100% reward CS (x-axis) and between 50% CS and 0% reward CS responses (y-axis). The responses in the appetitive and aversive blocks are shown separately (left and right). Filled circles indicate neurons that displayed significant variability across the 3 reward (left) or punishment (right) predicting CSs (Kruskal-Wallis test; $p<0.01$)

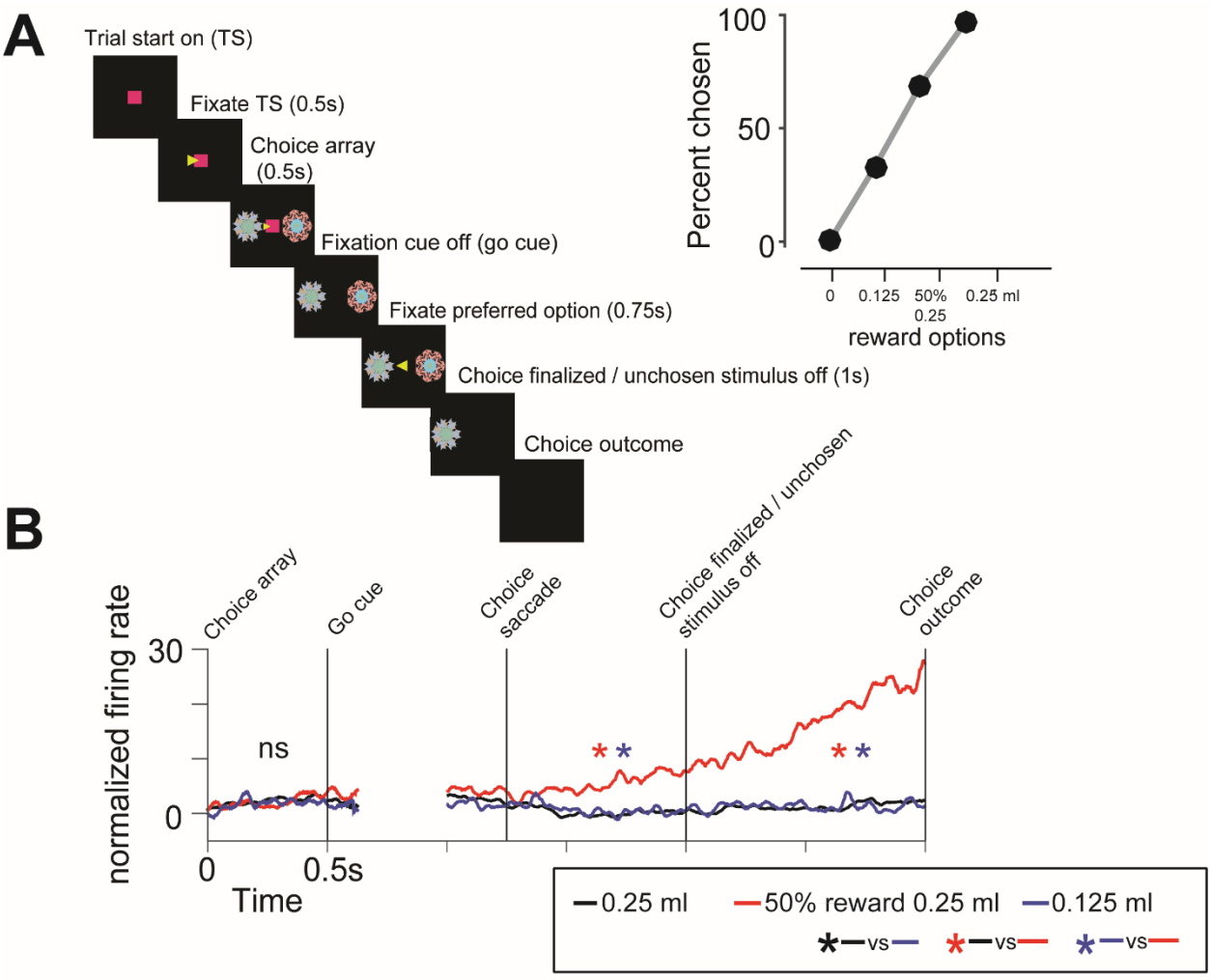

Supplementary Figure 2.4: U+ neurons' responses during choice. **(A)** Choice-trial structure (left) and the monkeys' choice behavior (right). Monkeys made a choice between two CSs among the six well-learned CSs (three indicating reward amounts, and three indicating reward probabilities). The inset shows the proportion of trials the monkeys chose 0, 0.125, 50% 0.25, and 0.25 CSs over all other CSs. **(B)** Average normalized neuronal responses of U+ neurons during choice trials sorted by the monkeys' choices. Specifically, neuronal activity was sorted into trials in which the monkey chose the object associated with 0.25 ml of juice, (black), the object associated with 50% of 0.25 ml of juice (red), or 0.125 ml of juice (blue). Asterisks above task epochs indicate statistical differences amongst the 3 trial types (first Kruskal Wallis test $p<0.01$ across three trial types, then Wilcoxon rank sum tests; $p<0.01$; inset shows the meanings of asterisk color). Normalization was done by subtracting the average activity during trial start fixation epoch.

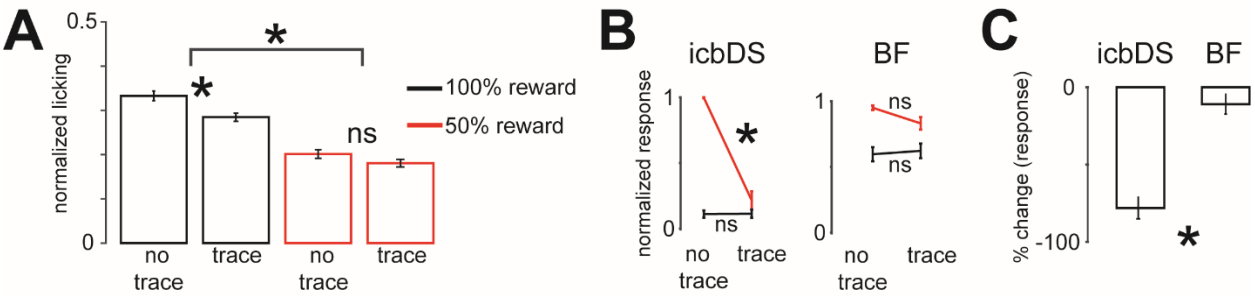

Supplementary Figure 2.5: Trace conditioning: behavior and comparison of striatum and basal forebrain U+ neurons' responses **(A)** Licking behavior of two monkeys during trace conditioning (measured from CS presentation to outcome). The licking behavior during 50% reward trace and non-trace trials was not significantly different ($p>0.05$). Asterisks indicate significant differences ($p<0.05$; Wilcoxon rank sum test). Error bars denote standard error. **(B)** Comparison between ramping uncertainty selective neurons in the icbDS and the medial basal forebrain (BF). Average normalized responses of icbDS U+ neurons (left; n = 32) and BF uncertainty selective neurons (right; n=17) during trace and no-trace conditions. Responses are shown for 100% (black) and 50% (red) CSs separately. Asterisk denotes significant change (sign rank test; $p<0.05$). **(C)** Uncertainty response % change (trace versus no-trace) for icbDS and BF. Asterisk denotes significant difference (Wilcoxon rank sum test; $p<0.05$).

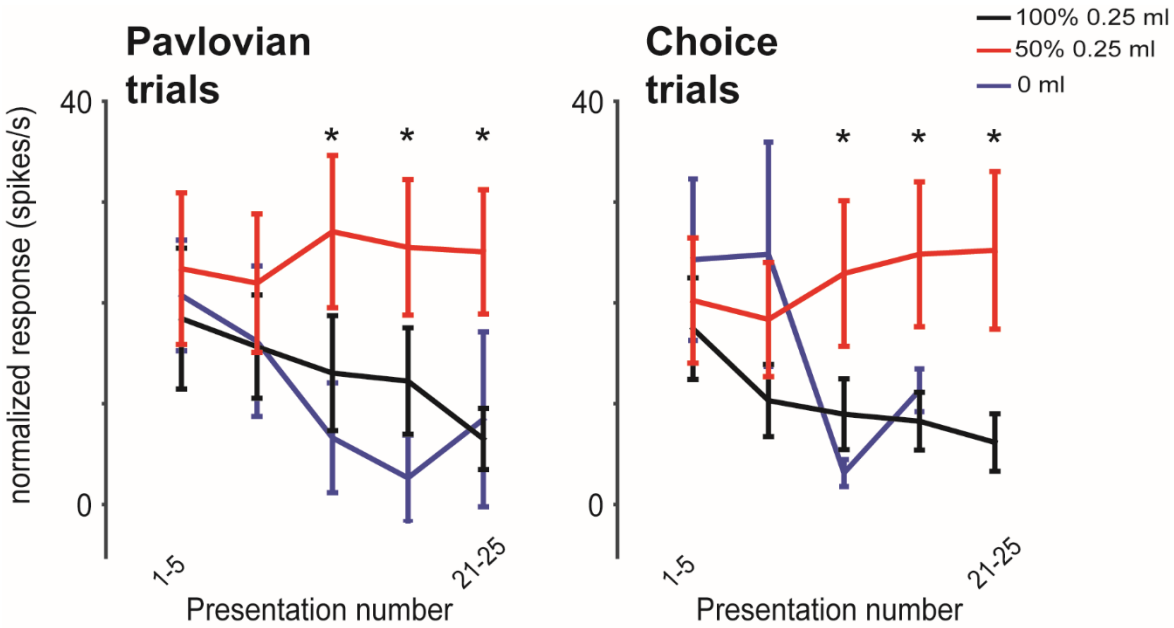

Supplementary Figure 2.6: U+ neurons' responses during learning for Pavlovian and choice trials. Binned neuronal population response across learning (30 learning sessions) shown separately for 100, 50, and 0% reward associated novel objects. Asterisks indicate significant variance across the three conditions ($p<0.05$; Kruskal-Wallis test).

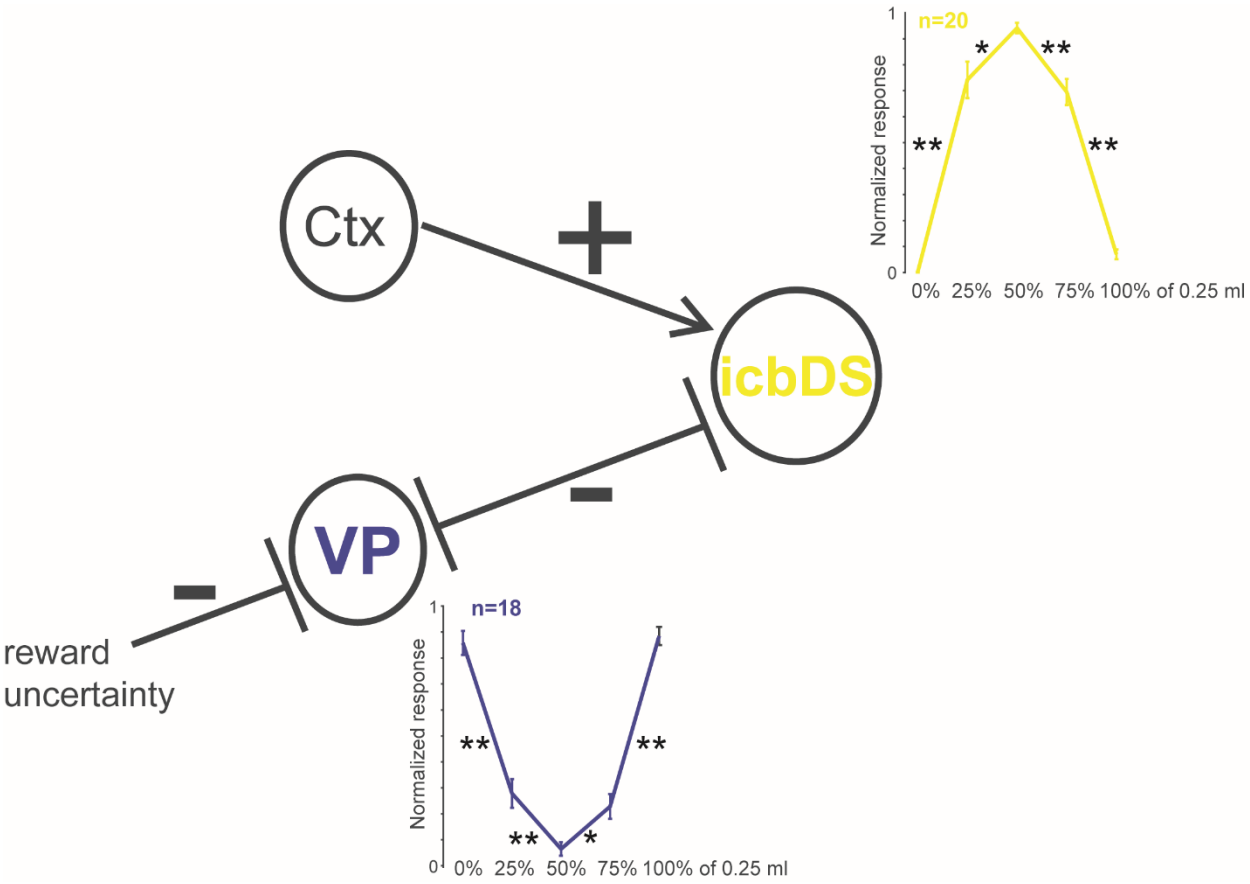

Supplementary Figure 2.7: The ventral pallidum as one source of uncertainty signals in the striatum. The ventral pallidal regions are known to send inhibitory projections to icbDS. These regions contain uncertainty-suppressed neurons (Ledbetter, Chen, Monosov, 2016; Journal of Neuroscience). Here, we present a schematic of a hypothetical gating of icbDS by pallidal inputs. When the pallidum is inhibited by uncertainty, cortical inputs can further shape and drive the icbDS response. We recorded the activity of 23 uncertainty-sensitive neurons in the ventral pallidum while two monkeys (B and W) experienced familiar/over-trained CSs associated with 0, 25, 50, 75, and 100 % chance of reward delivery (same as in Experiment 2). 18 neurons were suppressed by uncertainty, 5 were enhanced. Consistent with the proposed circuit, we found that the average CS responses of the 18 VP uncertainty-suppressed neurons (blue) form approximately an inverted mirror image of the response function of icbDS U+ neurons (shown in yellow). ** - $p < 0.01$ (sign rank test); * - $p<0.025$ (sign rank test).

Chapter 3: A primate neural network that controls information seeking

Adapted from:
J. Kael White*, Ethan S. Bromberg-Martin*, Kaining Zhang, Julia Pai, Sarah H. Heilbronner, Suzanne N. Haber, Ilya E. Monosov. *A neural network for information seeking.* (in review)
**denotes shared first authorship and equal contribution to the manuscript*

Humans and other animals often express a strong desire to know the uncertain rewards their future has in store, even when there is no way to use this information to influence the outcome.[23,26,28,29,31,171,183] However, while much is known about how the brain predicts rewards after information has been received[184], it is unknown how the brain predicts information itself, and how such neural predictions motivate information seeking behavior. Here we show that neurons in a network of interconnected subregions of the primate anterior cingulate cortex and basal ganglia predict the moment of gaining information about uncertain future rewards. We demonstrate that animals preferentially direct their gaze at objects that resolve uncertainty and that pharmacological disruptions of this network reduce the motivation to seek information. These findings demonstrate a novel cortico-basal ganglia mechanism responsible for motivating actions to resolve uncertain situations by seeking knowledge about the future.

3.1 Introduction

Stimuli do not often predict outcomes with absolute certainty. As such, humans and nonhuman animals have evolved complex nervous systems which can make predictions about future outcomes and adjust behaviors to seek information that can resolve uncertainty about these predictions. By seeking information that reduces uncertainty about the future, animals can maximize the value of interacting with environmental objects. Therefore, a mechanism for

signaling when uncertainty surrounding an outcome will be resolved and for directing behavior towards seeking information that reduces uncertainty could be useful in complex environments. Information-seeking behavior has been demonstrated in a range of species. Interestingly, findings in both humans[185] and nonhuman primates[26–28] demonstrated that the brain screens for opportunities to resolve uncertainty by obtaining information. Further, these representations are present in areas of the brain implicated in reinforcement learning and motivational control[26,27] and signals in these areas produce information prediction errors[26] much like the reward prediction errors which in-part guide reward-seeking behaviors.[34,186–188] Interestingly, advance information about the delivery of future reward is valued enough that humans[31] and nonhuman animals[28] will sacrifice levels of this reward in order to obtain this information. Despite its importance to survival and its value to human and nonhuman subjects alike, little is known about how and where in the brain information is valued and where information-seeking behaviors are promoted.

Insight into how this may be accomplished comes from research investigating how the brain promotes reward-seeking behaviors. The brain has populations of neurons which encode RPEs[35,37] and help guide behaviors towards primary rewards.[32,36,189] The activity of these cells is sustained from when the reward is first predicted and ramps to the expected time of reward delivery.[184] In many cases, these reward prediction signals were directly linked to online reward-seeking behavior; the strength of these signals are correlated to reward-seeking behaviors[77,190–192] and disrupting the signals alters reward seeking.[193,194]

But what are the requirements for a neural network to motivate behavior towards information-seeking behavior? It must (A) monitor the level of uncertainty about future events, (B) anticipate the time when information will become available to resolve the uncertainty, and

(C) causally motivate behavior to obtain information. Here we demonstrate that these criteria are met by an anatomically interconnected network comprising three areas of the primate brain: ACC and two subregions of the basal ganglia (BG), the internal-capsule-bordering portion of the dorsal striatum (icbDS) and the anterior pallidum including anterior globus pallidus and the pallidum (Pal).

3.2 Materials and methods

3.2.1 General procedures

Four adult male rhesus monkeys (*Macaca mulatta*) were used for behavioral, recording, and inactivation experiments (Animals B, R, Z, and W). All procedures conformed to the Guide for the Care and Use of Laboratory Animals and were approved by the Washington University Institutional Animal Care and Use Committee. A plastic head holder and plastic recording chamber were fixed to the skull under general anesthesia and sterile surgical conditions. The chambers were tilted laterally by 35-40° and aimed at the anterior cingulate and the anterior regions of the basal ganglia. After the animals recovered from surgery, they participated in the experiments.

3.2.2 Data acquisition

While the animals participated in the behavioral tasks we recorded single neurons in the anterior cingulate cortex, internal capsule-bordering regions of the dorsal striatum, and anterior pallidum including the ventral pallidum and the anterior-most part of the globus pallidus internal segment. Electrode trajectories were determined with 1 mm-spacing grid system and with the aid of MR images (3T) obtained along the direction of the recording chamber. This MRI-based estimation of neuron recording locations was aided by custom-built software (PyElectrode[195]). In addition, in order to further verify the location of recording sites, after a subset of experiments

the electrode was temporarily fixed in place at the recording site and the electrode tip's location in the target area was verified by MRI (Figure 3.1).

Single-unit recording was performed using glass-coated electrodes (Alpha Omega). The electrode was inserted through a stainless-steel guide tube and advanced by an oil-driven micromanipulator (MO-97A, Narishige). Signal acquisition (including amplification and filtering) was performed using Alpha Omega 44 kHz SNR system. Action potential waveforms were identified online by multiple time-amplitude windows with an additional template matching algorithm (Alpha-Omega). Neuronal recording was restricted to single neurons that were isolated online. Neuronal and behavioral analyses were conducted offline in Matlab (Mathworks, Natick, MA).

Eye position was obtained with an infrared video camera (Eyelink, SR Research). Behavioral events and visual stimuli were controlled by Matlab (Mathworks, Natick, MA) with Psychophysics Toolbox extensions. Juice, used as reward, was delivered with a solenoid delivery reward system (CRIST Instruments). Juice-related licking was measured and quantified using previously described methods.[15]

3.2.3 Behavioral tasks

We analyzed data recorded from several behavioral tasks which can be grouped into three major categories: standard uncertainty tasks, information viewing task (used for recording), and information seeking task (used for inactivations).

3.2.3.1 Standard uncertainty tasks

These tasks are described in detail in previous work.[15,18] They each used a distinct set of fractal visual CSs with different associated outcomes. However, they all shared the following general outline. Animals were presented with a small white circular trial start cue at the center of

the screen. In some tasks animals were required to fixate the trial start cue for a fixed duration (typically 0.5-1 s) for the trial to continue; if they failed to fulfill this requirement within a grace period (typically 5 s) the trial would be considered an error, they would receive a timeout, and the trial would repeat. In other tasks animal were not required to fixate the trial start cue; it was simply shown for a fixed duration (typically 1 s). After the trial start period, the trial start cue disappeared and a fractal visual conditioned stimulus (CS) appeared on the screen for a fixed duration (2.5 s). The CS was randomly positioned at one of three locations: the center of the screen, the left side of the screen, or the right side of the screen (at 10 or 12.5 degrees eccentricity). In some sessions only the left and right locations were used. Animals were not required to gaze at or interact with the CS in any way. At the end of the CS period, the CS disappeared and simultaneously the trial's outcome was delivered. Finally, there was an inter-trial interval during which the screen was blank (typically randomized between 1-8 s, with different durations for different animals and tasks). In some sessions, a small fraction of inter-trial intervals included the unexpected presentation of different salient events, which could be appetitive (juice), aversive (an airpuff, ~35 psi, delivered through a narrow tube placed ~6-8 cm from the face[15]), or audiovisual (an auditory tone sounding and the screen flashing white).

The standard uncertainty tasks primarily differed in their CSs, outcomes, and block structure:

- Task A[15]: Trials were presented in two distinct blocks. In the Probability block, there were five CSs associated with 0, 25, 50, 75, and 100% probabilities of 0.25 mL juice. In the Amount block, there were five CSs associated with 100% probability of 0, 0.0625, 0.125, 0.1875, and 0.25 mL juice. Hence for each CS in the Probability block there was a matched CS in the Amount block that was associated with an identical mean amount of juice, but for which the outcome was certain rather than probabilistic. Each block

consisted of 20 trials (4 presentations of each of its 5 CSs, shuffled in a randomized order). The two blocks were presented repeatedly in an alternating manner, with each block continuing until its 20 trials were correctly completed and then immediately transitioning into the other block.

- Task B[16]: Same as task A, except it used three Probability CSs (0, 50, 100%) and the three corresponding Amount CSs (0, 0.125, 0.25 mL), and each block consisted of 6 or 9 trials (2 or 3 presentations of each of its 3 CSs). In some sessions, blocks also included interleaved choice trials in which two CSs were presented and animals were allowed to choose between them with a saccade; our analysis here is of non-choice trials.
- Task C[15]: Trials were presented in two distinct blocks. In the Appetitive block, there were three CSs associated with 0, 50, and 100% probabilities of 0.4 mL juice. In the Aversive block, there were three CSs associated with 0, 50, and 100% probabilities of airpuffs. Each block consisted of 12 trials (4 presentations of each of its 3 CSs).
- Task D[15]: There were 9 CSs. Four CSs were associated with 25, 50, 75, and 100% probabilities of 0.4 mL juice. Four other CSs were associated with 25, 50, 75, and 100% probabilities of airpuff. One final CS was associated with no outcome (i.e. 0% probability of both reward and airpuff). The CSs were presented in a pseudorandom order.
- Task E: Three CSs were associated with 0, 50, and 100% probabilities of 0.25 mL juice. The CSs were presented in a pseudorandom order.

3.2.3.2 Information viewing task

This task began with the appearance of a small circular trial start cue at the center of the screen which animals were required to fixate for a fixed duration (typically 0.5 or 1 s). The trial start cue then disappeared and was followed in succession by a CS that was displayed for a fixed

duration (typically 1 s), which was then replaced by a cue at the same location that was displayed for a fixed duration (typically 2 s). The cue then disappeared, and simultaneously the outcome was delivered. The trial then completed with a 1 s inter-trial interval. The CSs were presented randomly on either the left or right side of the screen (10 degrees eccentricity). There were three *Info CSs* that yielded juice reward (0.25 mL) with 0, 50, and 100% probabilities, and were followed by one of two informative cues whose color indicated the trial's outcome (Figure 3.3A). There were three analogous *Noinfo CSs* that also yielded juice reward with 0, 50, and 100% probabilities, but which were followed by one of two non-informative cues whose colors were randomized on each trial and hence did not convey any information about the trial's outcome (Figure 3.3A). In some sessions Noinfo CSs were followed by a single non-informative visual cue. There was no apparent difference in behavior or neural activity between sessions with one or two non-informative cues; hence their data was pooled. The 6 total CSs were presented in a pseudo-random order.

3.2.3.3 Information seeking task

This task also began with animals fixating a trial start cue for a fixed duration, followed by a CS presented randomly on either the left or right side of the screen. However, the trial start cue remained visible for a fixed duration after CS onset during which animals were required to maintain fixation on the trial start cue (typically for 1 s in animal B, 0.25 s in animal R, and 0.5 or 1 s in animal Z). Fixation breaks were treated as errors: the screen went blank, there was a 1-2 s penalty delay period, and then the trial repeated from the beginning. After the fixation period, the trial start cue disappeared, and animals were free to move their eyes. The task then detected the first moment when animals gazed at the CS, defined as the eye position entering a square window centered on the CS (i.e. when horizontal and vertical eye positions were within 4° of the

center of the CS). If animals gazed at an Info CS it was immediately replaced with the appropriate informative cue; if they gazed at a Noinfo CS it was immediately replaced with a non-informative cue; if they did not gaze at a CS, no cue was shown. Importantly, regardless of their gaze behavior, all stimuli disappeared and the outcome was delivered at the same, fixed time after CS onset on all trials in the session (typically 3 s). Thus, gazing at the CS gave animals access to the cues but did not give them earlier access to the juice reward. In the version of the information seeking task used for inactivation experiments and controls, there were only two CSs – an Info CS and a Noinfo CS – that were both associated with 50% probability of 0.25 mL juice reward. By ensuring that the probability, amount, and timing of juice reward were identical for all CSs on all trials, we minimized the possibility that gaze behavior to the CSs could be influenced by different reward expectations or reward prediction errors induced by CS onset.

In some sessions, neurons recorded using the information viewing task were also recorded in interleaved trials or in separate blocks with a version of the information seeking task. These information seeking trials were indicated to the animal by a distinct green color of the trial start cue (Figure 3.7A). These trials also used six CSs: Info and Noinfo CSs associated with 0, 50, and 100% reward probability. These six fractal CSs on information seeking trials were visually identical to the analogous six fractal CSs used for information viewing trials. Information-related neural responses in these information seeking trials were typically similar to activity in information viewing trials (e.g. activity ramping up to the time the informative cue would become available and to the time a non-informed outcome would be delivered). Note, however, that the task design of information seeking trials induced a link between gaze and receipt of information: gaze behavior was not completely 'free' because it was required if the animal wanted to produce the cue, and the cue appeared with variable timing depending on the animal's

behavior. Therefore, to be conservative, data from the information seeking trials was only included in our analysis of information signals (Figure 3.4) in a small number of neurons for which no data from information viewing trials was available (n=4 ACC neurons in monkey Z).

Analysis of neural activity in Figure 3.2 and Supplementary Figures 3.1-3.2 uses data from all neurons recorded using standard uncertainty tasks in which CSs were associated with all five reward probabilities (tasks A and D). Analysis of neural activity during information tasks (Figure 3.4) uses data from neurons recorded using an information task.

3.2.4 Muscimol injections

On *muscimol injection* sessions, a 33-gauge cannula was inserted through a 23-gauge guide tube into a grid hole and to a depth previously identified to be in icbDS or Pal and to contain information-related neurons (Supplementary Figure 3.3). The other end of the cannula was connected to a 10 µL Hamilton syringe. Behavioral data from the information seeking task were collected in blocks of 70-150 correct trials. Before the injection we collected a 'pre-injection' behavioral data set from the animal performing the information seeking task, typically for one block (median: 96 correct trials, standard deviation: 24, range: 48-164). After recording the baseline data, we used a manual syringe pump (Stoelting) or automated syringe pump (Harvard Apparatus) to inject muscimol dissolved in saline. Muscimol concentrations were 8 mg/mL, injection rates were typically 0.1 µL/min (range: 0.09-0.2), and injection volumes ranged from 1.0-2.5 µL in icbDS and 0.545-1.4 µL in Pal. After each injection we collected a 'post-injection' behavioral data set (median: 303 correct trials, standard deviation: 157, range: 43-839). All pre- and post-injection blocks of data were included in our analysis regardless of the animal's response times or other gaze behavior, as long as the animal remained engaged in the task (i.e. generally initiating trials quickly and performing them correctly). On two sessions pre-

injection data from the same day was not available, so we used the first block of behavioral data collected from the same animal on days immediately before or after the session to obtain a comparable baseline. On *saline injection* control sessions, the same procedure was followed except that only the saline vehicle was injected (with the same volumes previously used for muscimol injections). On *sham* control sessions, the same procedure was followed (including pauses in procedure to simulate setting up the cannula, advancing the cannula, performing the injection, etc.), except no cannula was inserted and no injection was given.

3.2.5 Data analysis

Neurons recorded in the standard uncertainty tasks were included in our dataset if they showed significant responsiveness to uncertainty (activity on uncertain reward CS trials significantly different from both 0% reward CS trials and 100% reward CS trials, rank-sum tests, both $p < 0.05$ and both differences with the same sign). For this purpose, activity was measured in a broad time window encompassing the CS period to avoid making any assumptions about the time course of neural responses (0.1-2.5 s after CS onset). The neuron's sign of uncertainty coding was defined as +1 if its ROC area for discriminating between uncertain reward CS trials vs pooled data from 0% and 100% reward CS trials was > 0.5, and defined as -1 if its ROC area was < 0.5. Similarly, to avoid making any assumptions about the nature or time course of information-related signals, all neurons recorded in the information tasks were included in our dataset if they were classified online as potentially uncertainty responsive based on their activity on Noinfo trials or during any other uncertainty-related task. The neuron's sign of uncertainty coding was defined in the same manner as in standard uncertainty tasks, using activity from Noinfo trials in a 0.5 s window before outcome onset.

Neural activity was converted to normalized activity as follows. Each neuron's spiking activity was smoothed with a causal exponential kernel (mean = 30 ms) and then z-scored and sign-normalized using the following procedure. The neuron's average activity timecourse aligned at CS onset was calculated for each condition (defined here as each combination of CS and cue). These average activity timecourses from the different conditions were all concatenated into a single vector, and its mean and standard deviation were calculated. Henceforth, all future analyses converted that neuron's firing rates to normalized activity by (1) subtracting the mean of that vector, (2) dividing by the standard deviation of that vector, (3) multiplying by the neuron's sign of uncertainty coding. Thus, normalized activity of +1 in a given task condition means that the neuron's firing rate deviated away from its average firing rate in the same direction that it responded to uncertainty, by an amount equivalent to 1 SD of its overall distribution of average firing rates during the task.

Neural uncertainty signals were calculated in specific time windows (e.g. pre-cue, pre-outcome, etc.) as the ROC area for distinguishing activity on uncertain reward CS trials (25, 50, and 75%) from pooled data from 0% and 100% certain reward trials. In the information viewing task uncertainty signals were calculated separately for Info and Noinfo trials. To visualize their timecourses, they were calculated on neural activity at millisecond resolution after activity was smoothed with a gaussian kernel (SD = 50 ms) and sign-normalized based on the neuron's sign of uncertainty coding on Noinfo trials in a 0.5 s pre-outcome window (Figure 3.4). The Info Cue Anticipation Index was defined as the difference between its uncertainty signal for Info and Noinfo trials in a 0.5 s pre-cue time window. Hence the index was positive if a neuron had a higher uncertainty signal in anticipation of Info CSs, and negative if a neuron had a higher uncertainty signal in anticipation of Noinfo CSs. The Uncertain Outcome Anticipation Index was

defined as the difference between its uncertainty signals computed on two different time windows on Noinfo trials: a 0.5 s pre-outcome window, and a 0.5 s post-cue window (0.15-0.65 s after cue onset). Hence the index was positive if a neuron's uncertainty signal grew more positive between the cue and outcome, and negative if it grew more negative between the cue and outcome. Neurons were classified as information-responsive if their Info Cue Anticipation Index was significantly different from 0 ($p < 0.05$, permutation tests conducted by comparing the index calculated on the true data to the distribution of indexes calculated on 20000 permuted datasets that shuffled the assignment of trials to Info and Noinfo conditions). Neurons were classified as having a significant Uncertain Outcome Anticipation Index using the analogous permutation test ($p < 0.05$, shuffling the assignment of data to the post-cue and pre-outcome time windows). For analysis of information-oriented gaze behavior, the same two indexes were calculated for each neuron except that instead of using neural data they used the behavioral gaze data (equal to 1 for milliseconds when the animal's gaze was classified as being in the stimulus window and 0 otherwise). Finally, to plot the timecourse of uncertainty signals from the population including neurons with different signs of uncertainty coding, the normalized uncertainty signal (Figure 3.4F) was defined as the 'absolute' ROC area, i.e. as 0.5 + |Uncertainty signal – 0.5|. Thus if the uncertainty signal was excitatory (> 0.5) it was left intact, while it was flipped to become > 0.5 if it was inhibitory (< 0.5).

Latency of uncertainty coding. Each neuron's smoothed normalized activity aligned at CS onset was further smoothed with a 101 ms causal boxcar kernel and then tested at each millisecond after CS onset for whether it met the following criteria: (1) highly significant ROC area for distinguishing pooled data from uncertain reward CSs from the certain 0% reward CS ($p < 0.005$), (2) highly significant ROC area for distinguishing pooled data from uncertain reward

CSs from the certain 100% reward CS ($p < 0.005$); (3) both ROC areas have the same 'sign' (i.e. both > 0.5 indicating activation by uncertainty or < 0.5 indicating inhibition by uncertainty). A neuron's uncertainty coding latency was defined as the first millisecond after which it met these criteria for at least 24 consecutive milliseconds. See Supplementary Figure 3.1 for the latencies and full ROC timecourses in all neurons with detected latencies. This method was chosen to produce latencies that resemble those seen in raw traces of neural activity, but the same key result (i.e. Pal having shorter latency than ACC and icbDS) was found with other latency detection methods (e.g. different smoothing methods, significance criteria, required number of consecutive time bins,etc). Each area's latency was defined as the 1st percentile of its distribution of single neuron latencies, and areas were compared by testing whether the difference between their latencies was significantly different from that expected by chance ($p < 0.05$, permutation test, conducted by comparing the latency difference calculated on the true data to the distribution of latency differences calculated on 20000 permuted datasets that shuffled the assignment of neurons between the two areas being compared).

Rough vs graded uncertainty coding. In standard uncertainty tasks, a neuron's rough uncertainty activity was calculated as the difference in normalized activity between pooled data from all uncertain reward CSs and pooled data from the certain 0% and 100% reward CSs. Its graded uncertainty activity was calculated as the difference in normalized activity between data from the uncertain 50% reward CS and pooled data from the uncertain 25% and 75% reward CSs. Neurons were classified as having significant graded uncertainty coding if their graded uncertainty activity was significantly different from 0 ($p < 0.05$, rank-sum test). Areas were classified as having graded uncertainty coding if the number of neurons with significant graded coding was significantly different from chance levels ($p < 0.05$, binomial test).

Quantification of information seeking behavior during inactivations. Response times (RTs) were computed online and used to determine when the CS was replaced by the cue, defined as the time between the 'go' signal (i.e. the trial start cue's disappearance) and the gaze entering the response window around the CS. To improve the accuracy of RT measurements for our offline analysis, RTs were recomputed offline using response windows that were corrected for session-to-session variability in eye tracker settings using the procedure described above (i.e. centering the window on the observed peak gaze location separately for each CS location and each session). We then analyzed the RTs from all correctly performed trials in which the animal made a response and there was at least rough agreement between the online and offline RTs (i.e. within 0.2 s of each other). These criteria were met by nearly all correctly performed trials (n=17968/18035; 99.6%). We then quantified the information seeking bias using an Infobias Index based on the mean RTs for the Info and Noinfo CSs:

Infobias Index = (Noinfo RT – Info RT) / (Noinfo RT + Info RT)

The Infobias Index was computed separately for each session, and separately for each of the 2 x 2 combinations of time in session (pre- vs post-injection) and CS location relative to injection site (contralateral vs ipsilateral). We then derived two additional measures. For session and each CS location, we defined the change in Infobias index as the difference between post-injection and pre-injection Infobias indexes. We defined the change in Infobias laterality as the difference between the changes in Infobias Index for the contralateral and ipsilateral sides.

To test whether icbDS and Pal inactivations affected information seeking behavior (Figure 3.7C), we computed the mean change in Infobias index and tested whether it was significantly different from zero ($p < 0.05$, permutation test conducted by comparing the true mean change in Infobias Index to the distribution of mean changes in Infobias Index computed

on 20000 permuted datasets in which pre- and post-injection data were shuffled with each other). For pooled data from all inactivation sessions and for control sessions (Figure 3.7C) we used the same procedure, except to be conservative we included an additional correction for the different numbers of sessions of each type that were collected from each animal, by using weighted means such that each animal's data was weighted by the number of inactivation sessions that animal contributed to the dataset. The same key results were obtained in uncorrected data (significant change in contralateral Infobias Index during inactivation sessions, $p = 0.0015$; no significant change in Control sessions, $p = 0.8786$; inactivation sessions significantly different from control sessions, $p = 0.0243$).

To test how inactivations interfered with information seeking behavior, we analyzed RTs separately for Info and Noinfo CSs. RTs were normalized by z-scoring all RTs separately for each session and CS location. The mean normalized RT was then calculated for each combination of session, time in session (pre- or post-injection), and CS type (Info or Noinfo CS). Then for each session and CS type we calculated the change in mean normalized RT (post-injection – pre-injection). Finally, we tested whether the RT changes for each CS type were different from 0 (signed-rank test on per-session normalized RT changes), and whether the RT changes for the two CS types were different from each other (signed-rank test on per-session difference between normalized RT changes for the two CS types).

3.3 Results

3.3.1 Anatomically-connected regions of ACC, icbDS, and Pal contain ramping neurons that signal reward uncertainty

To identify neural networks that are selectively responsive to reward uncertainty, we presented monkeys with fractal visual conditioned stimuli (CSs) predicting the delivery of a

future juice reward with 0%, 25%, 50%, 75%, and 100% probabilities[8,19] while recording across areas of ACC, icbDS, and Pal (Figure 3.1). All three areas contained numerous neurons that were strongly activated or inhibited by all the CSs that cued uncertain rewards (Figure 3.2A; Figure 3.2B, cyan, blue, turquoise; 25%, 50%, and 75% reward CSs). These responses were primarily excitatory in ACC and icbDS and often inhibitory in Pal (Figure 3.2A). The average responses consisted of sustained ramping to the moment when the uncertain outcome would occur (Figure 3.2A,B). Importantly, unlike conventional reward-related neurons in these areas[15,16], these neurons were more responsive to reward uncertainty than reward value; their responses were substantially lower for the CSs that cued certain outcomes, even though they had the highest and lowest values in the task (black, 100%, certain reward; gray, 0%, certain no-reward; Figure 3.2A-C). Furthermore, many of these neurons responded to uncertainty in a graded manner[8]: they responded most in the condition with maximal uncertainty (50% reward), less in conditions with intermediate uncertainty (75% and 25% reward), and least in conditions with no uncertainty (100% and 0% reward).[15] Specifically, neurons with a significantly greater average response to the 50% CS than to the 75 and 25% CSs were found in all three areas (Figure 3.2D, dark blue; $p < 0.05$, signed-rank test), with much greater prevalence than expected by chance ($p < 0.001$ in each area, binomial tests), and were significantly more prevalent than the opposite response pattern (Figure 3.2D, cyan; $p < 0.05$ in each area, binomial tests).

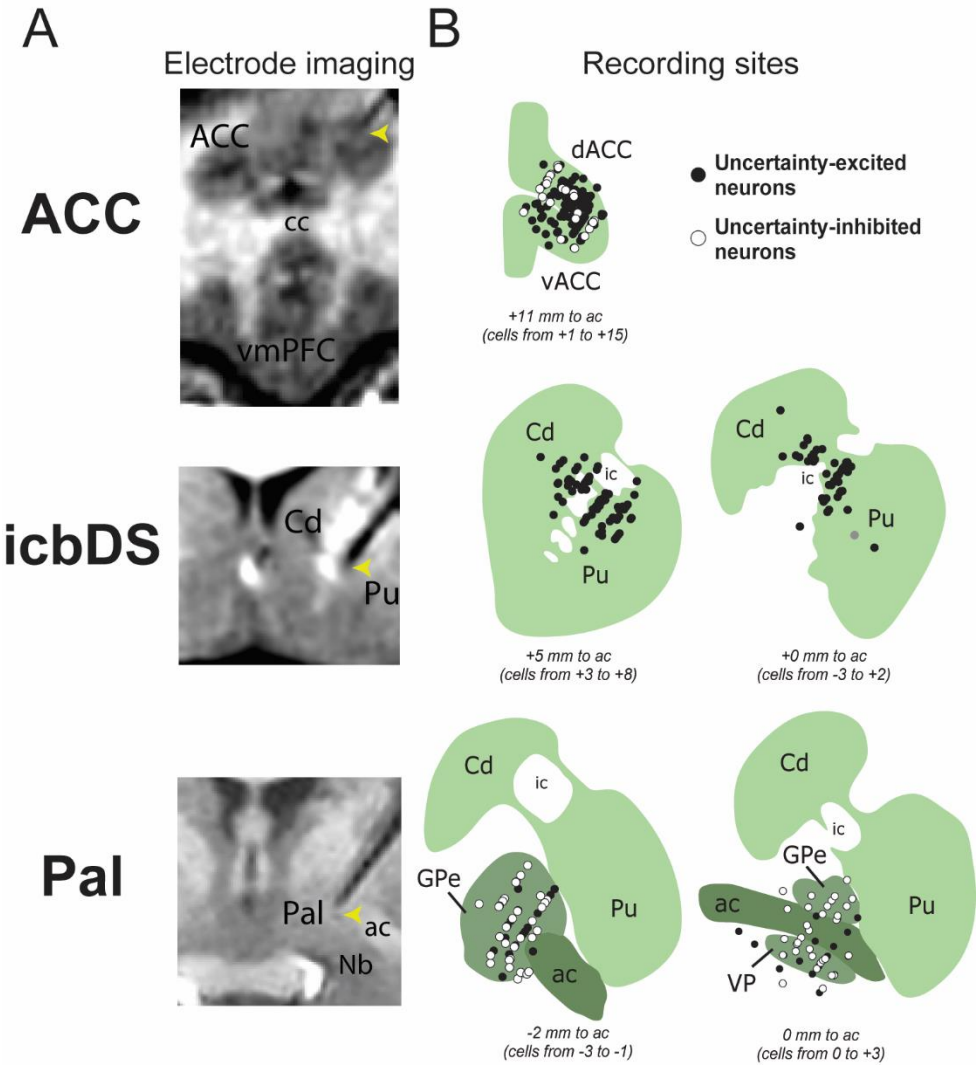

Figure 3.1: **(A)** MRIs were taken immediately after recording uncertainty coding neurons with the electrode still in place. Shown are coronal views in which the electrode track is visible as a black 'shadow' on the MRI; the yellow arrow indicates the location of the electrode tip. Top: recording site in ACC, at a location symmetrical to the ACC in the opposite hemisphere. Middle: recording site in icbDS, at a location intermediate between the body of the caudate and putamen. Bottom: recording site in Pal, with the tip adjacent to the ventral boundary of the anterior commissure. Abbreviations: cc, corpus callosum; vmPFC, ventromedial prefrontal cortex; Cd, caudate; Pu, putamen; ac, anterior commissure; Nb, nucleus basalis. **(B)** Reconstruction of recording sites in ACC (top), icbDS (middle), and Pal (bottom). Circles indicate locations of neurons that responded to uncertainty with significant excitation (black) or inhibition (white). Structures are shown in the coronal plane. Neurons are projected onto the nearest shown plane; text indicates the range of neuron locations.

The network refined its uncertainty signals over time. Uncertainty signals emerged markedly earlier in Pal (Figure 3.2A, arrows; Supplementary Figures 3.1,3.2; significantly shorter latency in Pal than ACC and icbDS, both $p < 0.001$, permutation tests) but this initial signal did not yet encode the graded level of uncertainty (i.e. similar activity for 25, 50, and 75%; Supplementary Figure 3.2). Uncertainty signals later emerged in both ACC and icbDS at roughly similar latencies (Figure 3.2A; Supplementary Figure 3.1; no significant latency difference, $p = 0.11$), and those two areas first significantly encoded the graded level of uncertainty, doing so before Pal (50 > 25,75%, Figure 3.2A; Supplementary Figure 3.2). These results indicate that a rapid but rough Pal uncertainty signal is followed by a slower, graded signal in cortico-striatal areas. Further, these results match the precise anatomical tracers performed by our collaborators in the Dr. Suzanne Haber Laboratory outlined in detail in the full manuscript from which this chapter was adapted.

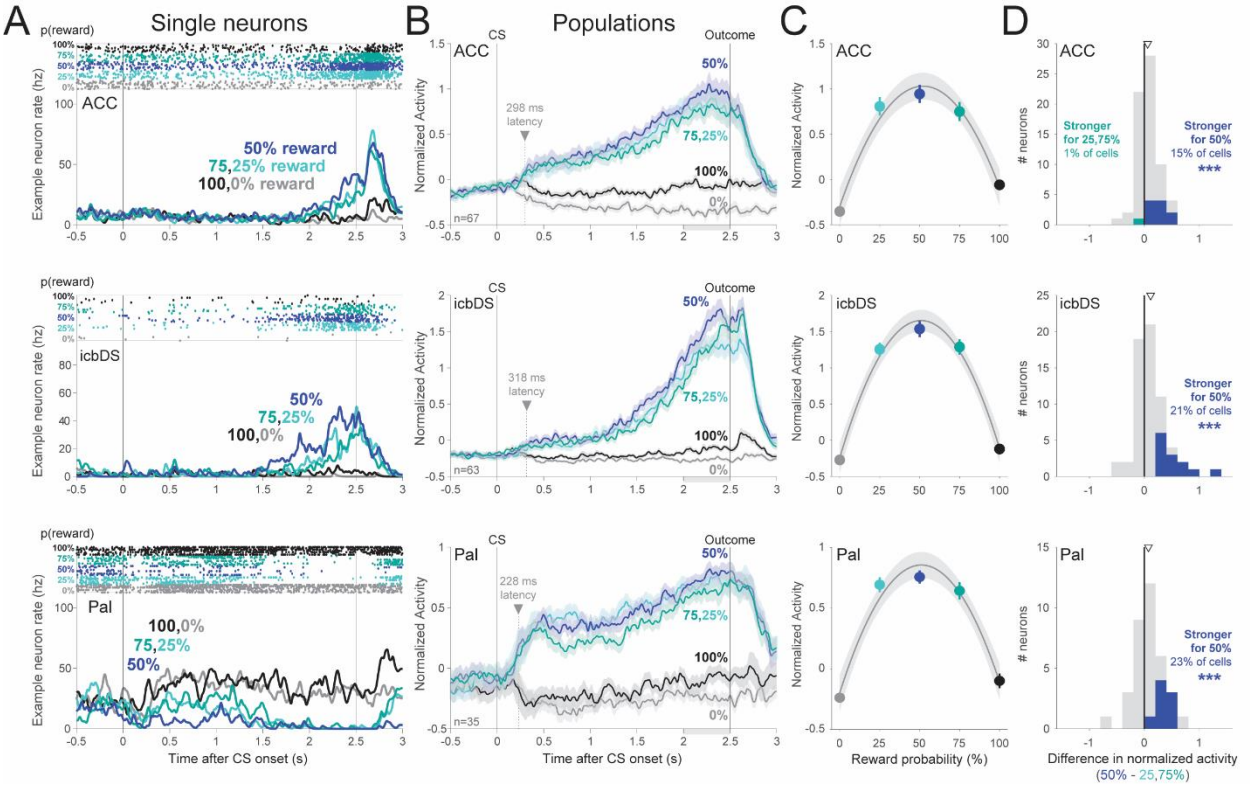

Figure 3.2: **(A)** Example responses to the uncertainty task from neurons in ACC (top), icbDS (middle), and Pal (bottom). The ACC and icbDS neurons have excitatory ramping activity up to the time of uncertain reward: strongest for highly uncertain rewards (blue, 50%), strong for moderately uncertain rewards (turquoise colors, 25% and 75%), and weak or absent for certain outcomes (black, 100%; gray, 0%). The Pal neuron has similar ramping activity with an opposite, inhibitory direction of response. *Top of panel:* times of each spike (dots) on each trial (rows). *Bottom of panel:* smoothed firing rate for each CS. **(B)** The population average normalized activity of uncertainty coding neurons in each area ramps up to the time of the uncertain outcome. Shaded areas are ± 1 SE. Arrow, dashed line, and text indicate each area's latency of uncertainty coding. Gray area below x-axis is the pre-outcome analysis time window. **(C)** Population average pre-outcome normalized activity is well fitted with a second-order polynomial function of reward probability (gray lines; shaded areas are ± 1 bootstrap SE) indicating an inverted-U relationship between reward probability and neural responses, as expected for uncertainty coding. **(D)** Graded coding of reward uncertainty. Histograms show each neuron's difference in normalized activity between CSs with high (50%) vs. moderate (25,75%) reward uncertainty. Arrows indicate the mean. Colored neurons have significantly differential activity. In all areas, more neurons are significantly more active for high uncertainty (blue) than moderate uncertainty (turquoise). *** indicates more neurons than expected by chance ($p \leq 0.001$).

3.3.2 Many uncertainty-selective neurons across this network anticipate uncertainty resolution through the delivery of advance information

Our findings thus far identify an interconnected cortico-BG network that signals reward uncertainty with ramping anticipatory activity. This raises a few key questions: what event is the network anticipating? Most crucially, does the network anticipate the moment of receiving an uncertain outcome *per se*, or the moment of receiving *information* to resolve the uncertainty?

To answer these questions, we designed a task to separate the time of receiving information from the time of receiving the outcome (information viewing task, Figure 3.3A). On each trial the monkey was shown a fractal CS that indicated that a reward would be delivered in 3 seconds with 100%, 50%, or 0% probability. There were two types of CSs. *Informative CSs* (Info CSs) were followed after 1 second by an informative visual cue whose color indicated the upcoming outcome (e.g. orange → reward, gray → no reward). *Non-informative CSs* (Noinfo CSs) were followed by a non-informative cue whose color was randomized on each trial and hence did not indicate the upcoming outcome. Importantly, there was no way for animals to use the information to control or influence the outcome. Thus, neurons that simply anticipate uncertain rewards should respond differently during the Info and Noinfo 50% reward CSs, because only the Noinfo 50% outcome is uncertain at the time of delivery (Figure 3.3C). However, neurons that anticipate information should activate specifically in advance of the time when the animal expects to be informed of the outcome, which occurs at different times on Info and Noinfo trials: on Info trials information is delivered after 1 second by the informative cue (Figure 3.3C, red arrow), while on Noinfo trials the animal is first informed of the outcome after 3 seconds by receiving the outcome (juice delivery or omission) at the end of the trial (Figure 3.3C, blue arrow).

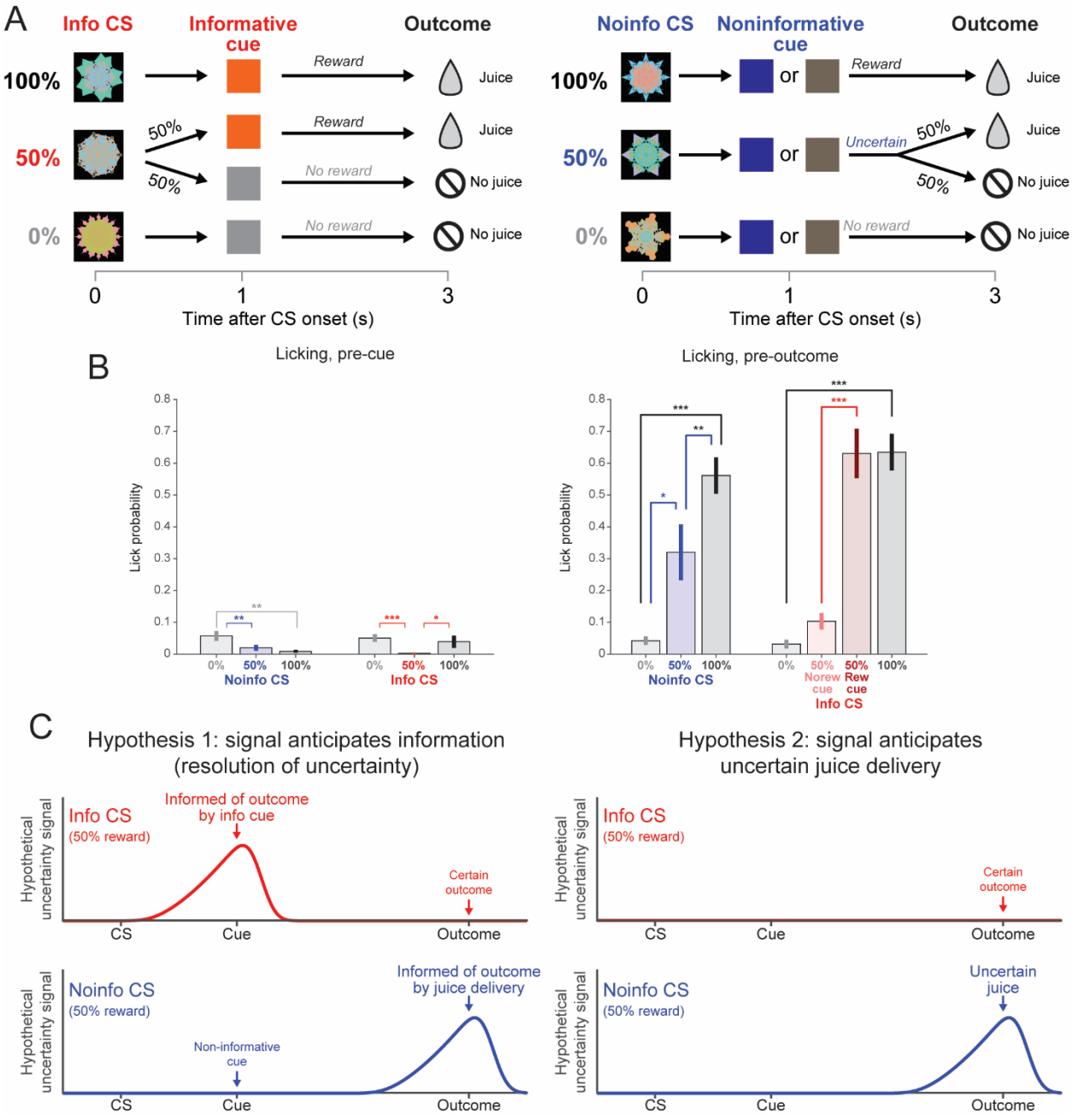

Figure 3.3: **(A)** Information viewing task. On Info CS trials, CSs predict 100, 50, or 0% reward, and are followed by an informative cue that indicates the outcome with certainty. On Noinfo CS trials, analogous CSs are followed by one of two non-informative cues that are randomized and hence leave the outcome uncertain until it is delivered at the end of the trial. **(B)** Left: Mean fraction of trials of each type in which a lick was detected in the 500 ms before cue onset. Data are from n=18 sessions in which licking was measured and there was reliable differential licking that distinguished 100% reward from 0% reward trials. Licks occurred before the cue on ~5% or fewer trials, indicating that animals had little or no expectation that juice would be delivered at the time of the cue. Notably, the Info 50% reward CS evoked intense gaze and neural activity in anticipation of the informative cue (Fig 3), but evoked near-zero licking, indicating that the information-related behavior and neural activity cannot be accounted for by expectation of juice

reward. If anything, there was slightly but significantly less licking for the Info 50% reward CS than for the other Info CSs. There were significant but small differences in licking between some other conditions as well (Noinfo 50% vs 0%, $p = 0.005$; Info 50% vs 0%, $p = 0.001$; Info 50% vs 100%, $p = 0.032$). Right: Same as left, for the 500 ms before outcome delivery. Licks occurred on a large fraction of trials, indicating that animals expected juice to be delivered at the time of the outcome. Licking was generally consistent with the mean reward in each condition. On Noinfo trials licking significantly increased with reward probability (100% > 50%, $p = 0.003$; 50% > 0%, $p = 0.044$; signed-rank tests). On Info trials licking was significantly greater after reward was cued than after no-reward was cued, both for trials in which reward was initially uncertain (50%→reward > 50%→no reward, $p = 0.001$) and trials when reward was initially certain (100% > 0%, $p < 0.001$). **(C)** Left: if neurons ramp to the receipt of information, they should also ramp to informative cues on Info trials (red). Right: if neural uncertainty signals simply anticipate uncertain juice delivery, they should only ramp up to uncertain outcomes on Noinfo trials (blue).

Indeed, the cortico-BG network contained a substantial population of neurons that anticipated the receipt of information to resolve reward uncertainty. We quantified each neuron's uncertainty signal using the ROC area for using its firing rate to distinguish trials with uncertain rewards vs certain rewards (50% vs 100% and 0%). We then calculated an "Info Cue Anticipation Index" defined as its uncertainty signal during the last 0.5 sec of the Info CSs (just before an informative cue) minus its uncertainty signal during the same time window for the Noinfo CSs (just before a non-informative cue). Neurons with significant Info Cue Anticipation Indexes were highly prevalent in all three areas of the network (Figure 3.4D,E; 47%, 54%, and 50% of recorded neurons in ACC, icbDS, and Pal (n=9/19, 13/24, and 21/42, respectively); more than expected by chance, all $p < 0.05$, binomial tests).

Importantly, as expected for an information-anticipatory signal, the same neurons that anticipated informative cues on Info trials also commonly anticipated uncertain outcomes on Noinfo trials, and did so in similar manners. For example, the icbDS neuron in Figure 3.4A was strongly activated on uncertain reward trials in advance of both informative cues (top, red) and uninformed outcomes (bottom, blue), while the Pal neuron in Figure 3.4B was inhibited in advance of these task events. To quantify this, we defined an analogous "Uncertain Outcome Anticipation Index" as the change in a neuron's uncertainty signal from the beginning to the end of the cue period on Noinfo trials. This index was significant in a substantial number of single neurons in all three areas (21%, 63%, and 31% of neurons in ACC, icbDS, and Pal; more neurons than expected by chance in all areas, binomial tests, all $p < 0.05$) and was most prevalent in icbDS (higher fraction of significant neurons in icbDS than ACC or Pal, both $p < 0.05$, binomial tests). There was a strong correlation between the two neural anticipation indexes (rank correlation = 0.45, $p < 0.001$, Figure 3.4E). That is, many neurons, especially in ACC and icbDS,

were activated in anticipation of receiving information from both cues and outcomes, while other neurons, especially in Pal, were inhibited for both. Thus, when examining neurons whose uncertainty signals on Noinfo trials significantly anticipated the outcome, the average timecourse of their uncertainty signals on Info trials bore a strong resemblance to a hypothetical information-anticipatory signal (Figure 3.3C, Figure 3.4F; similar results for all three areas, Supplementary Figure 3.4).

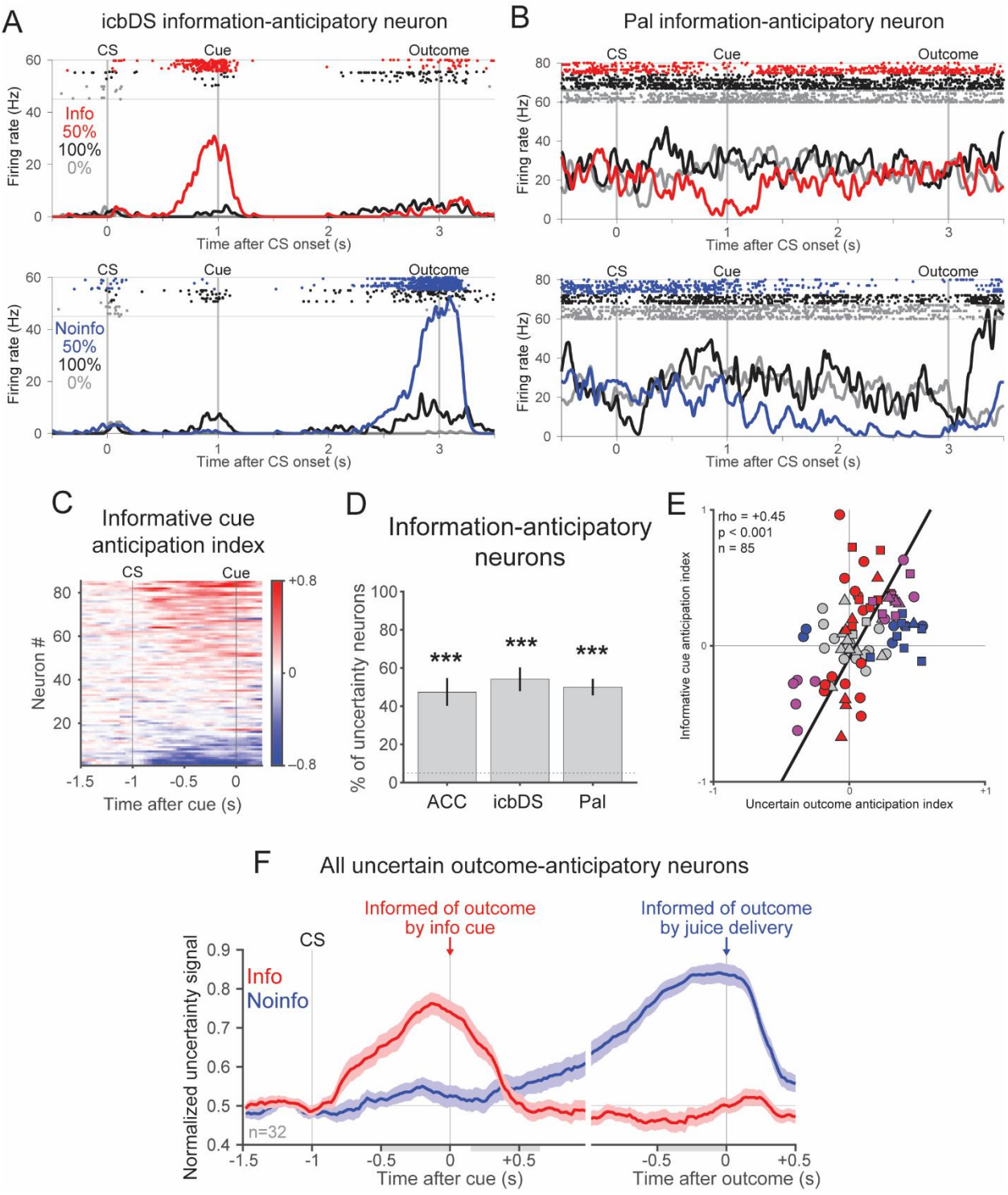

Figure 3.4: **(A)** An example icbDS neuron had strong ramping activity anticipating the time of receiving information about uncertain rewards: the informative cue on Info trials (top, red) and outcome delivery on Noinfo trials (bottom, blue). This activity was greatly reduced or absent when the outcome was certain (black, gray). **(B)** An example Pal neuron had a similar response pattern but with ramping inhibition instead of excitation. **(C)** Differential uncertainty signals

emerge in anticipation of informative cues. Each row is a neuron, and the color at each time point indicates the difference between its uncertainty signals on Info vs Noinfo trials. Color indicates sign of coding (red: more positive uncertainty signal for Info; blue: more negative uncertainty signal for Info; color bar indicates scale). **(D)** Information-anticipatory activity was significantly present in approximately half of uncertainty-related neurons in each area. *** indicates significantly more neurons than expected by chance, $p < 0.001$. **(E)** Correlated anticipation of the two reward-informative task events. Many neurons have significant Informative Cue Anticipation Indexes (red, y-axis), Uncertain Outcome Anticipation Indexes (blue, x-axis), or both (purple). The two indexes are highly correlated; text indicates rank correlation and its p-value. ACC, icbDS, and Pal neurons are indicated by triangles, squares, and circles. Black line is a linear fit with type 2 regression. **(F)** The population average uncertainty signal from neurons with ramping uncertainty signals on Noinfo trials (blue) closely resembles Hypothesis 2: they also have strong ramping activity on Info trials that anticipates the time of viewing the informative cue (red). Error bars are ± 1 SE. Gray areas are the time windows for calculating the indexes of cue anticipation (pre-cue window) and outcome anticipation (post-cue, pre-outcome windows).

3.3.3 Monkeys preferentially direct their gaze towards objects associated with uncertainty

Given the cortico-BG network's strong information-predictive signal, we next asked whether information predictions evoke information seeking behavior in monkeys. Since monkeys, like humans, scan uncertain environments for information with their eyes[15,26,171], we hypothesized that monkeys may anticipate information by directing their gaze to objects in their environment associated with the uncertainty to be resolved. Consistent with previous work, we found that monkeys licked in anticipation of juice rewards (Figure 3.3B) and that their gaze was attracted to visual objects based on their expected reward value (Figure 3.5A, 100% CS > 0% CS (black > gray), informative reward cue > no-reward cue (dark red > light red)).

Strikingly, however, monkeys' gaze was even more strongly attracted to objects based on their uncertainty, especially in the moments before receiving information to resolve that uncertainty. On Info trials, monkeys could anticipate receiving information during the Info 50% reward CS as they awaited the upcoming informative cue (Figure 3.5A, red arrow). Monkeys were substantially more likely to gaze at the Info 50% reward CS than all other CSs (signed-rank tests, all $p < 0.001$). Importantly, this attraction of gaze was specifically related to upcoming information rather than to reward value or uncertainty per se. Monkeys gazed at the Info 50% reward CS more than at the Noinfo 50% reward CS, which was associated with exactly the same reward value and uncertainty but was not followed by information (Figure 3.5B), and more than at the 100% reward CSs, which were associated with *double* the reward value but had no uncertainty to resolve (Figure 3.5A,B). Furthermore, this intense gaze at the Info 50% reward CS occurred despite near-zero licking, indicating that animals were anticipating the delivery of information, not juice reward (Figure 3.3B).

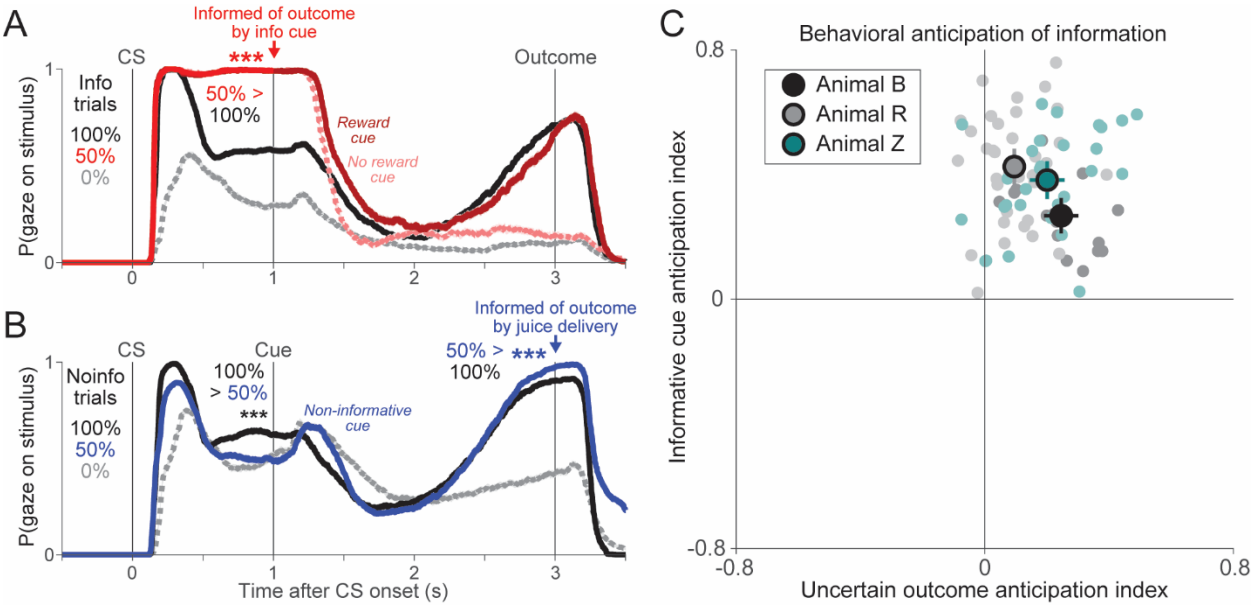

Figure 3.5: **(A)** Monkey's gaze on Noinfo trials is attracted to objects in anticipation of outcome delivery Lines indicate the probability at each millisecond that the animal gazes at the stimulus. Shaded areas indicate ± 1 SE (most too small to see). On uncertain 50% reward trials monkeys gazed less at the CS than on 100% reward trials, but while viewing the non-informative cues their gaze ramped up in anticipation of the outcome until it became greater on uncertain 50% than on 100% reward trials. **(B)** Monkeys' gaze on Info trials is attracted to CSs in anticipation of receiving informative cues about uncertain rewards. Same format as (A). Monkeys gazed more at the 100% CS (black) than the 0% CS (gray), but gazed most of all at the uncertain 50% CS (red) which could be followed by informative cues indicating either reward (dark red) or no reward (pink). *, **, *** indicates $p < 0.05$, 0.01, 0.001. Monkeys' gaze at reward cues then ramped up to the time of reward delivery, while gaze at no-reward cues was minimal. **(C)** Uncertainty-related gaze behavior in each animal significantly anticipated informative cues (y-axis) and uncertain outcomes (x-axis). Same format as Fig 3.4E, but analyzing gaze instead of neural activity. Colors indicate animals; light dots are single sessions; dark dots are means ± 1 SE

Similarly, on Noinfo trials, monkeys could anticipate receiving information at the end of the cue period as they awaited the upcoming reward delivery or omission (Figure 3.5B, blue arrow). Again, at that time the monkeys gazed at the cue more during Noinfo 50% reward trials than all other conditions (all $p < 0.001$), even 100% reward trials that had double the reward value (Figure 3.5A,B). They did so even though the upcoming information about the outcome was delivered through a non-visual modality (receipt of juice or no juice), and even though 100%, 50%, and 0% Noinfo trials all used exactly the same set of visual cue stimuli; they gazed at those cues most avidly on Noinfo 50% reward trials when they were associated with an uncertain reward, and did so specifically in the moments before the uncertainty was going to be resolved. These monkeys also behaved consistently in standard uncertainty-related tasks that lacked informative cues (essentially treating all trials as Noinfo because no cues were available). Thus, when we analyzed monkeys' gaze behavior in the same way that we analyzed neural spiking activity, we found that all monkeys had significantly positive Info Cue Anticipation and Uncertain Outcome Anticipation indexes, indicative of information-anticipatory behavior (Figure 3.5C, all $p < 0.001$, signed-rank test). Next, we compared neuronal activity preceding information delivery when the monkeys' gaze was on the stimulus compared to when the gaze was off of the stimulus. We found that neural information signals were present even at moments when the monkeys' gaze was away from the stimuli, but were significantly enhanced during matched time points from other trials when the monkeys' gaze was off the stimulus. This was true in both the information and standard uncertainty tasks (Figure 3.6).

This data suggested that the cortico-BG network's information signals could be well suited to motivate the animal's information-oriented behavior – a hypothesis we next tested through direct pharmacological disruption.

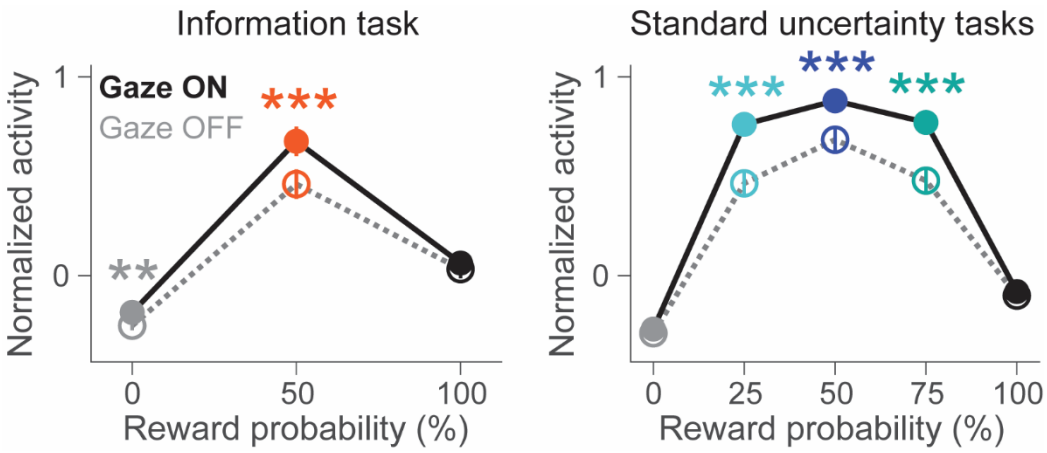

Figure 3.6: Mean normalized activity before receipt of information is enhanced when gaze is on the stimulus (dark dots/lines) compared to when gaze is off the stimulus (light dots/lines), especially for intermediate reward probabilities when reward is uncertain. Error bars are ± 1 SE; asterisks indicate significance.

3.3.4 Pharmacologically inactivating areas of BG that contain uncertainty-selective neurons causally decreases information-seeking behaviors

Given these findings, we hypothesized that information-predictive neurons in the basal ganglia have a causal role in motivating gaze shifts to gain information. If so, then temporarily inactivating the basal ganglia subregions that contain these neurons should impair the motivation to seek information. We therefore trained monkeys to perform a task in which gaze shifts were required to gain information (information seeking task, Figure 3.7A). Monkeys fixated a spot of light and then continued to fixate during a delay period while a 50% reward CS was presented on either the left or right side of the screen. After the fixation point disappeared ('go' signal) the monkey was free to gaze in any manner they chose. On trials with an Info CS, gazing at the CS caused it to be immediately replaced by an informative cue indicating the trial's outcome (reward or no reward). On trials with a Noinfo CS, gazing at the CS caused it to be replaced by a non-informative cue. Importantly, the monkeys' gaze at the CS allowed them to gain information about the outcome but did not allow them to influence the outcome itself in any way (i.e. the outcome always occurred a fixed time after the 'go' signal regardless of whether and how they gazed at the CS). In addition, we used a fixed-duration delay period between CS onset and the go signal to allow animals to anticipate the moment when information would become available. Indeed, animals had strongly anticipatory behavior, at times shifting their gaze onto the CS at short latencies before they could have perceived and reacted to the 'go' signal (Figure 3.7B, response times (RTs) < 50 ms). Monkeys were highly motivated to seek information, shown by their much faster RTs to shift their gaze onto Info CSs than Noinfo CSs (Figure 3.7B). We quantified the response bias favoring the info CSs with an "Infobias Index" (Figure 3.7B) which

was significantly positive in every session for every animal (n=43/43 sessions, all $p < 0.05$, permutation tests).

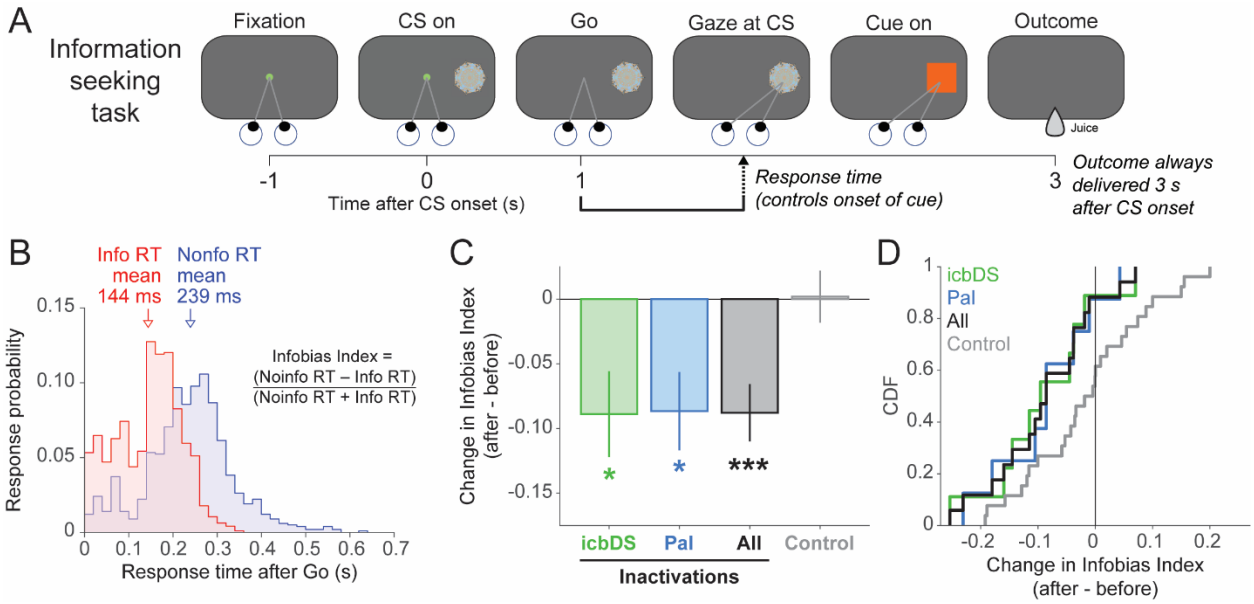

Figure 3.7: **(A)** Information seeking task. Monkeys were shown a CS, waited for a 'go' signal, and then were allowed to gaze at it. Gazing at an Info or Noinfo CS caused it to be replaced with an appropriate informative or non-informative cue. Regardless of whether or when animals gazed at the CS, the outcome was delivered a fixed time after CS onset. **(B)** RT distribution for animal B. The animal had much faster RTs for Info trials (red, mean = 144 ms) than Noinfo trials (blue, mean = 239 ms). The animal often anticipated the time that information would become available, as indicated by the prevalence of anticipatory saccades especially on Info trials (e.g. RTs < 50 ms). This histogram includes all data that was collected when inactivations were not being performed. It shows n=1962/1966 (99.8%) of those RTs; not visible are four outliers from Noinfo trials (RT = 0.741, 0.748, 1.326, 1.335 s). Text indicates the equation for the Infobias Index. **(C)** Muscimol inactivation effect on RTs to contralateral CSs, quantified as the change in Infobias Index (after– before). There are significant reductions in Infobias Index for icbDS inactivations (green), Pal inactivations (blue), and all inactivations (black), but not control sessions (gray). *, **, *** indicate $p < 0.05, 0.01, 0.001$. Error bars are ± 1 SE. **(D)** Cumulative distributions showing each session's inactivation effect on the Infobias Index for contralateral CSs. Inactivation sessions consistently reduce the information bias while control sessions do not.

Consistent with the lateralized functions of basal ganglia circuitry[196,197], we predicted that unilateral inactivations would reduce information seeking behavior directed toward objects in contralateral space. Indeed, unilateral injections of muscimol, a $GABA_A$ agonist, into either icbDS or Pal in the vicinity where information-anticipatory neurons were recorded caused the information seeking response bias to be significantly reduced in contralateral space (Figure 3.7C,D; icbDS, n=9 sessions, $p = 0.028$; Pal, n=8 sessions, $p = 0.031$; all inactivations, n=17, $p = 0.001$; permutation tests; see Supplementary Figures 3.3 for injection sites and effects in each session). No significant change was observed in a control dataset consisting of sham and saline injections (Figure 3.7C, gray, n=26 sessions, $p = 0.93$). In addition, inactivations had no significant effect on information seeking for ipsilateral CSs (all $p > 0.4$, Supplementary Figure 3.5). Thus, relative to control sessions, inactivations caused the information seeking bias to become lateralized – significantly shifted away from the contralateral side ($p = 0.019$, Supplementary Figure 3.5).

We further investigated the mechanism by which icbDS and Pal activity promote information seeking. Our data suggest that icbDS and Pal have reciprocal inhibitory connections and tend to encode information predictions in opposite manners, with icbDS neurons activated and Pal neurons commonly inhibited (Figures 3.2,3.3). We therefore hypothesized that icbDS and Pal activity have opposite influences on motivated gaze behavior, such that information-oriented gaze shifts are motivated by icbDS activity and suppressed by Pal activity. The icbDS is primarily active during the Info CS, so inactivation should slow gaze shifts to the Info CS while leaving responses to the Noinfo CS relatively intact. Conversely, Pal is normally inhibited during the Info CS, so inactivation should leave responses to the Info CS relatively intact while speeding gaze shifts to the Noinfo CS. Both of these predictions were borne out in the data.

Inactivation of icbDS slowed gaze shifts to the Info CS but did not significantly change RTs to the Noinfo CS (Supplementary Figure 3.6B, left, Info CS $p = 0.0003$, Noinfo CS $p = 0.64$, rank-sum tests; significantly different changes for Info vs Noinfo, $p = 0.0081$, permutation tests). Conversely, inactivation of Pal speeded gaze shifts to the Noinfo CS but did not significantly change RTs to the Info CS (Supplementary Figure 3.6B, center, Info CS $p = 0.17$, Noinfo CS $p = 0.001$; significantly different changes for Info vs Noinfo, $p = 0.0046$). Thus, icbDS activity motivated gaze shifts to gain information, while Pal activity suppressed motivation to gaze at objects that would not yield information.

Importantly, these inactivation effects on information seeking were not caused by generalized effects on overall motivation to perform the task, which could potentially be affected by inactivation of striatum and pallidum circuitry involved in primary reward seeking behavior.[198–202] Specifically, icbDS inactivations slowed RTs to the Info CS without reducing measures of general motivation, while Pal inactivations speeded RTs to the Noinfo CS without increasing measures of general motivation (Supplementary Figure 3.7). If anything, Pal inactivations speeded RTs to the Noinfo CS in spite of a modest reduction in general motivation to perform the task (Supplementary Figure 3.7), consistent with similar reductions of motivation from previous Pal inactivations.[198–201]

3.4 Discussion

Our work demonstrates the existence of a neural network responsible for motivating actions to resolve uncertain situations by seeking knowledge about future rewards. Previous studies identified cortical and basal ganglia networks that make conventional predictions about when future rewards are available and motivate behavior to seek those rewards.[2,184,196,203] Indeed, our monkeys had strong tendencies to gaze at visual stimuli based on their reward value.

However, the novel ACC-icbDS-Pal neurons we report here have relatively little response to reward value, and hence their primary function is not likely to be control of such reward value-oriented behavior. Instead, they have a quite distinct function: they predict when information will become available to resolve reward uncertainty and motivate gaze behavior to obtain that information. This information seeking gaze behavior can be even more potent than the attraction of gaze to primary reward: our monkeys gazed much more avidly at the CS that provided informative cues than at any other stimulus, even CSs and cues that were associated with *double* its expected reward value. Our data show that this information seeking gaze behavior is very similar to activity observed in the cortico-BG network.

Our data is crucial evidence for theories of reward learning, overt attention, and economic decision making, which propose that objects and events in the world are assigned salience both by neural systems that track primary reward value and its uncertainty[170,179,204,205], and by a system that anticipates information to resolve uncertainty.[26,29,206–208] Furthermore, our data demonstrates a neural mechanism through which information seeking can compete and interact with primary reward to drive ongoing behavior.[28,171,209,210]

In fact, information seeking goes hand-in-hand with primary reward seeking in natural environments. Most experimental studies of reward seeking begin with the presentation of a cue stimulus (or an environmental context) that tells the subject what reward to predict and what actions are needed to obtain it. However, rewards in natural environments can be scarce and uncertain, and fully predictive reward cues rarely come for free or materialize from thin air. In these situations, organisms must first seek and obtain information about the rewards that are available in their environment; only then can they predict the value of those rewards and use that value to motivate reward seeking behavior. In this sense, the cortico-BG network for information

seeking may be critical to ensure that organisms seek out the reward-related cues in their environment that are necessary for the proper operation of the well-known networks that predict and seek primary rewards.[2,184,196,203,210] Indeed, information-related neurons in all three areas were intermixed with other neurons that encoded the reward value of stimuli and outcomes[2,184,196,203,210], indicating that information- and reward-related neurons are well-positioned to support each other's computations.

While information-anticipatory signals were present in all three areas of the cortico-BG network, each area also had distinct features suitable for unique contributions to information seeking. Notably, fluctuations in ACC information signals were the earliest predictor of future behavior. ACC information signals changed several hundred milliseconds before gaze shifts, while BG signals changed more proximally to behavior. This finding supports and extends theories that ACC is especially important for motivating behavioral shifts to explore available prospects and learn their reward value and other properties[211–213], tracking their level of uncertainty and how it evolves over time as beliefs are updated in response to surprising outcomes[4,212,214–218], and using this information to decide how to control future cognition and behavior.[212,219] In particular, while it is well acknowledged that the ACC needs to receive a broad array of reward- and uncertainty-related information to perform these functions[209,219], our data indicates that the ACC is not merely a passive recipient of this information; rather, the ACC is tightly linked to the emergence of motivational drive to actively seek out that information from the environment.

In addition, our findings indicate that information seeking behavior is motivated by a BG circuit mechanism that is analogous but distinct from the BG circuits that motivate conventional reward-seeking behavior. There are two key parallels. First, behavior-related fluctuations in BG

information signals follow fluctuations in cortex and are proximal to behavioral gaze shifts. This is consistent with classic theories of cortico-BG circuits[90] and work on cortex-striatum interactions[220–222] suggesting that cognitive and motivational signals can be computed in cortex and then sent to BG where they are processed and used to guide behavior. Second, the specific functions of each BG subregion in information seeking are consistent with classical BG circuit motifs: notably, icbDS and Pal neurons commonly encode information signals with opposite signs and these areas have opposite causal influences on behavior, such that icbDS activity speeds gaze shifts to gain information while Pal activity slows gaze shifts that will not provide information. This resembles analogous findings for BG areas involved in primary reward seeking: antagonizing D1 receptors in visuomotor dorsal striatum slows gaze shifts to gain large juice rewards[87], while inactivation of Pal speeds gaze shifts to gain small juice rewards.[199] Importantly, however, the BG mechanisms underlying physical reward- and information-oriented behavior are at least partially distinct at the neuronal and behavioral levels: (1) when animals avidly gazed at the Info CS in anticipation of viewing the informative cue, they had near-zero licking behavior, indicating that they were not anticipating juice reward; (2) the cortical and BG neurons we identified that are linked to information-anticipatory behavior primarily anticipated the moment of gaining information, not the moment of gaining juice reward; and (3) inactivation effects on information seeking could not be explained as a result of generalized effects on juice reward seeking. Thus, this cortico-BG network appears to be specially focused on online information seeking behavior. This is in contrast to other BG circuits and interconnected areas involved in reward prediction errors and reinforcement, which commonly encode information and primary reward in a common currency.[26,28] In addition, whereas classical theories of cortico-BG circuits that classify Pal as an output structure[90,223], our

data extends previous results[201] by showing that Pal in fact responds earliest to uncertainty-related events. This is consistent with theories that BG rapidly selects salient stimuli to guide future behavior.[224,225] Our data supports a scenario in which (A) Pal first signals a rapid, rough assessment of reward uncertainty; (B) ACC and icbDS first signal the precise graded level of uncertainty; and (C) the resulting representation of uncertainty ramps up to the time of its resolution by information, and drives ongoing information seeking behavior.

Given the link between the ACC-icbDS-Pal network and information seeking behavior, variations in the network's activity could be responsible for the natural variations in information seeking behavior that are commonly found across individuals[185,210,216] and tasks.[226,227] In the same vein, it is notable that ACC and BG are implicated as sites of dysfunction and targets for treatment in human disorders of motivated behavior (such as obsessive-compulsive disorder[228,229], Parkinson's disease[230], and drug addiction[58]) that are known to affect reward- and uncertainty-related behavior.[231–236] Our results raise the possibility that these disorders and treatments may also affect the motivation to seek information about future events. While this has been little studied, there is evidence that Parkinson's disease reduces the motivation to gather information needed for upcoming decisions[237] and impairs learning from early access to information about uncertain outcomes[238] Taken together, our work provides a foundation for understanding the neural network mechanisms by which information is detected, predicted, and used to motivate behavior.

3.5 Supplementary material

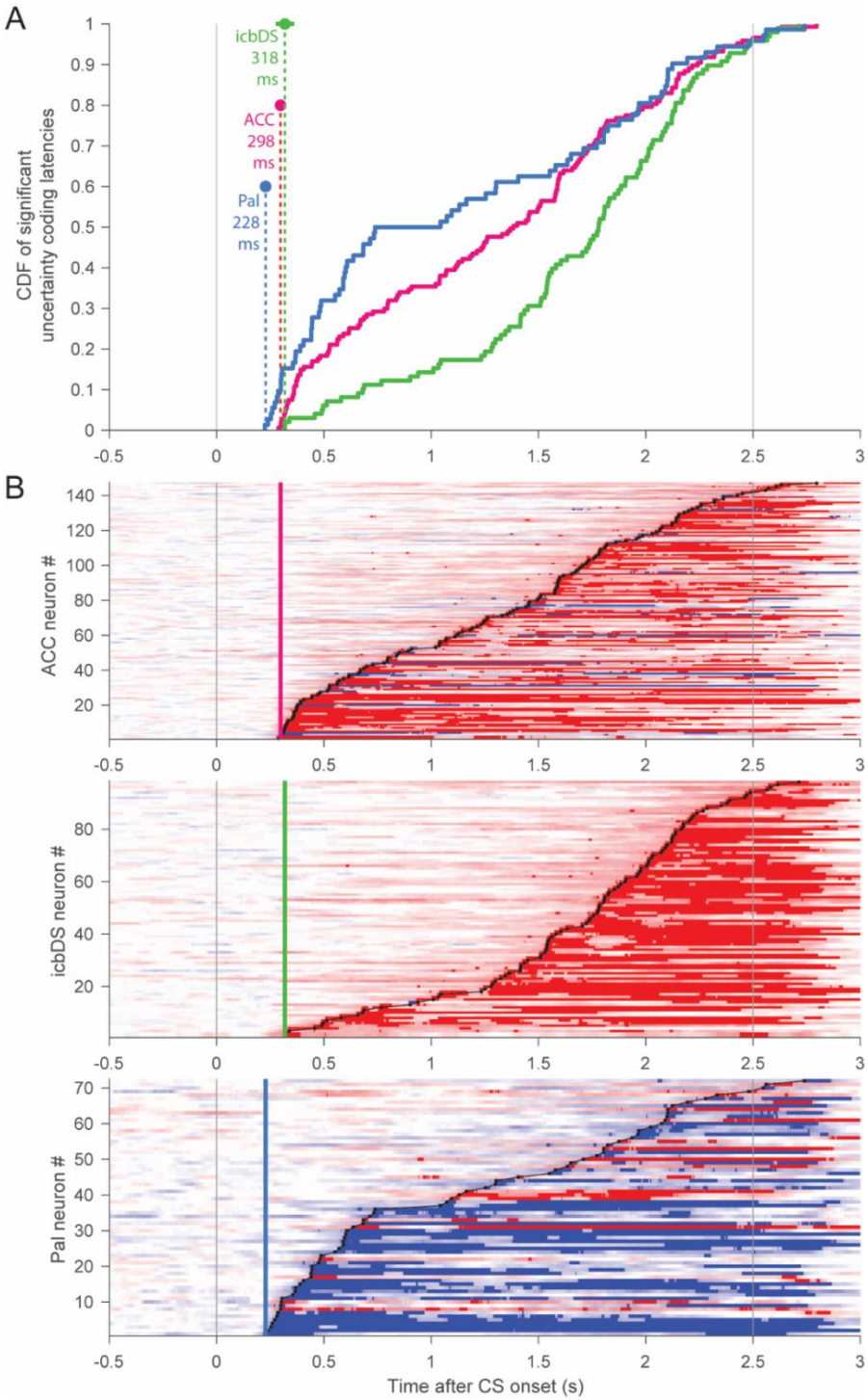

Supplementary Figure 3.1: **(A)** Cumulative distribution of latencies for all single neurons recorded during standard uncertainty tasks that had detected latencies of uncertainty coding. Circles, dashed vertical lines, and text indicate the estimated population latency of uncertainty coding in each area (error bars are ± 1 bootstrap SE). Uncertainty signals emerge first in Pal, followed by ACC and icbDS at similar latencies. **(B)** Heat map of uncertainty coding over time for the neurons in (A). Top: ACC; middle: icbDS; bottom: Pal. Each row is a neuron. Black dots indicate the detected latency of uncertainty coding. Color indicates the neuron's uncertainty

coding at each time during the task (red = more active for uncertain than certain CSs, blue = less active for uncertain than certain CSs, white = no uncertainty coding). Uncertainty coding for is quantified based on the ROC area for using the neuron's activity to discriminate between uncertain vs certain CSs. For this latency analysis we conservatively calculate the uncertainty coding at each time point as the least extreme of two ROC areas: one for discriminating all uncertain CSs from the 100% reward CS, and the other for discriminating all uncertain CSs from the 0% reward CS. Uncertainty coding is predominantly excitatory in ACC, almost exclusively excitatory in icbDS, and predominantly inhibitory in Pal.

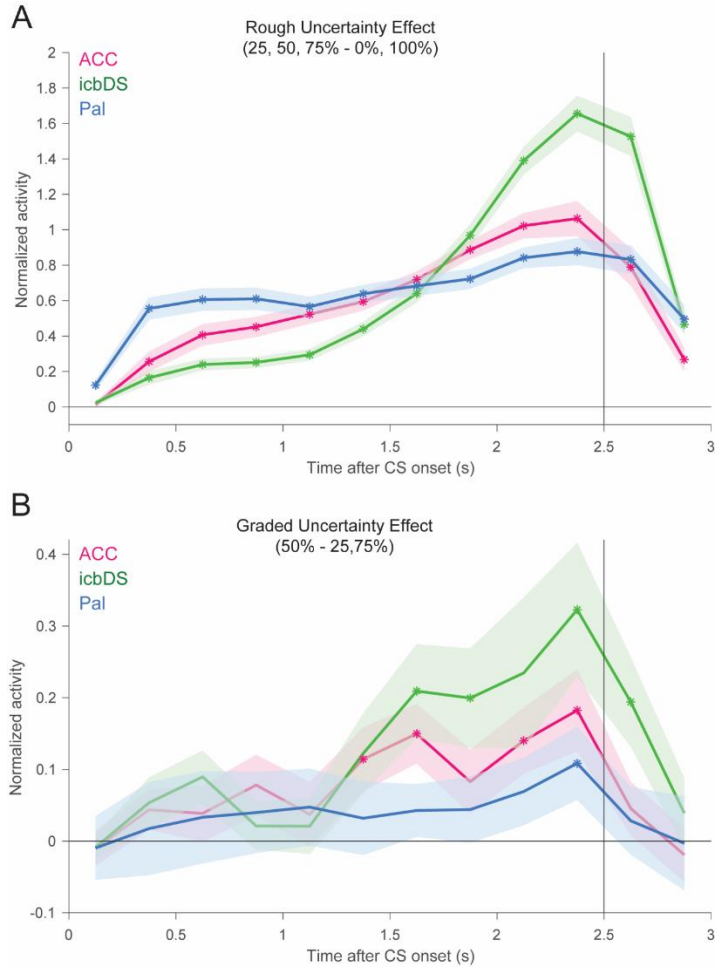

Supplementary Figure 3.2: In order to directly compare rough and graded uncertainty-related activity, they are both quantified here in terms of normalized activity. **(A)** Population average rough uncertainty signal for each area, defined as the difference in mean normalized activity between uncertain CSs (25%,50%, and 75%) and certain CSs (0% and 100%). The shaded area is ± 1 SE. Asterisks indicate significant differences from 0 (signed-rank test, $p < 0.05$). Consistent with the latency analysis in Fig S1, the rough uncertainty signal reaches significance first in Pal and later in ACC and icbDS. **(B)** Population average graded uncertainty signal in each area, defined as the difference in mean normalized activity between the maximally uncertain CS (50%) and the moderately uncertain CSs (25% and 75%). There is a trend for a graded uncertainty coding at all time points in all areas, but it grows and reaches significance first in ACC and icbDS, and later in Pal. Thus, while rough uncertainty coding emerges first in Pal, graded uncertainty coding becomes prevalent first in ACC and icbDS.

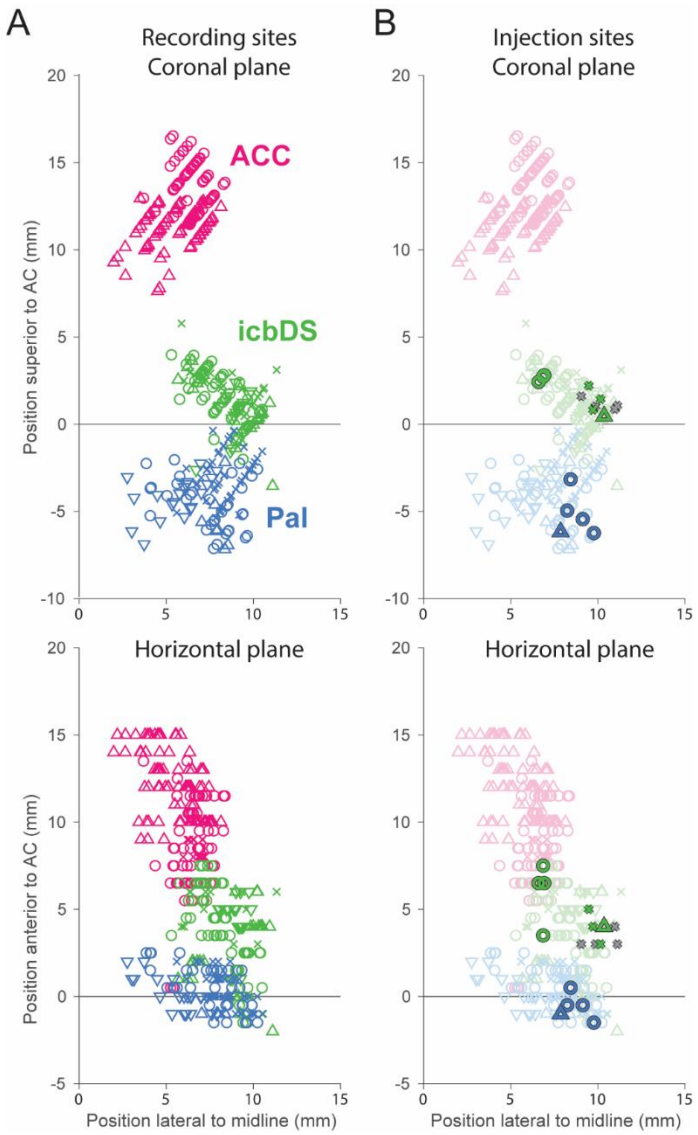

Supplementary Figure 3.3: **(A)** Reconstructed 3D coordinates of each neuron in the dataset, shown for all areas (indicated by colors) and all animals (indicated by symbols; see legend). Coordinates are relative to the midline, superior tip of the anterior commissure (AC). *Top* shows coordinates in the horizontal plane. *Bottom* shows coordinates in the coronal plane. The three areas where uncertainty-responsive neurons were found were clearly anatomically distinct from each other, and were located in similar, overlapping locations in all animals. **(B)** Same as (A) with an overlay showing the reconstructed coordinates of the injection sites. Colors indicate area (icbDS or Pal) and substance (muscimol or saline; see legend). The injection sites for icbDS and Pal were clearly distinct from each other and overlapped the locations of uncertainty-responsive neurons in their respective areas. The injection sites for saline overlapped with the injection sites for muscimol in the same area.

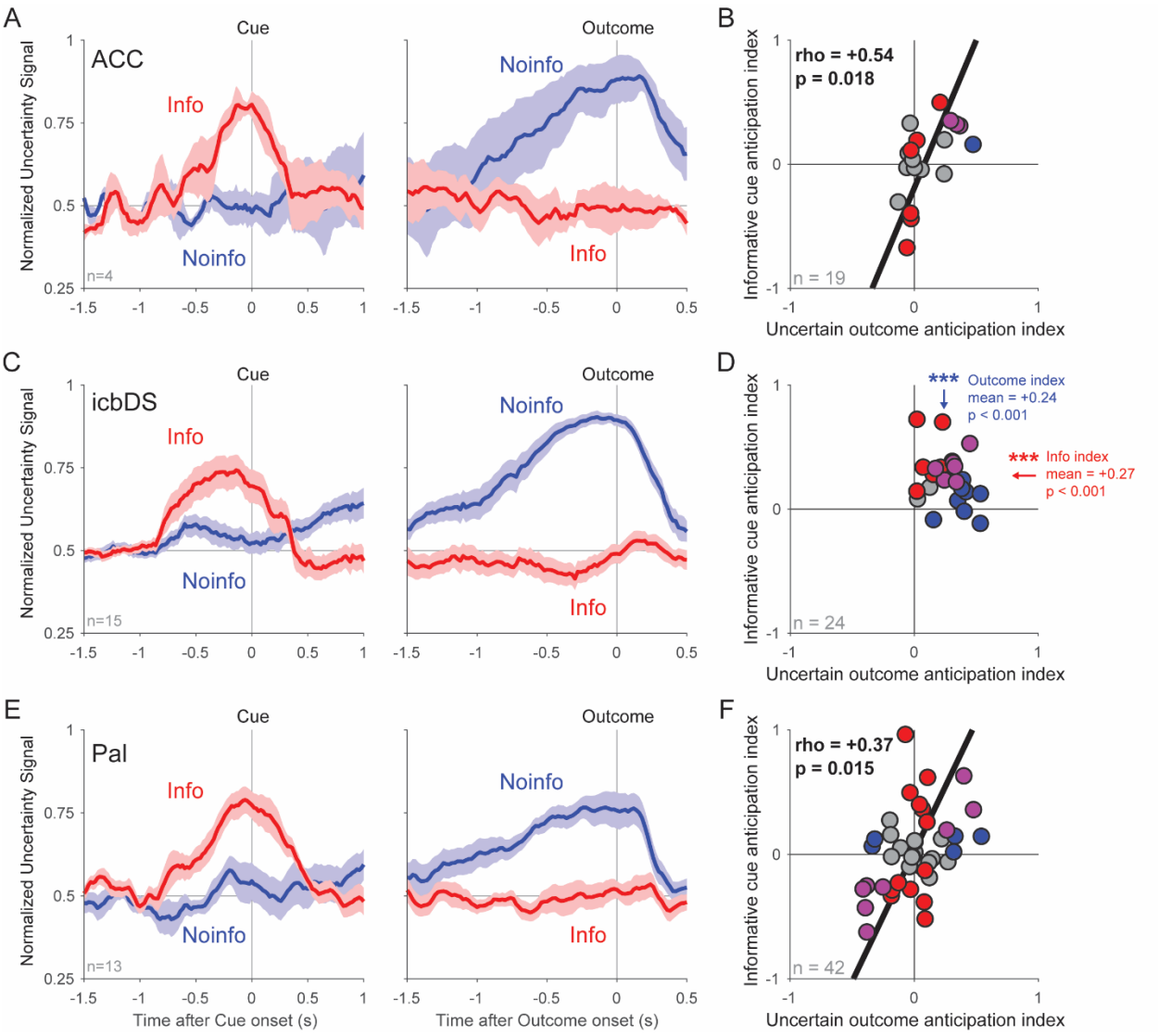

Supplementary Figure 3.4: Same as Fig 3.2G,H, plotted separately for each area. **(A,C,E)** Same as Fig 2H for each area. The average uncertainty signal of neurons that had a significant ramping uncertainty activity measured only using Noinfo trials (i.e. cells with a significant Uncertain Outcome Anticipation Index, $p < 0.05$, permutation test). Note that these neurons are selected solely based on their activity anticipating the outcome on Noinfo trials. Even so, in all areas these populations show a strong uncertainty signal in the same direction anticipating the cue on Info trials. Thus, these neural populations had information-anticipatory activity resembling the theoretical pattern in Fig 2G. **(B,D,F)** Same as Fig 2G for each area. Best-fit lines from type 2 regression are plotted for all areas with significant correlations ($p < 0.05$); arrows are plotted for all areas with significant mean indexes different from 0 ($p < 0.05$). All areas show coding indexes consistent with information-anticipatory activity, though in different manners due to the different signs of neural coding in icbDS vs ACC and Pal. icbDS shows an especially strong pattern of information-anticipatory activity. icbDS neurons only encode uncertainty with a

positive sign, and nearly all neurons are in the upper right quadrant, indicating positive anticipation of both informative cues and uncertain outcomes (mean Info Cue Anticipation Index = +0.27, mean Uncertain Outcome Anticipation Index = +0.24; both significantly greater than 0, signed-rank tests, both $p < 0.0001$). These two indexes are generally consistent across neurons with relatively low variability so there is no significant correlation between them (rho = -0.27, $p = 0.195$). By contrast, ACC and Pal populations included subsets of neurons with different signs and variable strengths of uncertainty coding in standard uncertainty tasks (Fig S1). As a result, information-anticipatory activity should not necessarily lead to non-zero population average indexes, but should result in the two indexes being correlated, indicating that individual neurons anticipate both informative cues and uncertain outcomes in similar manners. Indeed, in both areas there is a strong and significant correlation such that cells with a more positive Info Cue Anticipation Index also have a more positive Uncertain Outcome Anticipation Index (ACC: $p = 0.018$; Pal: $p = 0.015$) – the same pattern seen in Fig 2I for the population of all uncertainty-responsive neurons across the network.

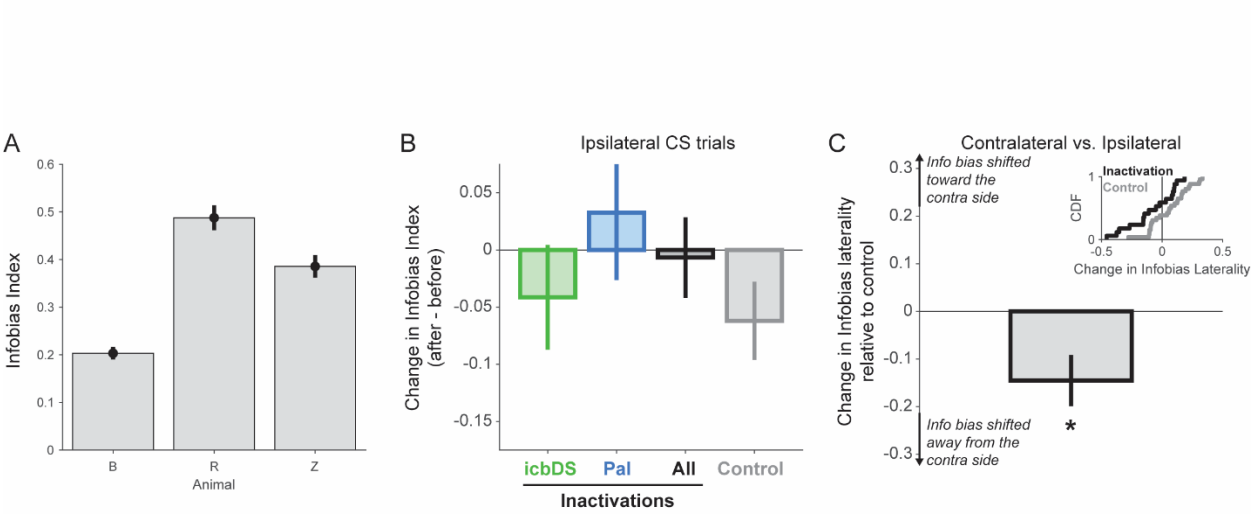

Supplementary Figure 3.5: **(A)** Mean Infobias Index in each animal. All animals had significantly positive Infobias Indexes in the mean over all sessions shown here and in all individual sessions (n=43/43; all $p < 0.05$, permutation tests). **(B)** No apparent change in Infobias Indexes for ipsilateral CSs. Same format as Fig 4C, but for ipsilateral CSs. There is no significant change resulting from inactivations and no significant difference between inactivations and control. **(C)** Inactivations change the laterality of information seeking behavior relative to control sessions. *Inset*: cumulative distributions of change in infobias laterality for inactivations (black) and controls (gray). Change in infobias laterality was quantified as: (change in Infobias Index for contralateral CSs) – (change in Infobias Index for ipsilateral CSs). *Bar plot*: difference in the change in infobias laterality between inactivations and controls. Error bars are ± bootstrap SE. The change in infobias laterality was more negative for inactivations than controls ($p = 0.019$, permutation test), indicating that information seeking behavior was shifted away from the contralateral side relative to controls.

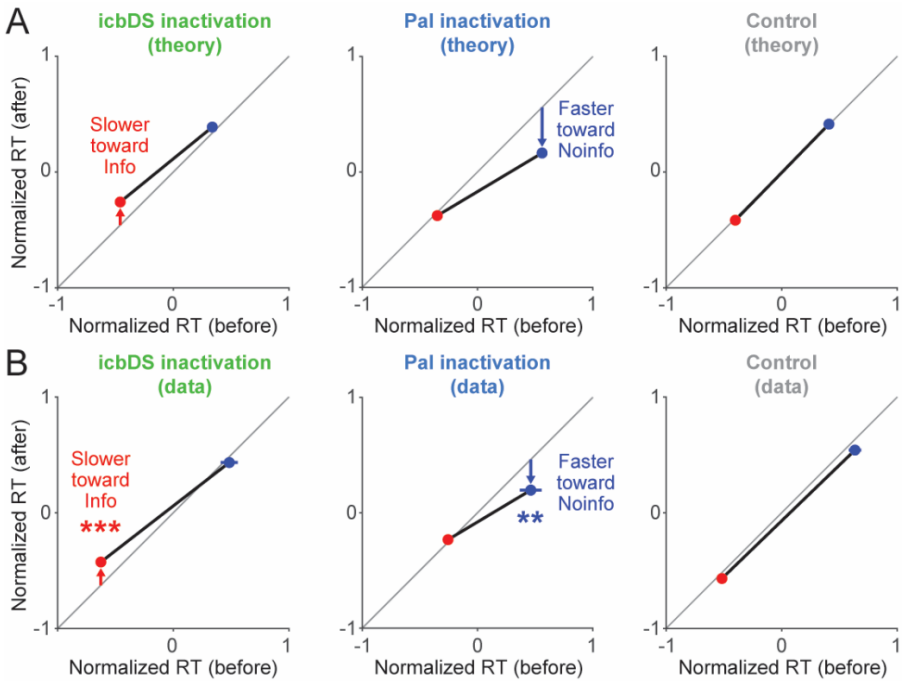

Supplementary Figure 3.6: **(A)** Predictions: the two BG areas should influence information seeking in distinct manners, such that icbDS inactivation slows RTs to obtain information (left, Info CS, red), Pal inactivation speeds RTs that will not obtain information (middle, Noinfo CS, blue), and controls have no effect (right). **(B)** Inactivation results, quantified by comparing normalized RTs (Methods) for the Info CS (red) and Noinfo CS (blue) before vs. after inactivation. icbDS inactivation slowed RTs to the Info CS without any significant effect on Noinfo RTs (left); Pal inactivation speeded RTs to Noinfo CS without any significant effect on Info RTs (middle); control sessions had no significant effect on RTs to either CS (right). Error bars are ± 1 SE.

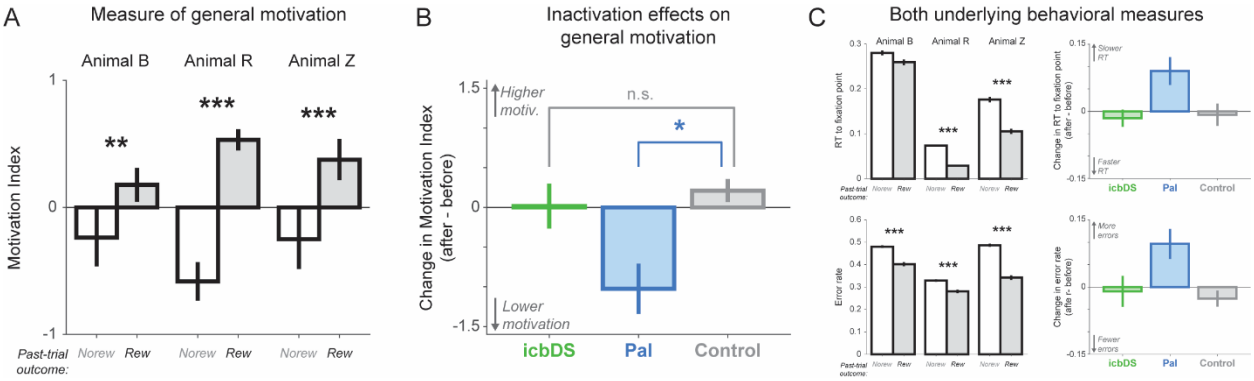

Supplementary Figure 3.7: Inactivation effects on general motivation and reward responsiveness. We quantified the animal's motivation to perform the task using two conventional measures of general motivation: the response time to initiate a trial by fixating on the fixation point on correctly performed trials and the probability of making an error during the trial **(C)**. To summarize these measures and gain statistical power to detect any potential small effect of inactivation on motivation, we created a composite Motivation Index **(A,B)** pooling these measures by z-scoring each measure within each animal, averaging the two measures within each session, and then flipping its sign (so that positive Motivation Index indicates higher motivation to perform the task).

Chapter 4: Conclusion

Neuroscientists, psychologists, and economists alike have long reported that humans and nonhuman animals often prefer to resolve uncertainty about the future at the earliest possible timepoint. This preference is strong enough that humans and nonhuman primates are willing to sacrifice an amount of upcoming reward in order to obtain information about uncertain outcomes, even if this information does nothing to change the value or timing of the outcome. These findings suggest that the information about uncertain outcomes itself has motivational value. In this thesis, we drew inspiration from the large body of research which identifies and describes how the brain monitors, predicts, and motivates behaviors toward pursuing primary rewards. Prior studies detailed diverse cortico-BG networks which contribute to these reward-seeking behaviors. Despite the importance of reward-related information to survival, there remain expansive gaps in there literature as to how the brain motivates behaviors towards uncertainty resolution through information seeking.

Here we presented two studies which expand our understanding of signals within the primate brain that underlie reward uncertainty processing and may play a direct role in motivating information-seeking behaviors:

In the first study we identified a population of neurons within specific, internal capsule-bordering regions of the dorsal striatum which selectively respond to objects associated with uncertain outcomes. We found that the response of these neurons was selective only to uncertain rewarding outcomes and not punishing ones and that it discriminated between objects which predicted different levels of reward uncertainty. We reported that this activity was largely object-presence-dependent and could be reduced by removing the object prior to outcome delivery and that it evolved rapidly as animals learned the value of new object-outcome associations.

Working with our collaborators in the Dr. Suzanne Haber Laboratory, we were able determine the locations of projection sites from ACC to icbDS, as well as between areas of icbDS and pallidum. The regions that project or receive inputs from icbDS contained uncertainty and information anticipation signals similar to icbDS.

In the second study we interrogated the response of single neurons across an identified neural network which spans areas of cortex and BG and found that this activity motivates information-seeking behaviors that resolve uncertain outcomes. First, we confirmed the existence of neurons whose activity was modulated by reward uncertainty in areas of ACC, icbDS, and pallidum. We then demonstrated that a significant portion of neurons in each of these three areas 'shifted' their uncertainty-anticipatory signal to task epochs where uncertainty was resolved by the delivery of advance information, rather than by the task outcome itself. Moreover, we found that each brain area had distinct characteristics in its information-anticipatory signal and that the sign of each signal is congruent with observed anatomy between these structures. We demonstrated that during uncertainty monkeys preferentially direct their gaze at objects associated with gaining information to resolve uncertainty, looking more frequently at these objects in the time preceding uncertainty resolution. This behavior is much like the observed changes in uncertainty-related activity in the ACC, icbDS, and pallidum neurons. Finally, we demonstrated that monkeys shift their gaze faster towards objects which give information about uncertain outcomes and that differences between reaction times to informed and non-informed objects can be altered by disrupting the activity of BG members of this network. By inactivating areas of either the DS or pallidum, we were able to decrease information-seeking bias by differentially influencing reaction time towards informative and non-informative secondary cues.

Following inactivations in DS, subjects were slower to shift their gaze towards informative cues where inactivations in pallidum resulted in faster gaze shifts towards non-informative cues.

In natural environments reward-seeking and information-seeking behaviors are often performed in conjunction with one another; animals must first seek out information about primary rewards within their environment and then act to pursue those rewards. The level of uncertainty in a situation is a crucial variable for determining when information is necessary and when it can be learned from objects within an environment. Our research sheds light on the mechanisms by which similar brain areas- and even similar network structure motifs- that motivate behaviors towards pursuing primary rewards also motivate behavior towards seeking information to resolve uncertainty about those rewards.

Within the BG, for example, previous studies identified contrasting roles of the dorsal striatum and pallidum in guiding behavior towards primary rewards of different sizes. When DS activity was disrupted, animals' gazes were slower to shift towards objects which gave large rewards.[87] Conversely, inactivations within pallidum produced faster reaction times to objects which gave small rewards.[199] Here, we reported corresponding effects, but which are specific to information-seeking preferences rather than reward size.

Our findings also provide insight into the internal circuitry of the BG more broadly. The striatum is typically considered an input nucleus of the BG and the pallidum an output nucleus, suggesting that a signal within the BG would emerge first within the striatum and then later in pallidum. Instead, we report that generalized uncertainty signals emerge first in pallidum and later in icbDS and ACC. These findings support more recent theories that implicate the BG in rapid responses to objects in an environment that can influence future interactions with these objects.[231,232] Indeed, we observed that uncertainty responses in pallidum were very fast to

emerge, but that these responses lacked information on specific levels of uncertainty predicted by an object. In contrast, later signals in ACC and icbDS contained a refined signal of uncertainty, which significantly discriminating between objects and differentiated between levels of uncertainty. This supports popular concepts of ACC, which suggest its importance in foraging and exploration, combining cognitive and motivational variables.[4,154,155] These integrated signals could then be projected to the BG to guide behaviors through known pathways.[46–49]

Clinically, there are large gaps in our understanding of both how emotion and cognition are impacted by uncertain states and how the brain alters behaviors during information-seeking to reduce these states. As a result, mental states associated with mis-evaluation or intolerance of uncertainty in a patient's life, such as generalized anxiety disorder[238,239], obsessive-compulsive disorder[239–241], and impulsive risk-taking[242–244], remain inadequately treated. Indeed, studies suggested that disease states such as these could, at least in part, be driven by pathology in the striatum and related cortico-BG pathways. Furthermore, diseases which disrupt normal function of the striatum have noted consequences on a patient's ability to accurately gauge levels of uncertainty and risk in their daily lives.[245,246] Bettering our understanding of how the brain responds to uncertain states and how these states might drive behaviors towards seeking information to reduce this uncertainty could help to develop more precise interventions for these ailments.

Ultimately, this work identifies novel mechanisms by which the brain anticipates uncertainty and motivates behavior towards seeking information to resolve it. It demonstrates that information-driven behaviors can be reduced by disrupting these mechanisms. Our findings add to the field's understanding of interactions within basal ganglia and across cortico-basal ganglia network motifs and offers insight into how the brain might use analogous cortico-basal

ganglia networks to motivate the concurrent information-seeking and reward-seeking behaviors necessary for survival in our complex and uncertain world.

References

1. Bach DR, Dolan RJ. Knowing how much you don't know: a neural organization of uncertainty estimates. *Nat Rev Neurosci*. 2012;13(8):572-586. doi:10.1038/nrn3289

2. Rushworth MFS, Behrens TEJ. Choice, uncertainty and value in prefrontal and cingulate cortex. *Nat Neurosci*. 2008;11(4):389-397. doi:10.1038/nn2066

3. Platt ML, Huettel SA. Risky business: the neuroeconomics of decision making under uncertainty. *Nat Neurosci*. 2008;11(4):398-403. doi:10.1038/nn2062

4. Behrens TEJ, Woolrich MW, Walton ME, Rushworth MFS. Learning the value of information in an uncertain world. *Nat Neurosci*. 2007;10(9):1214-1221. doi:10.1038/nn1954

5. Dayan P, Kakade S, Montague PR. Learning and selective attention. *Nat Neurosci*. 2000;3 Suppl:1218-1223. doi:10.1038/81504

6. Yu AJ, Dayan P. Uncertainty, neuromodulation, and attention. *Neuron*. 2005;46(4):681-692. doi:10.1016/j.neuron.2005.04.026

7. Paulsen DJ, Platt ML, Huettel SA, Brannon EM. From Risk-Seeking to Risk-Averse: The Development of Economic Risk Preference from Childhood to Adulthood. *Front Psychol*. 2012;3. doi:10.3389/fpsyg.2012.00313

8. Schultz W, Preuschoff K, Camerer C, et al. Explicit neural signals reflecting reward uncertainty. *Philos Trans R Soc Lond B Biol Sci*. 2008;363(1511):3801-3811. doi:10.1098/rstb.2008.0152

9. Hirsh JB, Mar RA, Peterson JB. Psychological entropy: a framework for understanding uncertainty-related anxiety. *Psychol Rev*. 2012;119(2):304-320. doi:10.1037/a0026767

10. Hsu M, Bhatt M, Adolphs R, Tranel D, Camerer CF. Neural systems responding to degrees of uncertainty in human decision-making. *Science*. 2005;310(5754):1680-1683. doi:10.1126/science.1115327

11. Preuschoff K, Bossaerts P, Quartz SR. Neural Differentiation of Expected Reward and Risk in Human Subcortical Structures. *Neuron*. 2006;51(3):381-390. doi:10.1016/j.neuron.2006.06.024

12. Stern ER, Gonzalez R, Welsh RC, Taylor SF. Updating beliefs for a decision: Neural correlates of uncertainty and underconfidence. *J Neurosci*. 2010;30(23):8032-8041. doi:10.1523/JNEUROSCI.4729-09.2010

13. Christopoulos GI, Tobler PN, Bossaerts P, Dolan RJ, Schultz W. Neural correlates of value, risk, and risk aversion contributing to decision making under risk. *J Neurosci*. 2009;29(40):12574-12583. doi:10.1523/JNEUROSCI.2614-09.2009

14. Preuschoff K, Quartz SR, Bossaerts P. Human insula activation reflects risk prediction errors as well as risk. *J Neurosci*. 2008;28(11):2745-2752. doi:10.1523/JNEUROSCI.4286-07.2008

15. Monosov IE. Anterior cingulate is a source of valence-specific information about value and uncertainty. *Nature Communications*. 2017;8(1):134. doi:10.1038/s41467-017-00072-y

16. Ledbetter NM, Chen CD, Monosov IE. Multiple Mechanisms for Processing Reward Uncertainty in the Primate Basal Forebrain. *J Neurosci*. 2016;36(30):7852-7864. doi:10.1523/JNEUROSCI.1123-16.2016

17. Monosov IE, Leopold DA, Hikosaka O. Neurons in the Primate Medial Basal Forebrain Signal Combined Information about Reward Uncertainty, Value, and Punishment Anticipation. *J Neurosci*. 2015;35(19):7443-7459. doi:10.1523/JNEUROSCI.0051-15.2015

18. Monosov IE, Hikosaka O. Selective and graded coding of reward-uncertainty by neurons in the primate anterodorsal septal region. *Nat Neurosci*. 2013;16(6):756-762. doi:10.1038/nn.3398

19. O'Neill M, Schultz W. Economic risk coding by single neurons in the orbitofrontal cortex. *J Physiol Paris*. 2015;109(1-3):70-77. doi:10.1016/j.jphysparis.2014.06.002

20. O'Neill M, Schultz W. Coding of reward risk by orbitofrontal neurons is mostly distinct from coding of reward value. *Neuron*. 2010;68(4):789-800. doi:10.1016/j.neuron.2010.09.031

21. Monosov IE, Hikosaka O. Regionally distinct processing of rewards and punishments by the primate ventromedial prefrontal cortex. *J Neurosci*. 2012;32(30):10318-10330. doi:10.1523/JNEUROSCI.1801-12.2012

22. McCoy AN, Platt ML. Risk-sensitive neurons in macaque posterior cingulate cortex. *Nat Neurosci*. 2005;8(9):1220-1227. doi:10.1038/nn1523

23. Wyckoff Jr. LB. The role of observing responses in discrimination learning. Part I. *Psychological Review*. 1952;59(6):431-442. doi:10.1037/h0053932

24. Zeigler HP, Jr LBW. Observing responses and discrimination learning. *Quarterly Journal of Experimental Psychology*. 1961;13(3):129-140. doi:10.1080/17470216108416486

25. Shahan TA. Observing behavior: effects of rate and magnitude of primary reinforcement. *J Exp Anal Behav*. 2002;78(2):161-178. doi:10.1901/jeab.2002.78-161

26. Bromberg-Martin ES, Hikosaka O. Midbrain Dopamine Neurons Signal Preference for Advance Information about Upcoming Rewards. *Neuron*. 2009;63(1):119-126. doi:10.1016/j.neuron.2009.06.009

27. Bromberg-Martin ES, Hikosaka O. Lateral habenula neurons signal errors in the prediction of reward information. *Nature Neuroscience*. 2011;14(9):1209-1216. doi:10.1038/nn.2902

28. Blanchard TC, Hayden BY, Bromberg-Martin ES. Orbitofrontal Cortex Uses Distinct Codes for Different Choice Attributes in Decisions Motivated by Curiosity. *Neuron*. 2015;85(3):602-614. doi:10.1016/j.neuron.2014.12.050

29. Kreps DM, Porteus EL. Temporal Resolution of Uncertainty and Dynamic Choice Theory. *Econometrica*. 1978;46(1):185-200. doi:10.2307/1913656

30. Chew SH, Ho JL. Hope: An empirical study of attitude toward the timing of uncertainty resolution. *J Risk Uncertainty*. 1994;8(3):267-288. doi:10.1007/BF01064045

31. Eliaz K, Schotter A. Experimental Testing of Intrinsic Preferences for NonInstrumental Information. *American Economic Review*. 2007;97(2):166-169. doi:10.1257/aer.97.2.166

32. Montague PR, Hyman SE, Cohen JD. Computational roles for dopamine in behavioural control. *Nature*. 2004;431(7010):760-767. doi:10.1038/nature03015

33. Holroyd CB, Coles MGH. The neural basis of human error processing: reinforcement learning, dopamine, and the error-related negativity. *Psychol Rev*. 2002;109(4):679-709. doi:10.1037/0033-295X.109.4.679

34. Wise RA. Dopamine, learning and motivation. *Nature Reviews Neuroscience*. 2004;5(6):483-494. doi:10.1038/nrn1406

35. Romo R, Schultz W. Dopamine neurons of the monkey midbrain: contingencies of responses to active touch during self-initiated arm movements. *Journal of Neurophysiology*. 1990;63(3):592-606. doi:10.1152/jn.1990.63.3.592

36. Bayer HM, Glimcher PW. Midbrain dopamine neurons encode a quantitative reward prediction error signal. *Neuron*. 2005;47(1):129-141. doi:10.1016/j.neuron.2005.05.020

37. Schultz W, Dayan P, Montague PR. A Neural Substrate of Prediction and Reward. *Science*. 1997;275(5306):1593-1599. doi:10.1126/science.275.5306.1593

38. Dickinson A, Smith J, Mirenowicz J. Dissociation of Pavlovian and instrumental incentive learning under dopamine antagonists. *Behav Neurosci*. 2000;114(3):468-483.

39. Chase HW, Kumar P, Eickhoff SB, Dombrovski AY. Reinforcement Learning Models and Their Neural Correlates: An Activation Likelihood Estimation Meta-Analysis. *Cogn Affect Behav Neurosci*. 2015;15(2):435-459. doi:10.3758/s13415-015-0338-7

40. Beierholm UR, Dayan P. Pavlovian-Instrumental Interaction in 'Observing Behavior.' *PLoS Comput Biol*. 2010;6(9). doi:10.1371/journal.pcbi.1000903

41. Iigaya K, Story GW, Kurth-Nelson Z, Dolan RJ, Dayan P. The modulation of savouring by prediction error and its effects on choice. *Elife*. 2016;5. doi:10.7554/eLife.13747

42. Bennett D, Bode S, Brydevall M, Warren H, Murawski C. Intrinsic Valuation of Information in Decision Making under Uncertainty. *PLoS Comput Biol*. 2016;12(7):e1005020. doi:10.1371/journal.pcbi.1005020

43. Wise SP, Jones EG. Cells of origin and terminal distribution of descending projections of the rat somatic sensory cortex. *Journal of Comparative Neurology*. 1977;175(2):129-157. doi:10.1002/cne.901750202

44. McGeorge AJ, Faull RL. The organization of the projection from the cerebral cortex to the striatum in the rat. *Neuroscience*. 1989;29(3):503-537.

45. Alexander GE, Crutcher MD. Functional architecture of basal ganglia circuits: neural substrates of parallel processing. *Trends in Neurosciences*. 1990;13(7):266-271. doi:10.1016/0166-2236(90)90107-L

46. Haber SN. The primate basal ganglia: parallel and integrative networks. *Journal of Chemical Neuroanatomy*. 2003;26(4):317-330. doi:10.1016/j.jchemneu.2003.10.003

47. Sesack SR, Grace AA. Cortico-Basal Ganglia Reward Network: Microcircuitry. *Neuropsychopharmacology*. 2010;35(1):27-47. doi:10.1038/npp.2009.93

48. Ferry AT, Ongür D, An X, Price JL. Prefrontal cortical projections to the striatum in macaque monkeys: evidence for an organization related to prefrontal networks. *J Comp Neurol*. 2000;425(3):447-470.

49. Haber SN, Knutson B. The reward circuit: linking primate anatomy and human imaging. *Neuropsychopharmacology*. 2010;35(1):4-26. doi:10.1038/npp.2009.129

50. Haber SN, Kim K-S, Mailly P, Calzavara R. Reward-Related Cortical Inputs Define a Large Striatal Region in Primates That Interface with Associative Cortical Connections, Providing a Substrate for Incentive-Based Learning. *Journal of Neuroscience*. 2006;26(32):8368-8376. doi:10.1523/JNEUROSCI.0271-06.2006

51. François C, Yelnik J, Tandé D, Agid Y, Hirsch EC. Dopaminergic cell group A8 in the monkey: anatomical organization and projections to the striatum. *J Comp Neurol*. 1999;414(3):334-347.

52. Langer LF, Graybiel AM. Distinct nigrostriatal projection systems innervate striosomes and matrix in the primate striatum. *Brain Res*. 1989;498(2):344-350.

53. Haber SN, Fudge JL. The primate substantia nigra and VTA: integrative circuitry and function. *Crit Rev Neurobiol*. 1997;11(4):323-342.

54. Joel D, Weiner I. The connections of the dopaminergic system with the striatum in rats and primates: an analysis with respect to the functional and compartmental organization of the striatum. *Neuroscience*. 2000;96(3):451-474.

55. Kötter R. Postsynaptic integration of glutamatergic and dopaminergic signals in the striatum. *Progress in Neurobiology*. 1994;44(2):163-196. doi:10.1016/0301-0082(94)90037-X

56. Tepper JM, Bolam JP. Functional diversity and specificity of neostriatal interneurons. *Curr Opin Neurobiol*. 2004;14(6):685-692. doi:10.1016/j.conb.2004.10.003

57. Tepper JM, Plenz D. MICROCIRCUITS IN THE STRIATUM STRIATAL CELL TYPES AND THEIR INTERACTION. *The MIT Press*.:12.

58. Volkow ND, Wang G-J, Fowler JS, Tomasi D. Addiction Circuitry in the Human Brain. *Annu Rev Pharmacol Toxicol*. 2012;52:321-336. doi:10.1146/annurev-pharmtox-010611-134625

59. Koepp MJ, Gunn RN, Lawrence AD, et al. Evidence for striatal dopamine release during a video game. *Nature*. 1998;393(6682):266-268. doi:10.1038/30498

60. Breiter HC, Aharon I, Kahneman D, Dale A, Shizgal P. Functional imaging of neural responses to expectancy and experience of monetary gains and losses. *Neuron*. 2001;30(2):619-639.

61. O'Doherty JP, Deichmann R, Critchley HD, Dolan RJ. Neural responses during anticipation of a primary taste reward. *Neuron*. 2002;33(5):815-826.

62. Knutson B, Cooper JC. Functional magnetic resonance imaging of reward prediction. *Curr Opin Neurol*. 2005;18(4):411-417.

63. Haruno M, Kawato M. Different Neural Correlates of Reward Expectation and Reward Expectation Error in the Putamen and Caudate Nucleus During Stimulus-Action-Reward Association Learning. *Journal of Neurophysiology*. 2006;95(2):948-959. doi:10.1152/jn.00382.2005

64. Delgado MR, Miller MM, Inati S, Phelps EA. An fMRI study of reward-related probability learning. *NeuroImage*. 2005;24(3):862-873. doi:10.1016/j.neuroimage.2004.10.002

65. Delgado MR, Nystrom LE, Fissell C, Noll DC, Fiez JA. Tracking the hemodynamic responses to reward and punishment in the striatum. *J Neurophysiol*. 2000;84(6):3072-3077. doi:10.1152/jn.2000.84.6.3072

66. Knutson B, Adams CM, Fong GW, Hommer D. Anticipation of increasing monetary reward selectively recruits nucleus accumbens. *J Neurosci*. 2001;21(16):RC159.

67. Knutson B, Westdorp A, Kaiser E, Hommer D. FMRI Visualization of Brain Activity during a Monetary Incentive Delay Task. *NeuroImage*. 2000;12(1):20-27. doi:10.1006/nimg.2000.0593

68. Kawagoe R, Takikawa Y, Hikosaka O. Expectation of reward modulates cognitive signals in the basal ganglia. *Nat Neurosci*. 1998;1(5):411-416. doi:10.1038/1625

69. Apicella P, Scarnati E, Ljungberg T, Schultz W. Neuronal activity in monkey striatum related to the expectation of predictable environmental events. *J Neurophysiol*. 1992;68(3):945-960. doi:10.1152/jn.1992.68.3.945

70. Hikosaka O, Sakamoto M, Usui S. Functional properties of monkey caudate neurons. I. Activities related to saccadic eye movements. *J Neurophysiol*. 1989;61(4):780-798. doi:10.1152/jn.1989.61.4.780

71. Apicella P, Ljungberg T, Scarnati E, Schultz W. Responses to reward in monkey dorsal and ventral striatum. *Exp Brain Res*. 1991;85(3):491-500. doi:10.1007/BF00231732

72. Graybiel AM, Grafton ST. The Striatum: Where Skills and Habits Meet. *Cold Spring Harb Perspect Biol*. 2015;7(8). doi:10.1101/cshperspect.a021691

73. Samejima K, Ueda Y, Doya K, Kimura M. Representation of action-specific reward values in the striatum. *Science*. 2005;310(5752):1337-1340. doi:10.1126/science.1115270

74. Lauwereyns J, Watanabe K, Coe B, Hikosaka O. A neural correlate of response bias in monkey caudate nucleus. *Nature*. 2002;418(6896):413-417. doi:10.1038/nature00892

75. Graybiel AM. Habits, rituals, and the evaluative brain. *Annu Rev Neurosci*. 2008;31:359-387. doi:10.1146/annurev.neuro.29.051605.112851

76. Kim HF, Hikosaka O. Distinct basal ganglia circuits controlling behaviors guided by flexible and stable values. *Neuron*. 2013;79(5):1001-1010. doi:10.1016/j.neuron.2013.06.044

77. Nakamura K, Santos GS, Matsuzaki R, Nakahara H. Differential reward coding in the subdivisions of the primate caudate during an oculomotor task. *J Neurosci*. 2012;32(45):15963-15982. doi:10.1523/JNEUROSCI.1518-12.2012

78. Lau B, Glimcher PW. Value representations in the primate striatum during matching behavior. *Neuron*. 2008;58(3):451-463. doi:10.1016/j.neuron.2008.02.021

79. Cai X, Kim S, Lee D. Heterogeneous coding of temporally discounted values in the dorsal and ventral striatum during intertemporal choice. *Neuron*. 2011;69(1):170-182. doi:10.1016/j.neuron.2010.11.041

80. Yin HH, Knowlton BJ, Balleine BW. Inactivation of dorsolateral striatum enhances sensitivity to changes in the action-outcome contingency in instrumental conditioning. *Behav Brain Res*. 2006;166(2):189-196. doi:10.1016/j.bbr.2005.07.012

81. Ricker JM, Kopchock RJ, Drown RM, Cromwell HC. Effects of striatal lesions on components of choice: Reward discrimination, preference, and relative valuation. *Behav Brain Res*. 2016;315:130-140. doi:10.1016/j.bbr.2016.08.031

82. Miyachi S, Hikosaka O, Miyashita K, Kárádi Z, Rand MK. Differential roles of monkey striatum in learning of sequential hand movement. *Exp Brain Res*. 1997;115(1):1-5. doi:10.1007/PL00005669

83. Yin HH, Knowlton BJ, Balleine BW. Lesions of dorsolateral striatum preserve outcome expectancy but disrupt habit formation in instrumental learning. *Eur J Neurosci*. 2004;19(1):181-189.

84. Yin HH, Knowlton BJ, Balleine BW. Blockade of NMDA receptors in the dorsomedial striatum prevents action-outcome learning in instrumental conditioning. *Eur J Neurosci*. 2005;22(2):505-512. doi:10.1111/j.1460-9568.2005.04219.x

85. Atallah HE, Lopez-Paniagua D, Rudy JW, O'Reilly RC. Separate neural substrates for skill learning and performance in the ventral and dorsal striatum. *Nature Neuroscience*. 2007;10(1):126-131. doi:10.1038/nn1817

86. Muranishi M, Inokawa H, Yamada H, et al. Inactivation of the putamen selectively impairs reward history-based action selection. *Exp Brain Res*. 2011;209(2):235-246. doi:10.1007/s00221-011-2545-y

87. Nakamura K, Hikosaka O. Role of Dopamine in the Primate Caudate Nucleus in Reward Modulation of Saccades. *J Neurosci*. 2006;26(20):5360-5369. doi:10.1523/JNEUROSCI.4853-05.2006

88. Heilbronner SR, Meyer MAA, Choi EY, Haber SN. How do cortico-striatal projections impact on downstream pallidal circuitry? *Brain Struct Funct*. 2018;223(6):2809-2821. doi:10.1007/s00429-018-1662-9

89. Chikama M, McFarland NR, Amaral DG, Haber SN. Insular Cortical Projections to Functional Regions of the Striatum Correlate with Cortical Cytoarchitectonic Organization in the Primate. *J Neurosci*. 1997;17(24):9686-9705. doi:10.1523/JNEUROSCI.17-24-09686.1997

90. Alexander GE, DeLong MR, Strick PL. Parallel organization of functionally segregated circuits linking basal ganglia and cortex. *Annu Rev Neurosci*. 1986;9:357-381. doi:10.1146/annurev.ne.09.030186.002041

91. Künzle H. Bilateral projections from precentral motor cortex to the putamen and other parts of the basal ganglia. An autoradiographic study inMacaca fascicularis. *Brain Research*. 1975;88(2):195-209. doi:10.1016/0006-8993(75)90384-4

92. Kunishio K, Haber SN. Primate cingulostriatal projection: Limbic striatal versus sensorimotor striatal input. *Journal of Comparative Neurology*. 1994;350(3):337-356. doi:10.1002/cne.903500302

93. Flaherty AW, Graybiel AM. Input-output organization of the sensorimotor striatum in the squirrel monkey. *J Neurosci*. 1994;14(2):599-610.

94. McFarland NR, Haber SN. Convergent inputs from thalamic motor nuclei and frontal cortical areas to the dorsal striatum in the primate. *J Neurosci*. 2000;20(10):3798-3813.

95. Isomura Y, Takekawa T, Harukuni R, et al. Reward-modulated motor information in identified striatum neurons. *J Neurosci*. 2013;33(25):10209-10220. doi:10.1523/JNEUROSCI.0381-13.2013

96. Van den Bercken JH, Cools AR. Evidence for a role of the caudate nucleus in the sequential organization of behavior. *Behav Brain Res*. 1982;4(4):319-327.

97. Berridge KC, Whishaw IQ. Cortex, striatum and cerebellum: control of serial order in a grooming sequence. *Exp Brain Res*. 1992;90(2):275-290.

98. Pellis SM, Castañeda E, McKenna MM, Tran-Nguyen LT, Whishaw IQ. The role of the striatum in organizing sequences of play fighting in neonatally dopamine-depleted rats. *Neurosci Lett*. 1993;158(1):13-15.

99. Yin HH. The Sensorimotor Striatum Is Necessary for Serial Order Learning. *J Neurosci*. 2010;30(44):14719-14723. doi:10.1523/JNEUROSCI.3989-10.2010

100. Aldridge JW, Anderson RJ, Murphy JT. Sensory-motor processing in the caudate nucleus and globus pallidus: a single-unit study in behaving primates. *Can J Physiol Pharmacol*. 1980;58(10):1192-1201.

101. Kimura M. The role of primate putamen neurons in the association of sensory stimuli with movement. *Neurosci Res*. 1986;3(5):436-443.

102. Hikosaka O, Sakai K, Miyauchi S, Takino R, Sasaki Y, Pütz B. Activation of human presupplementary motor area in learning of sequential procedures: a functional MRI study. *J Neurophysiol*. 1996;76(1):617-621. doi:10.1152/jn.1996.76.1.617

103. Boecker H, Dagher A, Ceballos-Baumann AO, et al. Role of the human rostral supplementary motor area and the basal ganglia in motor sequence control: investigations with H2 15O PET. *J Neurophysiol*. 1998;79(2):1070-1080. doi:10.1152/jn.1998.79.2.1070

104. Opris I, Lebedev M, Nelson RJ. Motor Planning under Unpredictable Reward: Modulations of Movement Vigor and Primate Striatum Activity. *Front Neurosci*. 2011;5:61. doi:10.3389/fnins.2011.00061

105. Faure A, Haberland U, Condé F, El Massioui N. Lesion to the nigrostriatal dopamine system disrupts stimulus-response habit formation. *J Neurosci*. 2005;25(11):2771-2780. doi:10.1523/JNEUROSCI.3894-04.2005

106. Jog MS, Kubota Y, Connolly CI, Hillegaart V, Graybiel AM. Building neural representations of habits. *Science*. 1999;286(5445):1745-1749.

107. Hikosaka O, Yamamoto S, Yasuda M, Kim HF. Why skill matters. *Trends Cogn Sci (Regul Ed)*. 2013;17(9):434-441. doi:10.1016/j.tics.2013.07.001

108. Haber SN, Kunishio K, Mizobuchi M, Lynd-Balta E. The orbital and medial prefrontal circuit through the primate basal ganglia. *J Neurosci*. 1995;15(7 Pt 1):4851-4867.

109. Hollerman JR, Tremblay L, Schultz W. Involvement of basal ganglia and orbitofrontal cortex in goal-directed behavior. In: *Progress in Brain Research*. Vol 126. Cognition, emotion and autonomic responses: The integrative role of the prefrontal cortex and limbic structures. Elsevier; 2000:193-215. doi:10.1016/S0079-6123(00)26015-9

110. Goto Y, Grace AA. Dopaminergic modulation of limbic and cortical drive of nucleus accumbens in goal-directed behavior. *Nat Neurosci*. 2005;8(6):805-812. doi:10.1038/nn1471

111. Hare TA, O'Doherty J, Camerer CF, Schultz W, Rangel A. Dissociating the Role of the Orbitofrontal Cortex and the Striatum in the Computation of Goal Values and Prediction Errors. *J Neurosci*. 2008;28(22):5623-5630. doi:10.1523/JNEUROSCI.1309-08.2008

112. Setlow B, Schoenbaum G, Gallagher M. Neural Encoding in Ventral Striatum during Olfactory Discrimination Learning. *Neuron*. 2003;38(4):625-636. doi:10.1016/S0896-6273(03)00264-2

113. Kelley AE. Ventral striatal control of appetitive motivation: role in ingestive behavior and reward-related learning. *Neuroscience & Biobehavioral Reviews*. 2004;27(8):765-776. doi:10.1016/j.neubiorev.2003.11.015

114. O'Doherty J, Dayan P, Schultz J, Deichmann R, Friston K, Dolan RJ. Dissociable Roles of Ventral and Dorsal Striatum in Instrumental Conditioning. *Science*. 2004;304(5669):452-454. doi:10.1126/science.1094285

115. McDannald MA, Lucantonio F, Burke KA, Niv Y, Schoenbaum G. Ventral Striatum and Orbitofrontal Cortex Are Both Required for Model-Based, But Not Model-Free, Reinforcement Learning. *J Neurosci*. 2011;31(7):2700-2705. doi:10.1523/JNEUROSCI.5499-10.2011

116. Saxena S, Rauch SL. FUNCTIONAL NEUROIMAGING AND THE NEUROANATOMY OF OBSESSIVE-COMPULSIVE DISORDER. *Psychiatric Clinics of North America*. 2000;23(3):563-586. doi:10.1016/S0193-953X(05)70181-7

117. Remijnse PL, Nielen MMA, Balkom AJLM van, et al. Reduced Orbitofrontal-Striatal Activity on a Reversal Learning Task in Obsessive-Compulsive Disorder. *Arch Gen Psychiatry*. 2006;63(11):1225-1236. doi:10.1001/archpsyc.63.11.1225

118. Menzies L, Chamberlain SR, Laird AR, Thelen SM, Sahakian BJ, Bullmore ET. Integrating evidence from neuroimaging and neuropsychological studies of obsessive-compulsive disorder: The orbitofronto-striatal model revisited. *Neuroscience & Biobehavioral Reviews*. 2008;32(3):525-549. doi:10.1016/j.neubiorev.2007.09.005

119. Ahmari SE, Spellman T, Douglass NL, et al. Repeated Cortico-Striatal Stimulation Generates Persistent OCD-Like Behavior. *Science*. 2013;340(6137):1234-1239. doi:10.1126/science.1234733

120. Barch DM, Dowd EC. Goal Representations and Motivational Drive in Schizophrenia: The Role of Prefrontal–Striatal Interactions. *Schizophr Bull*. 2010;36(5):919-934. doi:10.1093/schbul/sbq068

121. Fettes P, Schulze L, Downar J. Cortico-Striatal-Thalamic Loop Circuits of the Orbitofrontal Cortex: Promising Therapeutic Targets in Psychiatric Illness. *Front Syst Neurosci*. 2017;11. doi:10.3389/fnsys.2017.00025

122. Leh SE, Ptito A, Chakravarty MM, Strafella AP. Fronto-striatal connections in the human brain: A probabilistic diffusion tractography study. *Neuroscience Letters*. 2007;419(2):113-118. doi:10.1016/j.neulet.2007.04.049

123. Ballard IC, Murty VP, Carter RM, MacInnes JJ, Huettel SA, Adcock RA. Dorsolateral Prefrontal Cortex Drives Mesolimbic Dopaminergic Regions to Initiate Motivated Behavior. *J Neurosci*. 2011;31(28):10340-10346. doi:10.1523/JNEUROSCI.0895-11.2011

124. Ray R, Zald DH. Anatomical insights into the interaction of emotion and cognition in the prefrontal cortex. *Neurosci Biobehav Rev*. 2012;36(1):479-501. doi:10.1016/j.neubiorev.2011.08.005

125. Smith EE, Jonides J. Working memory: a view from neuroimaging. *Cogn Psychol*. 1997;33(1):5-42. doi:10.1006/cogp.1997.0658

126. Fuster JM. Prefrontal neurons in networks of executive memory. *Brain Res Bull*. 2000;52(5):331-336.

127. Frank MJ, Loughry B, O'Reilly RC. Interactions between frontal cortex and basal ganglia in working memory: A computational model. *Cognitive, Affective, & Behavioral Neuroscience*. 2001;1(2):137-160. doi:10.3758/CABN.1.2.137

128. O'Reilly RC, Frank MJ. Making Working Memory Work: A Computational Model of Learning in the Prefrontal Cortex and Basal Ganglia. *Neural Computation*. 2006;18(2):283-328. doi:10.1162/089976606775093909

129. Dahlin E, Neely AS, Larsson A, Bäckman L, Nyberg L. Transfer of Learning After Updating Training Mediated by the Striatum. *Science*. 2008;320(5882):1510-1512. doi:10.1126/science.1155466

130. Barbey AK, Koenigs M, Grafman J. Dorsolateral prefrontal contributions to human working memory. *Cortex*. 2013;49(5):1195-1205. doi:10.1016/j.cortex.2012.05.022

131. Eslinger PJ, Grattan LM. Frontal lobe and frontal-striatal substrates for different forms of human cognitive flexibility. *Neuropsychologia*. 1993;31(1):17-28. doi:10.1016/0028-3932(93)90077-D

132. Ragozzino ME, Ragozzino KE, Mizumori SJY, Kesner RP. Role of the dorsomedial striatum in behavioral flexibility for response and visual cue discrimination learning. *Behav Neurosci*. 2002;116(1):105-115.

133. Ragozzino ME. The Contribution of the Medial Prefrontal Cortex, Orbitofrontal Cortex, and Dorsomedial Striatum to Behavioral Flexibility. *Annals of the New York Academy of Sciences*. 2007;1121(1):355-375. doi:10.1196/annals.1401.013

134. Kehagia AA, Murray GK, Robbins TW. Learning and cognitive flexibility: frontostriatal function and monoaminergic modulation. *Current Opinion in Neurobiology*. 2010;20(2):199-204. doi:10.1016/j.conb.2010.01.007

135. Zheng T, Wilson CJ. Corticostriatal combinatorics: the implications of corticostriatal axonal arborizations. *J Neurophysiol*. 2002;87(2):1007-1017. doi:10.1152/jn.00519.2001

136. Haber SN, Fudge JL, McFarland NR. Striatonigrostriatal pathways in primates form an ascending spiral from the shell to the dorsolateral striatum. *J Neurosci*. 2000;20(6):2369-2382.

137. Percheron G, Filion M. Parallel processing in the basal ganglia: up to a point. *Trends in Neurosciences*. 1991;14(2):55-56. doi:10.1016/0166-2236(91)90020-U

138. Yelnik J, François C, Percheron G. Spatial relationships between striatal axonal endings and pallidal neurons in macaque monkeys. *Adv Neurol*. 1997;74:45-56.

139. Joel D, Weiner I. The connections of the primate subthalamic nucleus: indirect pathways and the open-interconnected scheme of basal ganglia-thalamocortical circuitry. *Brain Res Brain Res Rev*. 1997;23(1-2):62-78.

140. Balleine BW, Delgado MR, Hikosaka O. The Role of the Dorsal Striatum in Reward and Decision-Making. *J Neurosci*. 2007;27(31):8161-8165. doi:10.1523/JNEUROSCI.1554-07.2007

141. Cools R. Dopaminergic control of the striatum for high-level cognition. *Current Opinion in Neurobiology*. 2011;21(3):402-407. doi:10.1016/j.conb.2011.04.002

142. Kennerley SW, Walton ME, Behrens TEJ, Buckley MJ, Rushworth MFS. Optimal decision making and the anterior cingulate cortex. *Nat Neurosci*. 2006;9(7):940-947. doi:10.1038/nn1724

143. Rudebeck PH, Behrens TE, Kennerley SW, et al. Frontal cortex subregions play distinct roles in choices between actions and stimuli. *J Neurosci*. 2008;28(51):13775-13785. doi:10.1523/JNEUROSCI.3541-08.2008

144. Wallis JD, Kennerley SW. Heterogeneous reward signals in prefrontal cortex. *Curr Opin Neurobiol*. 2010;20(2):191-198. doi:10.1016/j.conb.2010.02.009

145. Cai X, Padoa-Schioppa C. Neuronal encoding of subjective value in dorsal and ventral anterior cingulate cortex. *J Neurosci*. 2012;32(11):3791-3808. doi:10.1523/JNEUROSCI.3864-11.2012

146. Shenhav A, Botvinick MM, Cohen JD. The expected value of control: an integrative theory of anterior cingulate cortex function. *Neuron*. 2013;79(2):217-240. doi:10.1016/j.neuron.2013.07.007

147. Kwan CL, Crawley AP, Mikulis DJ, Davis KD. An fMRI study of the anterior cingulate cortex and surrounding medial wall activations evoked by noxious cutaneous heat and cold stimuli. *Pain*. 2000;85(3):359-374.

148. Iwata K, Kamo H, Ogawa A, et al. Anterior cingulate cortical neuronal activity during perception of noxious thermal stimuli in monkeys. *J Neurophysiol*. 2005;94(3):1980-1991. doi:10.1152/jn.00190.2005

149. Rainville P, Duncan GH, Price DD, Carrier B, Bushnell MC. Pain affect encoded in human anterior cingulate but not somatosensory cortex. *Science*. 1997;277(5328):968-971.

150. Kennerley SW, Behrens TEJ, Wallis JD. Double dissociation of value computations in orbitofrontal and anterior cingulate neurons. *Nature Neuroscience*. 2011;14(12):1581-1589. doi:10.1038/nn.2961

151. Mulert C, Menzinger E, Leicht G, Pogarell O, Hegerl U. Evidence for a close relationship between conscious effort and anterior cingulate cortex activity. *International Journal of Psychophysiology*. 2005;56(1):65-80. doi:10.1016/j.ijpsycho.2004.10.002

152. Walton ME, Bannerman DM, Alterescu K, Rushworth MFS. Functional Specialization within Medial Frontal Cortex of the Anterior Cingulate for Evaluating Effort-Related Decisions. *J Neurosci*. 2003;23(16):6475-6479. doi:10.1523/JNEUROSCI.23-16-06475.2003

153. Bush G, Luu P, Posner MI. Cognitive and emotional influences in anterior cingulate cortex. *Trends in Cognitive Sciences*. 2000;4(6):215-222. doi:10.1016/S1364-6613(00)01483-2

154. Bryden DW, Johnson EE, Tobia SC, Kashtelyan V, Roesch MR. Attention for learning signals in anterior cingulate cortex. *J Neurosci*. 2011;31(50):18266-18274. doi:10.1523/JNEUROSCI.4715-11.2011

155. Kolling N, Behrens TEJ, Mars RB, Rushworth MFS. Neural Mechanisms of Foraging. *Science*. 2012;336(6077):95-98. doi:10.1126/science.1216930

156. Panagis G, Spyraki C, Miliaressis E. Poststimulation excitability of ventral pallidum self-stimulation neurons. *Behavioral Neuroscience*. 1995;109(4):777-781. doi:10.1037/0735-7044.109.4.777

157. Murray B, Shizgal P. Physiological measures of conduction velocity and refractory period for putative reward-relevant MFB axons arising in the rostral MFB. *Physiology & Behavior*. 1996;59(3):427-437. doi:10.1016/0031-9384(95)02077-2

158. Panagis G, Nomikos GG, Miliaressis E, et al. Ventral pallidum self-stimulation induces stimulus dependent increase in c-fos expression in reward-related brain regions. *Neuroscience*. 1997;77(1):175-186.

159. Stratford TR, Kelley AE, Simansky KJ. Blockade of GABAA receptors in the medial ventral pallidum elicits feeding in satiated rats. *Brain Res*. 1999;825(1-2):199-203.

160. Smith KS, Berridge KC. The ventral pallidum and hedonic reward: neurochemical maps of sucrose "liking" and food intake. *J Neurosci*. 2005;25(38):8637-8649. doi:10.1523/JNEUROSCI.1902-05.2005

161. Shimura T, Imaoka H, Yamamoto T. Neurochemical modulation of ingestive behavior in the ventral pallidum. *Eur J Neurosci*. 2006;23(6):1596-1604. doi:10.1111/j.1460-9568.2006.04689.x

162. Morgane PJ. Alterations in feeding and drinking behavior of rats with lesions in globi pallidi. *Am J Physiol*. 1961;201:420-428. doi:10.1152/ajplegacy.1961.201.3.420

163. Cromwell HC, Berridge KC. Where does damage lead to enhanced food aversion: the ventral pallidum/substantia innominata or lateral hypothalamus? *Brain Res*. 1993;624(1-2):1-10.

164. Berridge KC. Food reward: brain substrates of wanting and liking. *Neurosci Biobehav Rev*. 1996;20(1):1-25.

165. Miller JM, Vorel SR, Tranguch AJ, et al. Anhedonia after a selective bilateral lesion of the globus pallidus. *Am J Psychiatry*. 2006;163(5):786-788. doi:10.1176/ajp.2006.163.5.786

166. Vijayaraghavan L, Vaidya JG, Humphreys CT, Beglinger LJ, Paradiso S. Emotional and motivational changes after bilateral lesions of the globus pallidus. *Neuropsychology*. 2008;22(3):412-418. doi:10.1037/0894-4105.22.3.412

167. Schultz W. Behavioral theories and the neurophysiology of reward. *Annu Rev Psychol*. 2006;57:87-115. doi:10.1146/annurev.psych.56.091103.070229

168. Padoa-Schioppa C, Cai X. The orbitofrontal cortex and the computation of subjective value: consolidated concepts and new perspectives. *Ann N Y Acad Sci*. 2011;1239:130-137. doi:10.1111/j.1749-6632.2011.06262.x

169. Courville AC, Daw ND, Touretzky DS. Bayesian theories of conditioning in a changing world. *Trends Cogn Sci (Regul Ed)*. 2006;10(7):294-300. doi:10.1016/j.tics.2006.05.004

170. Pearce JM, Hall G. A model for Pavlovian learning: variations in the effectiveness of conditioned but not of unconditioned stimuli. *Psychol Rev*. 1980;87(6):532-552.

171. Daddaoua N, Lopes M, Gottlieb J. Intrinsically motivated oculomotor exploration guided by uncertainty reduction and conditioned reinforcement in non-human primates. *Sci Rep*. 2016;6:20202. doi:10.1038/srep20202

172. Burke CJ, Tobler PN. Coding of reward probability and risk by single neurons in animals. *Front Neurosci*. 2011;5:121. doi:10.3389/fnins.2011.00121

173. Yamada H, Inokawa H, Hori Y, et al. Characteristics of fast-spiking neurons in the striatum of behaving monkeys. *Neurosci Res*. 2016;105:2-18. doi:10.1016/j.neures.2015.10.003

174. Yamamoto S, Monosov IE, Yasuda M, Hikosaka O. What and where information in the caudate tail guides saccades to visual objects. *J Neurosci*. 2012;32(32):11005-11016. doi:10.1523/JNEUROSCI.0828-12.2012

175. Hayashi K, Nakao K, Nakamura K. Appetitive and aversive information coding in the primate dorsal raphé nucleus. *J Neurosci*. 2015;35(15):6195-6208. doi:10.1523/JNEUROSCI.2860-14.2015

176. Paton JJ, Belova MA, Morrison SE, Salzman CD. The primate amygdala represents the positive and negative value of visual stimuli during learning. *Nature*. 2006;439(7078):865-870. doi:10.1038/nature04490

177. Spooren WP, Lynd-Balta E, Mitchell S, Haber SN. Ventral pallidostriatal pathway in the monkey: evidence for modulation of basal ganglia circuits. *J Comp Neurol*. 1996;370(3):295-312. doi:10.1002/(SICI)1096-9861(19960701)370:3<295::AID-CNE2>3.0.CO;2-#

178. Grinband J, Hirsch J, Ferrera VP. A neural representation of categorization uncertainty in the human brain. *Neuron*. 2006;49(5):757-763. doi:10.1016/j.neuron.2006.01.032

179. Yanike M, Ferrera VP. Representation of Outcome Risk and Action in the Anterior Caudate Nucleus. *J Neurosci*. 2014;34(9):3279-3290. doi:10.1523/JNEUROSCI.3818-13.2014

180. Yamamoto S, Kim HF, Hikosaka O. Reward value-contingent changes of visual responses in the primate caudate tail associated with a visuomotor skill. *J Neurosci*. 2013;33(27):11227-11238. doi:10.1523/JNEUROSCI.0318-13.2013

181. Klein JT, Platt ML. Social information signaling by neurons in primate striatum. *Curr Biol*. 2013;23(8):691-696. doi:10.1016/j.cub.2013.03.022

182. Ongür D, Price JL. The organization of networks within the orbital and medial prefrontal cortex of rats, monkeys and humans. *Cereb Cortex*. 2000;10(3):206-219.

183. Marvin CB, Shohamy D. Curiosity and reward: Valence predicts choice and information prediction errors enhance learning. *J Exp Psychol Gen*. 2016;145(3):266-272. doi:10.1037/xge0000140

184. Schultz W. Multiple reward signals in the brain. *Nat Rev Neurosci*. 2000;1(3):199-207. doi:10.1038/35044563

185. Luhmann CC, Chun MM, Yi D-J, Lee D, Wang X-J. Neural dissociation of delay and uncertainty in inter-temporal choice. *J Neurosci*. 2008;28(53):14459-14466. doi:10.1523/JNEUROSCI.5058-08.2008

186. Ikemoto S, Panksepp J. The role of nucleus accumbens dopamine in motivated behavior: a unifying interpretation with special reference to reward-seeking. *Brain Res Brain Res Rev*. 1999;31(1):6-41.

187. Everitt BJ, Parkinson JA, Olmstead MC, Arroyo M, Robledo P, Robbins TW. Associative processes in addiction and reward. The role of amygdala-ventral striatal subsystems. *Ann N Y Acad Sci*. 1999;877:412-438.

188. Pessiglione M, Seymour B, Flandin G, Dolan RJ, Frith CD. Dopamine-dependent prediction errors underpin reward-seeking behaviour in humans. *Nature*. 2006;442(7106):1042-1045. doi:10.1038/nature05051

189. Morris G, Arkadir D, Nevet A, Vaadia E, Bergman H. Coincident but Distinct Messages of Midbrain Dopamine and Striatal Tonically Active Neurons. *Neuron*. 2004;43(1):133-143. doi:10.1016/j.neuron.2004.06.012

190. Mello GBM, Soares S, Paton JJ. A scalable population code for time in the striatum. *Curr Biol*. 2015;25(9):1113-1122. doi:10.1016/j.cub.2015.02.036

191. Belova MA, Paton JJ, Salzman CD. Moment-to-moment tracking of state value in the amygdala. *J Neurosci*. 2008;28(40):10023-10030. doi:10.1523/JNEUROSCI.1400-08.2008

192. Miyazaki K, Miyazaki KW, Doya K. Activation of dorsal raphe serotonin neurons underlies waiting for delayed rewards. *J Neurosci*. 2011;31(2):469-479. doi:10.1523/JNEUROSCI.3714-10.2011

193. Schoenbaum G, Roesch M. Orbitofrontal cortex, associative learning, and expectancies. *Neuron*. 2005;47(5):633-636. doi:10.1016/j.neuron.2005.07.018

194. Kusumoto-Yoshida I, Liu H, Chen BT, Fontanini A, Bonci A. Central role for the insular cortex in mediating conditioned responses to anticipatory cues. *PNAS*. 2015;112(4):1190-1195. doi:10.1073/pnas.1416573112

195. Daye PM, Monosov IE, Hikosaka O, Leopold DA, Optican LM. pyElectrode: an open-source tool using structural MRI for electrode positioning and neuron mapping. *J Neurosci Methods*. 2013;213(1):123-131. doi:10.1016/j.jneumeth.2012.12.012

196. Hikosaka O, Nakamura K, Nakahara H. Basal ganglia orient eyes to reward. *J Neurophysiol*. 2006;95(2):567-584. doi:10.1152/jn.00458.2005

197. Kravitz AV, Kreitzer AC. Striatal Mechanisms Underlying Movement, Reinforcement, and Punishment. *Physiology (Bethesda)*. 2012;27(3). doi:10.1152/physiol.00004.2012

198. Smith KS, Tindell AJ, Aldridge JW, Berridge KC. Ventral pallidum roles in reward and motivation. *Behav Brain Res*. 2009;196(2):155-167. doi:10.1016/j.bbr.2008.09.038

199. Tachibana Y, Hikosaka O. The primate ventral pallidum encodes expected reward value and regulates motor action. *Neuron*. 2012;76(4):826-837. doi:10.1016/j.neuron.2012.09.030

200. Root DH, Melendez RI, Zaborszky L, Napier TC. The ventral pallidum: Subregion-specific functional anatomy and roles in motivated behaviors. *Prog Neurobiol*. 2015;130:29-70. doi:10.1016/j.pneurobio.2015.03.005

201. Richard JM, Ambroggi F, Janak PH, Fields HL. Ventral Pallidum Neurons Encode Incentive Value and Promote Cue-Elicited Instrumental Actions. *Neuron*. 2016;90(6):1165-1173. doi:10.1016/j.neuron.2016.04.037

202. Saga Y, Richard A, Sgambato-Faure V, Hoshi E, Tobler PN, Tremblay L. Ventral Pallidum Encodes Contextual Information and Controls Aversive Behaviors. *Cereb Cortex*. 2017;27(4):2528-2543. doi:10.1093/cercor/bhw107

203. Heilbronner SR, Hayden BY. Dorsal Anterior Cingulate Cortex: A Bottom-Up View. *Annu Rev Neurosci*. 2016;39:149-170. doi:10.1146/annurev-neuro-070815-013952

204. Roesch MR, Esber GR, Li J, Daw ND, Schoenbaum G. Surprise! Neural correlates of Pearce-Hall and Rescorla-Wagner coexist within the brain. *Eur J Neurosci*. 2012;35(7):1190-1200. doi:10.1111/j.1460-9568.2011.07986.x

205. Ghazizadeh A, Griggs W, Hikosaka O. Ecological Origins of Object Salience: Reward, Uncertainty, Aversiveness, and Novelty. *Front Neurosci*. 2016;10:378. doi:10.3389/fnins.2016.00378

206. Berlyne DE. Uncertainty and conflict: a point of contact between information-theory and behavior-theory concepts. *Psychol Rev*. 1957;64, Part 1(6):329-339.

207. Golman R, Loewenstein G. An Information-Gap Theory of Feelings About Uncertainty. :24.

208. Gottlieb J. Understanding active sampling strategies: Empirical approaches and implications for attention and decision research. *Cortex*. 2018;102:150-160. doi:10.1016/j.cortex.2017.08.019

209. Zentall TR. Maladaptive "gambling" by pigeons. *Behav Processes*. 2011;87(1):50-56. doi:10.1016/j.beproc.2010.12.017

210. Charpentier CJ, Bromberg-Martin ES, Sharot T. Valuation of knowledge and ignorance in mesolimbic reward circuitry. *Proc Natl Acad Sci USA*. 2018;115(31):E7255-E7264. doi:10.1073/pnas.1800547115

211. Quilodran R, Rothé M, Procyk E. Behavioral shifts and action valuation in the anterior cingulate cortex. *Neuron*. 2008;57(2):314-325. doi:10.1016/j.neuron.2007.11.031

212. Kolling N, Wittmann MK, Behrens TEJ, Boorman ED, Mars RB, Rushworth MFS. Value, search, persistence and model updating in anterior cingulate cortex. *Nat Neurosci*. 2016;19(10):1280-1285. doi:10.1038/nn.4382

213. Karlsson MP, Tervo DGR, Karpova AY. Network resets in medial prefrontal cortex mark the onset of behavioral uncertainty. *Science*. 2012;338(6103):135-139. doi:10.1126/science.1226518

214. Hayden BY, Heilbronner SR, Pearson JM, Platt ML. Surprise signals in anterior cingulate cortex: neuronal encoding of unsigned reward prediction errors driving adjustment in behavior. *J Neurosci*. 2011;31(11):4178-4187. doi:10.1523/JNEUROSCI.4652-10.2011

215. Shenhav A, Straccia MA, Musslick S, Cohen JD, Botvinick MM. Dissociable neural mechanisms track evidence accumulation for selection of attention versus action. *Nat Commun*. 2018;9(1):2485. doi:10.1038/s41467-018-04841-1

216. Brydevall M, Bennett D, Murawski C, Bode S. The neural encoding of information prediction errors during non-instrumental information seeking. *Sci Rep*. 2018;8(1):6134. doi:10.1038/s41598-018-24566-x

217. Hunt LT, Malalasekera WMN, de Berker AO, et al. Triple dissociation of attention and decision computations across prefrontal cortex. *Nat Neurosci*. 2018;21(10):1471-1481. doi:10.1038/s41593-018-0239-5

218. Starkweather CK, Gershman SJ, Uchida N. The Medial Prefrontal Cortex Shapes Dopamine Reward Prediction Errors under State Uncertainty. *Neuron*. 2018;98(3):616-629.e6. doi:10.1016/j.neuron.2018.03.036

219. Shenhav A, Cohen JD, Botvinick MM. Dorsal anterior cingulate cortex and the value of control. *Nat Neurosci*. 2016;19(10):1286-1291. doi:10.1038/nn.4384

220. Fujii N, Graybiel AM. Time-varying covariance of neural activities recorded in striatum and frontal cortex as monkeys perform sequential-saccade tasks. *Proc Natl Acad Sci USA*. 2005;102(25):9032-9037. doi:10.1073/pnas.0503541102

221. Muhammad R, Wallis JD, Miller EK. A comparison of abstract rules in the prefrontal cortex, premotor cortex, inferior temporal cortex, and striatum. *J Cogn Neurosci*. 2006;18(6):974-989. doi:10.1162/jocn.2006.18.6.974

222. Seo M, Lee E, Averbeck BB. Action selection and action value in frontal-striatal circuits. *Neuron*. 2012;74(5):947-960. doi:10.1016/j.neuron.2012.03.037

223. Middleton FA, Strick PL. Basal ganglia and cerebellar loops: motor and cognitive circuits. *Brain Res Brain Res Rev*. 2000;31(2-3):236-250.

224. Krauzlis RJ, Bollimunta A, Arcizet F, Wang L. Attention as an effect not a cause. *Trends Cogn Sci (Regul Ed)*. 2014;18(9):457-464. doi:10.1016/j.tics.2014.05.008

225. Chatham CH, Badre D. Multiple gates on working memory. *Curr Opin Behav Sci*. 2015;1:23-31. doi:10.1016/j.cobeha.2014.08.001

226. Miller SM. Monitoring and blunting: validation of a questionnaire to assess styles of information seeking under threat. *J Pers Soc Psychol*. 1987;52(2):345-353.

227. Gormezano I, Wasserman EA. *Learning and Memory: The Behavioral and Biological Substrates*. Psychology Press; 2013.

228. Huey ED, Zahn R, Krueger F, et al. A psychological and neuroanatomical model of obsessive-compulsive disorder. *J Neuropsychiatry Clin Neurosci*. 2008;20(4):390-408. doi:10.1176/jnp.2008.20.4.390

229. Brown LT, Mikell CB, Youngerman BE, Zhang Y, McKhann GM, Sheth SA. Dorsal anterior cingulotomy and anterior capsulotomy for severe, refractory obsessive-compulsive disorder: a systematic review of observational studies. *J Neurosurg*. 2016;124(1):77-89. doi:10.3171/2015.1.JNS14681

230. DeLong MR, Wichmann T. Basal Ganglia Circuits as Targets for Neuromodulation in Parkinson Disease. *JAMA Neurol*. 2015;72(11):1354-1360. doi:10.1001/jamaneurol.2015.2397

231. Williams ZM, Bush G, Rauch SL, Cosgrove GR, Eskandar EN. Human anterior cingulate neurons and the integration of monetary reward with motor responses. *Nat Neurosci*. 2004;7(12):1370-1375. doi:10.1038/nn1354

232. Sheth SA, Mian MK, Patel SR, et al. Human dorsal anterior cingulate cortex neurons mediate ongoing behavioural adaptation. *Nature*. 2012;488(7410):218-221. doi:10.1038/nature11239

233. Vaghi MM, Luyckx F, Sule A, Fineberg NA, Robbins TW, De Martino B. Compulsivity Reveals a Novel Dissociation between Action and Confidence. *Neuron*. 2017;96(2):348-354.e4. doi:10.1016/j.neuron.2017.09.006

234. Frank MJ, Seeberger LC, O'reilly RC. By carrot or by stick: cognitive reinforcement learning in parkinsonism. *Science*. 2004;306(5703):1940-1943. doi:10.1126/science.1102941

235. Averbeck B, O'Sullivan S, Djamshidian A. Impulsive and Compulsive Behaviours in Parkinson's disease. *Annu Rev Clin Psychol*. 2014;10:553-580. doi:10.1146/annurev-clinpsy-032813-153705

236. Reynolds B. A review of delay-discounting research with humans: relations to drug use and gambling. *Behav Pharmacol*. 2006;17(8):651-667. doi:10.1097/FBP.0b013e3280115f99

237. de Rezende Costa FH, Averbeck B, O'Sullivan SS, et al. Jumping to conclusions in untreated patients with Parkinson's disease. *Neuropsychologia*. 2016;85:19-23. doi:10.1016/j.neuropsychologia.2016.03.002

238. Dugas MJ, Gagnon F, Ladouceur R, Freeston MH. Generalized anxiety disorder: a preliminary test of a conceptual model. *Behav Res Ther*. 1998;36(2):215-226.

239. Holaway RM, Heimberg RG, Coles ME. A comparison of intolerance of uncertainty in analogue obsessive-compulsive disorder and generalized anxiety disorder. *J Anxiety Disord*. 2006;20(2):158-174. doi:10.1016/j.janxdis.2005.01.002

240. Graybiel AM, Rauch SL. Toward a neurobiology of obsessive-compulsive disorder. *Neuron*. 2000;28(2):343-347.

241. Tolin DF, Abramowitz JS, Brigidi BD, Foa EB. Intolerance of uncertainty in obsessive-compulsive disorder. *J Anxiety Disord*. 2003;17(2):233-242.

242. Mitchell MR, Weiss VG, Beas BS, Morgan D, Bizon JL, Setlow B. Adolescent risk taking, cocaine self-administration, and striatal dopamine signaling. *Neuropsychopharmacology*. 2014;39(4):955-962. doi:10.1038/npp.2013.295

243. van Holst RJ, Sescousse G, Janssen LK, et al. Increased Striatal Dopamine Synthesis Capacity in Gambling Addiction. *Biol Psychiatry*. 2018;83(12):1036-1043. doi:10.1016/j.biopsych.2017.06.010

244. Kalivas BC, Kalivas PW. Corticostriatal circuitry in regulating diseases characterized by intrusive thinking. *Dialogues Clin Neurosci*. 2016;18(1):65-76.

245. Molina JA, Sáinz-Artiga MJ, Fraile A, et al. Pathologic gambling in Parkinson's disease: a behavioral manifestation of pharmacologic treatment? *Mov Disord*. 2000;15(5):869-872.

246. Merims D, Giladi N. Dopamine dysregulation syndrome, addiction and behavioral changes in Parkinson's disease. *Parkinsonism Relat Disord*. 2008;14(4):273-280. doi:10.1016/j.parkreldis.2007.09.007